

# Pairing symmetry in cuprate superconductors

C. C. Tsuei and J. R. Kirtley

IBM Thomas J. Watson Research Center, P.O. Box 218, Yorktown Heights,  
New York 10598

Pairing symmetry in the cuprate superconductors is an important and controversial topic. The recent development of phase-sensitive tests, combined with the refinement of several other symmetry-sensitive techniques, has for the most part settled this controversy in favor of predominantly  $d$ -wave symmetry for a number of optimally hole- and electron-doped cuprates. This paper begins by reviewing the concepts of the order parameter, symmetry breaking, and symmetry classification in the context of the cuprates. After a brief survey of some of the key non-phase-sensitive tests of pairing symmetry, the authors extensively review the phase-sensitive methods, which use the half-integer flux-quantum effect as an unambiguous signature for  $d$ -wave pairing symmetry. A number of related symmetry-sensitive experiments are described. The paper concludes with a brief discussion of the implications, both fundamental and applied, of the predominantly  $d$ -wave pairing symmetry in the cuprates.

## CONTENTS

I. Introduction	969	2. $c$ -axis twist junctions	1004
A. Evidence for Cooper pairing in cuprates	969	VI. Implications of $d_{x^2-y^2}$ Pairing Symmetry	1004
B. Order parameter in superconductors	970	A. Pairing interaction	1004
C. Broken symmetry and symmetry classification of the superconducting state	971	B. Quasiparticles in $d$ -wave superconductors	1006
1. Tetragonal crystal lattice	972	C. Surfaces and interfaces	1006
2. Orthorhombic crystal lattice	973	1. Zero-bias conductance peaks	1006
3. Cu-O square/rectangular lattice	973	2. Time-reversal symmetry breaking	1007
II. Non-Phase-Sensitive Techniques	974	3. Josephson junctions in $d$ -wave superconductors	1007
A. Penetration depth	974	D. Vortex state	1007
B. Specific heat	975	VII. Conclusions	1008
C. Thermal conductivity	975	Acknowledgments	1009
D. Angle-resolved photoemission	975	References	1009
E. Raman scattering	976		
F. Nuclear magnetic resonance	976		
G. Nonlinear Meissner effect	976		
III. Half-Integer Flux-Quantum Effect	977		
A. Josephson tunneling	977		
B. Flux quantization in a superconducting ring	980		
C. Paramagnetic Meissner effect	981		
IV. Phase-Sensitive Tests of Pairing Symmetry	982		
A. SQUID interferometry	982		
B. Single-Josephson-junction modulation	984		
C. Tricrystal and tetracrystal magnetometry	985		
1. Design and characterization of controlled-orientation multicrystals	985		
2. Magnetic-flux imaging	986		
3. Nature of the observed half-integer flux quantization	988		
4. Integer and half-integer Josephson vortices	989		
5. Evidence for pure $d$ -wave pairing symmetry	993		
a. Tetragonal $Tl_2Ba_2CuO_{6+\delta}$	994		
b. Orthorhombic $Bi_2Sr_2CaCu_2O_{8+\delta}$	995		
D. Thin-film SQUID magnetometry	997		
E. Universality of $d$ -wave superconductivity	997		
1. Hole-doped cuprates	998		
2. Electron-doped cuprates	998		
3. Temperature dependence of the $\Phi_0/2$ effect	1000		
V. Related Symmetry-Sensitive Experiments	1000		
A. Biepitaxial grain-boundary experiments	1000		
B. $c$ -axis pair tunneling	1001		
1. Tunneling into conventional superconductors	1001		

## I. INTRODUCTION

The normal-to-superconducting phase-transition temperature ( $T_c$ ) of a superconductor marks the inception of a macroscopic quantum phase-coherent pair state. It is well established that in the conventional low- $T_c$  superconductors (e.g., Pb, Al, Nb, and  $Nb_3Sn$ ), the phonon-mediated many-body electron-electron interaction leads to spin-singlet pairing with  $s$ -wave symmetry (Bardeen, Cooper, and Schrieffer, 1957). On the other hand, the internal structure of the Cooper pairs in the high- $T_c$  cuprate superconductors was a topic of intense debate for almost ten years after the discovery of high-temperature superconductivity (Bednorz and Müller, 1986). Recently a new class of pairing symmetry experiments have altered this situation significantly. These phase-sensitive tests, as well as a number of other techniques for measuring the magnitude of the energy gap, have firmly established predominantly  $d$ -wave pairing symmetry in a number of high- $T_c$  cuprate superconductors. In this review, we shall survey the current status of the field and assess the implications of  $d$ -wave pairing for our understanding of high-temperature superconductivity and for its applications.

### A. Evidence for Cooper pairing in cuprates

Given the unprecedented superconducting critical temperatures discovered in various cuprate systems (Wu *et al.*, 1987; Chu *et al.*, 1993), early researchers had cause

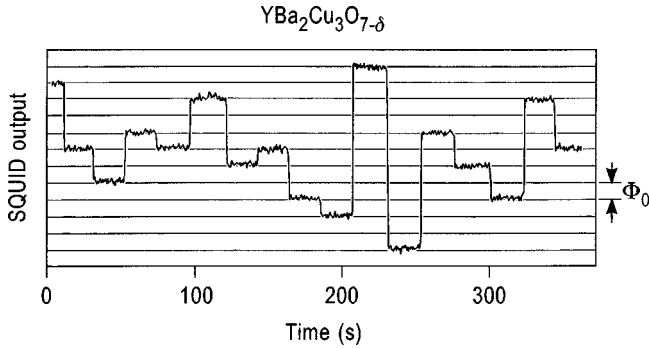


FIG. 1. The magnetic flux threading through a polycrystalline YBCO ring, monitored with a SQUID magnetometer as a function of time. The flux jumps occur in integral multiples of the flux quantum  $\Phi_0 = h/2e$ . Adapted from Gough *et al.* (1987).

to question whether Cooper pairing operates as in conventional superconductors. The most direct evidence for electronic pairing in cuprate superconductors was provided by a study of the magnetic-flux states of a polycrystalline  $\text{YBa}_2\text{Cu}_3\text{O}_{7-\delta}$  (YBCO) ring, monitored with a SQUID<sup>1</sup> magnetometer (Gough *et al.*, 1987; Fig. 1). The data showed that the magnetic flux  $\Phi$  threading through the ring was quantized in multiples of the basic flux quantum  $\Phi_0 = h/2e = 2.07 \times 10^{-15}$  Wb. This is the *integer flux-quantum effect*:

$$\Phi = n\Phi_0 \quad (n=0,1,2, \dots). \quad (1)$$

In addition to proving that the electronic charges are paired in the superconducting state, this experiment also established the existence of long-range quantum phase coherence of the pair wave function through thousands of individual grains around the YBCO ring. Since then, integer flux quantization has been demonstrated many times, in SQUID-related and other experiments, involving single-phase YBCO and other cuprate systems, and at liquid nitrogen temperatures and above (Koelle *et al.*, 1999).

Persistent current and integer flux quantization were also demonstrated in a YBCO ring interrupted by a segment of Nb, a conventional *s*-wave superconductor (Keene *et al.*, 1989). This experiment implicitly indicated that there is no difference in parity between the pair wave functions in a high- $T_c$  cuprate superconductor (e.g., YBCO) and a low- $T_c$  conventional superconductor (e.g., Nb). The effect of parity in Josephson junctions is reviewed by Fulde *et al.*, 1988. Other evidence for singlet pairing includes the results of Andreev-reflection (Hoevers *et al.*, 1988) and spin susceptibility measurements (Takigawa *et al.*, 1989; Barrett *et al.*, 1990).

In view of this experimental evidence, we shall focus on spin-singlet Cooper pairing in the following discussion.

<sup>1</sup>SQUID stands for superconducting quantum interference device. For a recent review on SQUID's and their applications, see Koelle *et al.* (1999).

## B. Order parameter in superconductors

The order parameter is a very useful concept in describing the ordered state of various phase transitions (see White and Geballe, 1979; Anderson, 1984). The superconducting pair state is characterized by an order parameter that represents the extent of macroscopic phase coherence. The concept of the superconducting order parameter was first introduced by Ginzburg and Landau (1950) in their phenomenological description of the superconducting state, based on the Landau theory of second-order phase transitions.

In the Ginzburg-Landau formalism, a complex position-dependent order parameter  $\Psi(\mathbf{r}) = |\Psi(\mathbf{r})|e^{i\varphi(\mathbf{r})}$  describes the macroscopic properties of a superfluid condensate. The temperature-dependent order parameter  $\Psi(\mathbf{r})$  is characterized by a phase  $\varphi(\mathbf{r})$  and a modulus  $|\Psi(\mathbf{r})|$ . The quantity  $|\Psi(\mathbf{r})|^2$  is a measure of the local superfluid density  $n_s(\mathbf{r})$ , suggesting that  $\Psi(\mathbf{r})$  is a wave function. To study the thermodynamic and magnetic properties of superconductors, the total free energy  $F_s$  with respect to its value in the normal state  $F_n$  is expanded in even powers of the order parameter  $\Psi(\mathbf{r})$  and its spatial gradients:

$$F_s = F_n + \int d^3r \left[ \alpha |\Psi(\mathbf{r})|^2 + \frac{1}{2} \beta |\Psi(\mathbf{r})|^4 + \sum_{i,j} K_{ij} \left( \frac{\partial \Psi(\mathbf{r})}{\partial r_i} \right) \left( \frac{\partial \Psi(\mathbf{r})}{\partial r_j} \right) + f_m + \dots \right], \quad (2)$$

where the second-rank tensor  $K_{ij}$  is reduced to the scalar  $\hbar^2/2m$  for superconductors with a cubic crystal structure. The magnetic-field term  $f_m$  is a function of  $\Psi(\mathbf{r})$ , the vector potential  $\mathbf{A}(\mathbf{r})$ , the magnetic induction  $\mathbf{B}(\mathbf{r})$ , and the applied magnetic field  $\mathbf{H}(\mathbf{r})$ . A minimization of the free-energy functional (2) with respect to variations in  $\Psi(\mathbf{r})$  and  $\mathbf{A}(\mathbf{r})$  leads to the two well-known Ginzburg-Landau differential equations, from which the order parameter can be defined. With appropriate boundary conditions, various properties of the most probable superconducting state can be calculated. There is a vast literature on the application of Ginzburg-Landau theory and its extensions to a variety of superconducting systems (Cyrot, 1973; Tinkham, 1996).

The link between the Ginzburg-Landau theory and the microscopic theory of superconductivity was established by Gor'kov (1959). In the vicinity of  $T_c$ , the Ginzburg-Landau equations can be derived from the BCS theory. The Ginzburg-Landau order parameter  $\Psi(\mathbf{r})$  is identified with the pair wave function and is proportional to the energy gap  $\Delta(\mathbf{r})$ . In principle, the validity of the Ginzburg-Landau theory should be limited to a temperature range near  $T_c$ , due to the inherent assumption that the order parameter is small and slowly varying close to the phase transition. In practice, the Ginzburg-Landau theory is often applied well beyond its range of validity with good results. There is justification for this unexpected success in terms of the rigidity of the superconducting wave function, and other theoretical arguments. As far as pairing symmetry is concerned, the

energy gap  $\Delta(\mathbf{r})$  as the microscopic identity of the Ginzburg-Landau order parameter is expected to be valid throughout the whole temperature range below  $T_c$ , as the superconducting order parameter, defined at either a phenomenological or a microscopic level, represents the degree of long-range phase coherence in the pair state.

An essential condition of macroscopic quantum phenomena such as superfluidity and superconductivity is the occurrence of off-diagonal long-range order, a concept that has no classical analog (Yang, 1962; Anderson, 1966a). The off-diagonal long-range order of a many-particle system stems from the existence of certain particle correlations, which can be expressed as a nonzero expectation value of the two-particle reduced density matrix:

$$\rho_2(\mathbf{r}, \mathbf{r}') = \langle \Psi_\alpha^\dagger(\mathbf{r}) \Psi_\beta^\dagger(\mathbf{r}) \Psi_\alpha(\mathbf{r}') \Psi_\beta(\mathbf{r}') \rangle, \quad (3)$$

where  $\Psi_\alpha^\dagger(\mathbf{r})$  and  $\Psi_\alpha(\mathbf{r})$  are the particle field operators<sup>2</sup> for creating and annihilating a particle at a relative coordinate  $\mathbf{r}$  with (pseudo-) spin state  $\mathbf{k}\uparrow$ . For the case of spin-singlet pairing ( $\alpha = -\beta$ ), the pair-correlation function can be expressed by

$$\rho_2(\mathbf{r}, \mathbf{r}') = \langle \Psi_\uparrow^\dagger(\mathbf{r}) \Psi_\uparrow^\dagger(\mathbf{r}) \rangle \langle \Psi_\downarrow(\mathbf{r}') \Psi_\downarrow(\mathbf{r}') \rangle \quad (4)$$

in the limit the pair separation  $|\mathbf{r} - \mathbf{r}'|$  becomes infinite.

It is clear from Eq. (4) that a finite value of the two-particle density matrix is a sure signature for the existence of pair correlation. The off-diagonal long-range order in superconductors then corresponds to a nonvanishing anomalous expectation value of the local pair amplitude  $\langle \Psi_\uparrow^\dagger(\mathbf{r}) \Psi_\uparrow^\dagger(\mathbf{r}) \rangle$ , which is indeed consistent with the order parameter defined in the Ginzburg-Landau formalism. In momentum-space representation, off-diagonal long-range order corresponds to a nonzero expectation value of  $\langle c_{\mathbf{k}\uparrow} c_{-\mathbf{k}\downarrow} \rangle \propto \Psi(\mathbf{k})$ , where the pair wave function  $\Psi(\mathbf{k})$  is a complex scalar function of wave vector  $\mathbf{k}$ , and is related to the gap function  $\Delta_{\mathbf{k}}$  through  $\Psi(\mathbf{k}) = \Delta_{\mathbf{k}}/2E_{\mathbf{k}}$ , where  $E_{\mathbf{k}}$  is the quasiparticle excitation energy.

Macroscopic phase coherence is one of the most remarkable characteristics of the BCS superfluid condensate and is inherently related to the fact that particle number in the BCS pair state is not well defined. It is a manifestation of the off-diagonal long-range order arising from BCS-type pairing. With the condition of off-diagonal long-range order fulfilled, one can derive macroscopic quantum phenomena such as flux quantization and the Meissner effect without needing to know the details of the pairing mechanism (Yang, 1962). Furthermore, it is recognized that off-diagonal long-range order is a property not only of BCS superconductors but also of other alternative types of superconductivity (Allen, 1990).

<sup>2</sup>The field operator  $\Psi_\uparrow(\mathbf{r})$  can be expressed by  $\Psi_\uparrow(\mathbf{r}) = \sum_{\mathbf{k}} \Psi_{\mathbf{k}}(\mathbf{r}) c_{\mathbf{k}\uparrow}$ , where  $c_{\mathbf{k}\uparrow}$  is the second-quantized annihilation operator for state  $\mathbf{k}\uparrow$ .

In short, off-diagonal long-range order exists in all superconductors. The use of the pair amplitude  $\langle c_{\mathbf{k}\uparrow} c_{-\mathbf{k}\downarrow} \rangle \sim \Delta_{\mathbf{k}}$  as the order parameter captures the essence of the macroscopic phase-coherent superconducting state. The gap parameter is well defined, and its symmetry can be experimentally determined, even in the absence of detailed knowledge about the microscopic origin of superconductivity.

### C. Broken symmetry and symmetry classification of the superconducting state

The concept of broken symmetry permeates nearly every branch of modern physics (Michel, 1980; Anderson, 1984). For example, the onset of any long-range order in condensed matter is always accompanied by a lowering in symmetry (Landau, 1957). As in any second-order phase transition, the symmetries above and below the transition from normal to superconducting state are related,<sup>3</sup> due to the fact that the symmetry breaking across the transition is continuous. In this context, the order parameter is just a measure of the amount of symmetry breaking in the ordered state. The symmetry group  $H$  describing the superconducting state must be a subgroup of the full symmetry group  $G$  describing the normal state:

$$G = X \times R \times U(1) \times T \quad \text{for } T > T_c \quad (5)$$

and

$$H \subset G \quad \text{for } T \leq T_c, \quad (6)$$

where  $X$  is the symmetry group of the crystal lattice,  $R$  the symmetry group of spin rotation,<sup>4</sup>  $U(1)$  the one-dimensional global gauge symmetry, and  $T$  the time-reversal symmetry operation. The existence of off-diagonal long-range order in BCS superconductors below  $T_c$  leads to a phase-coherent pair condensate in which the global gauge symmetry is spontaneously broken. Macroscopic phase-coherent quantum phenomena such as the Meissner effect, flux quantization, and the Josephson effects are all manifestations of the global gauge symmetry violation in the superconducting state. In an unconventional superconductor, one or more symmetries in addition to  $U(1)$  are broken at  $T_c$ . The degree of symmetry breaking involved in the pair state is reflected in the symmetry properties of the order parameter.

One can gain insight into the nature of the pair-condensate state based on symmetry considerations alone. For example, the parity of a superconductor with inversion symmetry can be specified using the Pauli

<sup>3</sup>There are possibly exceptions in certain one-dimensional systems (Anderson, 1984).

<sup>4</sup>In crystals with strong spin-orbit coupling such as the heavy-fermion systems, the spins can be considered as frozen into the crystal lattice. Rotation in spin space is coupled to that in coordinate space. Therefore spin rotation is no longer a separate symmetry.

principle. The crystal structures of existing bulk superconductors, including the heavy-fermion and cuprate systems, are all characterized by a center of inversion. Therefore superconductors can be classified via the parity of the pair state: The spin-triplet state (total spin  $S=1$ ) has a superconducting order parameter (gap function) with odd parity; the spin-singlet pair state ( $S=0$ ) corresponds to an orbital pair wave function  $\Psi(\mathbf{k}) \propto \Delta(\mathbf{k})$  with even parity [i.e.,  $\Delta(\mathbf{k}) = \Delta(-\mathbf{k})$ ]. Due to the absence of inversion symmetry close to a surface, the mixing of singlet and triplet pair states induced by spin-orbit interaction, which may be important in heavy-fermion superconductors, can result in an observable nonlinear magneto-optical effect (Schmalian and Hübner, 1996). In cuprate superconductors, the spin-orbit coupling is expected to be relatively small. Thus the spin-singlet and -triplet pair states are well defined.

Further classification of superconductors requires a knowledge of possible lattice symmetries,  $X$  in Eq. (5), that might be broken in the superconducting state. This assumes<sup>5</sup> that the symmetry of the superconducting pair wave function reflects that of the underlying crystal lattice.

It is a general result of the Landau theory of second-order phase transitions that the order parameter describing the transition must transform according to one of the irreducible representations of the symmetry group of the high-temperature phase (Landau and Lifshitz, 1979). This must be true for superconducting phase transitions, which are second order in the absence of a magnetic field. The forms of the order parameter can be categorized for various pair-condensate systems by decomposing the representation of the normal-state symmetry group into irreducible representations (Annett, 1991).

Point-group symmetry classification<sup>6</sup> of pair states has been extensively studied in superfluid He (Blount, 1985), heavy-fermion superconductors (Ozaki *et al.*, 1985, 1986; Ueda and Rice, 1985; Volovik and Gor'kov, 1985; Gor'kov, 1987; Fulde *et al.*, 1988; Sigrist and Ueda, 1991; Yip and Garg, 1993; Sauls, 1994), and also in cuprate superconductors (Sigrist and Rice, 1987; Annett *et al.*, 1990, 1996; Annett, 1991; Li *et al.*, 1993; Wenger and Östlund, 1993; Jha and Rajagopal, 1997).

The underlying microscopic pairing mechanism must be known to determine which of the candidate pair states prevails in a given crystal structure. Even without such knowledge, the gap function can be expressed as a

linear combination of the basis functions ( $\chi_\mu^j$ ) of the irreducible representation ( $\Gamma^j$ ) that corresponds to the highest  $T_c$  of all possible forms of the order parameter:

$$\Delta(\mathbf{k}) = \sum_{\mu=1}^{l_j} \eta_\mu \chi_\mu^j(\mathbf{k}), \quad (7)$$

where  $l_j$  is the dimensionality of  $\Gamma^j$ , and the complex number  $\eta_\mu$  is invariant under all symmetry operations of the normal-state group  $G$  in Eq. (5). The expansion coefficients  $\eta_\mu$  can be used to construct the Ginzburg-Landau free energy in Eq. (2), for example.

Yip and Garg (1993) have shown that the basis functions  $\chi_\mu^j$  can always be selected to be real, so that  $\eta_\mu^* \eta_\mu$  will contain information about the time-reversal symmetry. They further proved that time-reversal symmetry can be broken only when the representation is multidimensional.

The basis functions of the irreducible representations for various symmetry groups are well tabulated in the literature (Volovik and Gor'kov, 1985; Annett, 1991; Sigrist and Ueda, 1991) for various crystal structures.<sup>7</sup> In the following, we shall list the basis functions and other symmetry properties of spin-singlet even-parity pair states in two crystal structures that are especially relevant to cuprate superconductors.

### 1. Tetragonal crystal lattice

Cuprate superconductors such as  $\text{La}_{2-x}\text{Sr}_x\text{CuO}_4$  (LSCO),  $\text{Tl}_2\text{Ba}_2\text{CaCu}_2\text{O}_8$  (Tl-2212),  $\text{HgBa}_2\text{CaCu}_2\text{O}_6$  (Hg-1212), and some  $\text{YBa}_2\text{Cu}_3\text{O}_7$  (YBCO)-type compounds with significant cation substitution have a tetragonal crystal structure with point-group symmetry  $D_{4h}$ . Allowed pair states for a tetragonal superconductor are listed in Table I for spin-singlet even-parity pairing under the standard group-theoretic constraints (Annett *et al.*, 1990). The notation in Tables I and II is adopted from Tinkham (1964). The superconducting order parameter should transform like the basis function of an irreducible representation of the relevant point group. However, the basis function is not necessarily unique (Yip and Garg, 1993). An example is the case of the  $A_{1g}$  ( $s$ -wave) pair state in Table I. Each of the four one-dimensional irreducible representations corresponds to a single, scalar gap function of complex numbers. Therefore these pair states should exhibit only one superconducting transition. For the two-dimensional representation ( $E_g$ ), there are three possible states characterized by different residual symmetries (see Table I). Of the

<sup>5</sup>Strictly speaking, there is no *a priori* reason to rule out an order parameter with a symmetry lower than that of the crystal translation and point-group operations. Indeed, such a possibility has been mentioned (Volovik and Gor'kov, 1985) but has not been actively investigated.

<sup>6</sup>Nearly all group-theoretic classifications of superconducting states are based on point-group symmetry. There are exceptions when translational invariance is broken. For example, the presence of spin-density waves in certain heavy-fermion superconductors reduces the number of possible pair states (Ozaki and Machida, 1989; Annett, 1991).

<sup>7</sup>The crystal structures of cuprates have been intensively investigated (Shaked *et al.*, 1994). The atomic arrangement in this class of perovskite oxides is layered, with alternating  $\text{CuO}_2$  plane and charge reservoir blocks. The presence of Cu-O chains (as in  $\text{YBa}_2\text{Cu}_3\text{O}_7$ ) or incommensurate superlattice modulation in  $\text{Bi}_2\text{O}_2$  layers (as in  $\text{Bi}_2\text{Sr}_2\text{CaCu}_2\text{O}_8$ ) results in the orthorhombic variant of the basic tetragonal structure. Thus the crystal structure of the cuprates can be broadly divided into two categories: a tetragonal lattice with point-group symmetry  $D_{4h}$ , and an orthorhombic lattice with  $D_{2h}$ .

TABLE I. Spin-singlet even-parity pair states in a tetragonal crystal with point group  $D_{4h}$ .

Wave-function name	Group-theoretic notation, $T_j$	Residual symmetry	Basis function	Nodes
$s$ wave	$A_{1g}$	$D_{4h} \times T$	$1, (x^2 + y^2), z^2$	none
$g$	$A_{2g}$	$D_4[C_4] \times C_i \times T$	$xy(x^2 - y^2)$	line
$d_{x^2-y^2}$	$B_{1g}$	$D_4[D_2] \times C_i \times T$	$x^2 - y^2$	line
$d_{xy}$	$B_{2g}$	$D_4[D_2'] \times C_i \times T$	$xy$	line
$e_{(1,0)}$	$E_g(1,0)$	$D_4[C_2'] \times C_i \times T$	$xz$	line
$e_{(1,1)}$	$E_g(1,1)$	$D_2[C_2''] \times C_i \times T$	$(x+y)z$	line
$e_{(1,i)}$	$E_g(1,i)$	$D_4[E] \times C_i$	$(x+iy)z$	line

three states of  $E_g$ , only  $E_g(1,i)$  has broken time-reversal symmetry. The gap function  $\Delta(\mathbf{k})$  for each pair state can be expanded as a function of  $k_x$ ,  $k_y$ , and  $k_z$ , the wave-vector components along the principal axes in the Brillouin zone (Wenger and Östlund, 1993), using the basis functions listed in Table I. For example

$$\Delta_s(\mathbf{k}) = \Delta_s^o + \Delta_s^1(\cos k_x + \cos k_y) + \Delta_s^2 \cos k_z + \dots, \quad (8)$$

$$\Delta_g(\mathbf{k}) = \Delta_g^o(\sin 2k_x \sin k_y - \sin 2k_y \sin k_x) + \dots, \quad (9)$$

$$\Delta_{d_{x^2-y^2}}(\mathbf{k}) = \Delta_{d_{x^2-y^2}}^o(\cos k_x - \cos k_y) + \dots, \quad (10)$$

$$\Delta_{d_{xy}}(\mathbf{k}) = \Delta_{d_{xy}}^o(\sin k_x \sin k_y) + \dots, \quad (11)$$

$$\Delta_e(\mathbf{k}) = \Delta_e^o \sin k_z(\sin k_x \pm i \sin k_y) + \dots. \quad (12)$$

With the exception of the  $s$ -wave pair state, the order parameters have basis functions with node lines. However, the number and the location of the nodes at the Fermi-surface depends on the Fermi-surface topology, as well as the band filling of a given band structure (Chen *et al.*, 1993).

In addition to the pure states listed in Table I, the order parameter of various mixed pair states can be formed by combining a real subcomponent from one 1D representation with an imaginary subcomponent from another 1D representation. Following Wenger and Östlund (1993), the nodeless mixed pair states are

$$\Delta_s(\mathbf{k}) + i\Delta_g(\mathbf{k}), \quad (13)$$

$$\Delta_g(\mathbf{k}) + i\Delta_{d_{x^2-y^2}}(\mathbf{k}), \quad (14)$$

TABLE II. Spin-singlet even-parity pair states in an orthorhombic crystal (point group  $D_{2h}$ ).

Group-theoretic notations	Residual symmetry	Basis function	Nodes
$A_{1g}$	$D_{2h} \times T$	1	
$B_{1g}$	$D_2[C_2'] \times C_i \times T$	$xy$	line
$B_{2g}$	$D_2[C_2''] \times C_i \times T$	$xz$	line
$B_{3g}$	$D_2[C_2'''] \times C_i \times T$	$yz$	line

$$\Delta_s(\mathbf{k}) + i\Delta_{d_{xy}}(\mathbf{k}), \quad (15)$$

$$\Delta_{d_{x^2-y^2}}(\mathbf{k}) + i\Delta_{d_{xy}}(\mathbf{k}). \quad (16)$$

The mixed pair states with nodes are

$$\Delta_g(\mathbf{k}) + i\Delta_{d_{x^2-y^2}}(\mathbf{k}), \quad (17)$$

$$\Delta_g(\mathbf{k}) + i\Delta_{d_{xy}}(\mathbf{k}). \quad (18)$$

Time-reversal symmetry is broken in all these mixed states. It might be useful to reiterate that such states can only occur if the superconductivity is first order, or as a result of two successive phase transitions. This follows from the ideas of the Landau theory of second-order phase transitions stated earlier.

## 2. Orthorhombic crystal lattice

Cuprate superconductors such as  $\text{YBa}_2\text{Cu}_3\text{O}_{7-\delta}$  (YBCO) and  $\text{Bi}_2\text{Sr}_2\text{CaCu}_2\text{O}_8$  (Bi-2212) have an orthorhombic crystal structure with point-group symmetry  $D_{2h}$ . In the case of YBCO, the lattice distortion induced by the Cu-O chains results in inequivalent directions  $a$  and  $b$ . The orthorhombicity  $[(b-a)/(a+b)]$  of the YBCO structure has been experimentally established as about 2%. In the case of Bi-2212, an incommensurate superlattice modulation in the BiO layers, along the  $b$  direction, gives rise to unequal lattice constants  $a$  and  $b$  in the  $\text{CuO}_2$  planes. An important difference between the two crystal structures is that the in-plane Cu-O bonds coincide with the inequivalent  $a$  and  $b$  axes in YBCO, but not in Bi-2212. This has significant consequences on the symmetry of the order parameter in both superconductors (Sec. IV.C.5). The symmetry properties of the allowed spin-singlet even-parity pair states for a standard orthorhombic superconductor are tabulated in Table II (Annett *et al.*, 1990). Note that both the  $s$ - and  $d_{x^2-y^2}$ -wave pair states in the orthorhombic case belong to the same irreducible representation ( $A_{1g}$ ). Hence an admixture of these two states is allowed and only a single superconducting transition should be observed. This is apparently the case for YBCO.

## 3. Cu-O square/rectangular lattice

The cuprate superconductors, either tetragonal or orthorhombic, share one common structural ingredient, i.e., the  $\text{CuO}_2$  planes. In the tetragonal case, for example, in Hg-1201 or  $\text{Tl}_2\text{Ba}_2\text{CuO}_{6+\delta}$  (Tl-2201), the Cu and O atoms arrange themselves in a square lattice with point-group symmetry  $C_{4v}$  [Fig. 2(a)]. In the high- $T_c$  superconductors such as YBCO, the  $\text{CuO}_2$  plane takes the form of a Cu-O rectangular lattice<sup>8</sup> with the point-group symmetry  $C_{2v}$  [Fig. 2(b)]. The point group  $C_{4v}$  consists

<sup>8</sup>Structural subtleties such as the  $\text{CuO}_2$  plane buckling and  $\text{CuO}_5$  tilt are known to have an effect on  $T_c$  (Chmaissem *et al.*, 1999). However, we shall not consider the effect of these factors on pairing symmetry because they do not alter the basic crystal symmetry of the  $\text{CuO}_2$  planes.

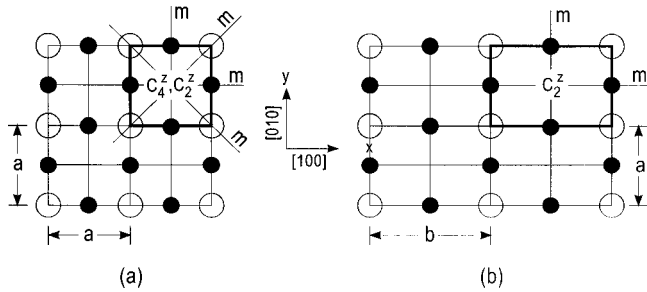


FIG. 2. A schematic of the  $\text{CuO}_2$  lattices: (a) square; (b) rectangular:  $\bullet$ , oxygen;  $\circ$  copper. The unit cells are underscored by heavy lines. Also shown are the symmetry operations of the point group for each lattice.

of the following symmetry elements: mirror reflections ( $m$ ) with respect to the lines  $x=0$ ,  $y=0$ , and  $x=\pm y$ ; a fourfold ( $C_4$ ) and a twofold ( $C_2$ ) rotation about the  $c$ -axis. The  $C_{2v}$  point group can be obtained by subtracting  $C_4$  and reflecting in the diagonals of the unit cell.

All cuprate superconductors are characterized by a relatively high ratio of  $c$ -axis to  $a$ -axis lattice constants,  $c/a$ , (3.0 for YBCO, 5.7 for Bi-2212, and 7.6 for Tl-2212). In the  $k$ -space presentation, these ratios of  $c/a$  translate into a flattened Brillouin zone possessing the basic symmetry properties of the unit cell of a square/rectangular lattice. Indeed, the results of band-structure calculations for various cuprates such as  $\text{YBa}_2\text{Cu}_3\text{O}_{7-\delta}$  (Krakauer *et al.*, 1988), Bi-2212 (Krakauer and Pickett, 1988), Tl-2201 (Hamann and Mattheiss, 1988), Hg-1201 (Singh, 1993a), and Hg-1223 (Singh, 1993b; Singh and Pickett, 1994) all show energy bands predominantly derived from the  $\text{CuO}_2$  planes, with no significant dispersion in the  $c$ -axis direction.

As measured from these band-structure calculations, the degree of two-dimensional characteristics increases with larger  $c/a$  ratio. For more details on band-structure calculations and comparison with experiments in cuprate superconductors, see Pickett (1989), Andersen *et al.* (1995), and Shen *et al.* (1995). The two-dimensional nature of the energy bands manifests itself in various normal-state and superconducting properties. For example, the room-temperature ratio of out-of-plane to in-plane resistivities ( $\rho_c/\rho_{ab}$ ) is about 30–100 for YBCO, and  $10^5$  for Bi-2212 (Poole *et al.*, 1995; Ong *et al.*, 1996). In the superconducting state, large anisotropy in the magnetic penetration depths ( $\lambda_{ab}/\lambda_c$ ) and the superconducting coherence length ( $\xi_{ab}/\xi_c$ ) is also observed (Jannossy *et al.*, 1990; Chien *et al.*, 1994). The observation of strong anisotropy in resistivity, penetration depth, and other physical properties does not necessarily determine whether the high- $T_c$  superconductors are truly two-dimensional or merely anisotropic three-dimensional electronic systems (Hussey *et al.*, 1996). However, investigations of  $c$ -axis charge dynamics and transport (Gray and Kim, 1993; Uchida *et al.*, 1994; Clarke *et al.*, 1995; Tajima *et al.*, 1997; Yurgens *et al.*, 1997, 1999; Kitano *et al.*, 1998) have provided strong evidence for charge confinement in the  $\text{CuO}_2$  layers. In-plane charge confinement blocks coherent interplane

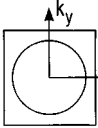
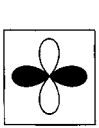
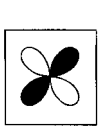
Group-theoretic notation	$A_{1g}$	$A_{2g}$	$B_{1g}$	$B_{2g}$
Order parameter basis function	constant	$xy(x^2-y^2)$	$x^2-y^2$	$xy$
Wave function name	s-wave	g	$d_{x^2-y^2}$	$d_{xy}$
Schematic representation of $\Delta(k)$ in B.Z.				

FIG. 3.  $k$ -space representation of allowed symmetry basis functions for the  $C_{4v}$  symmetry appropriate for the  $\text{CuO}_2$  planes in the high- $T_c$  superconductors.

charge transport, with important implications on the origin of high-temperature superconductivity (Anderson, 1997).

Furthermore, recent studies of interplane  $dc$  and  $ac$  intrinsic Josephson effects have convincingly shown that highly anisotropic high- $T_c$  superconductors such as Bi-2212 act as stacks of two-dimensional superconducting  $\text{CuO}_2$ -based layers coupled by Josephson interactions (Kleiner and Müller, 1994; Mros *et al.*, 1998). Similarly, it has been shown that the vortex state can be understood in terms of stacks of two-dimensional pancake vortices. The cores of these 2D vortices, localized in the  $\text{CuO}_2$  layers, are connected by Josephson vortices with cores confined in the nonsuperconducting charge-reservoir layers (Clem, 1998 and references therein; Drost *et al.*, 1999).

We conclude that superconductivity in cuprates basically originates from the  $\text{CuO}_2$  layers. Therefore pairing symmetry should reflect the symmetry of the underlying Cu-O square/rectangular lattices. We therefore concentrate our study of pairing symmetry on possible pair states in a square lattice. A schematic presentation in  $k$  space for these candidate states for point-group symmetry  $C_{4v}$  is shown in Fig. 3 where black and white represent opposite signs of the order parameter. Based on these pair states, the effects of orthorhombicity (point group  $C_{2v}$ ) and mixed pairing symmetries, including states with time-reversal symmetry breaking, will then be considered.

## II. NON-PHASE-SENSITIVE TECHNIQUES

There is now a preponderance of evidence from a number of non-phase-sensitive experimental techniques that pairing in the cuprates is highly anisotropic, with a line of nodes in the superconducting gap (Scalapino, 1995; Annett *et al.*, 1996):

### A. Penetration depth

In a superconductor in the local limit ( $\xi \ll \lambda$ , where  $\xi$  is the coherence length and  $\lambda$  is the penetration depth), the superfluid fraction can be expressed as  $x_s(T) = \lambda^2(0)/\lambda^2(T)$ . For conventional BCS superconductors,  $x_s$  saturates exponentially to 1 as  $T$  approaches zero. In

contrast,  $x_s(T)$  should approach unity linearly as  $T$  approaches zero for a superconductor with a line of nodes. The simple  $d_{x^2-y^2}$  pairing state (assuming tetragonal symmetry and ignoring dispersion in the  $c$ -axis direction) gives  $\Delta\lambda_{ab}(T)/\lambda_{ab}(0) \approx (\ln 2) \times (k_B T/\Delta_0)$ , where  $\Delta_0$  is the zero-temperature value of the  $d$ -wave gap amplitude. However, this depends sensitively on scattering. In the presence of scattering,  $\Delta\lambda_{ab}(T) \sim T^2$  as  $T \rightarrow 0$  (Annett *et al.*, 1991). Although sample quality was initially a problem, it is now generally agreed that in YBCO, the best-characterized high- $T_c$  material, the low-temperature penetration depth  $\Delta\lambda_{ab}$  is proportional to  $T$  for clean samples. Further, if impurities are added, the linear  $T$  dependence rolls over to a  $T^2$  dependence at low temperatures, as expected for a dirty  $d$ -wave superconductor (Hardy *et al.*, 1993; Bonn and Hardy, 1996; Kamal *et al.*, 1998). It has been predicted that the surface impedance of a  $d$ -wave superconductor should saturate at a fundamental minimum value at low temperatures, since there are always low-energy excitations available to it (Lee, 1993; Hirschfeld, Puttিকা, and Scalapino, 1993, 1994). Surface impedance measurements on YBCO, which can be fit well to a  $d$ -wave model (Hensen *et al.*, 1997), indicate that the quasiparticle lifetimes become very long in the superconducting state (Bonn *et al.*, 1992; Hosseini *et al.*, 1999), and the predicted fundamental limit has been below experimental sensitivity in all materials measured so far (Bonn and Hardy, 1996). Although these results are consistent with a pairing state with a line of nodes, they cannot distinguish between, for example,  $d$ -wave and extended  $s$ -wave symmetries. Further, it has been proposed that the linear dependence of  $\Delta\lambda_{ab}$  could also arise from proximity effects between alternating  $s$ -wave superconducting and normal layers in the cuprates (Atkinson and Carbotte, 1995; Klemm and Liu, 1995).

### B. Specific heat

The temperature dependence of the specific heat in the cuprates has a number of terms. An unconventional superconductor with a line of nodes is expected to have a zero-field density of states  $N(E) \sim |E - E_F|$ . This leads to a specific-heat term  $c_e = \alpha T^2 \approx \gamma_n T^2/T_c$ , where  $\gamma_n$  is the coefficient of the linear- $T$  term in the normal state. Thermodynamic calculations indicate that this  $T^2$  dependence extends over a very large temperature range in a spin-fluctuation model (Kruchinin and Patapis, 1997). Further, Volovik (1993) calculated that the dominant contribution to the magnetic-field dependence of the specific heat for a superconductor with a line of nodes comes from a Doppler shift of the quasiparticle excitations outside the vortex core. In the low-temperature limit,  $T/T_c \ll \sqrt{H/H_{c2}}$ , this term replaces the  $\alpha T^2$  term with a linear- $T$  term,  $c_{Volovik} = k\gamma_n T \sqrt{H/H_{c2}}$ , where  $k$  is a constant of order one. Moler *et al.* (1994) and Moler, Sisson, *et al.* (1997) measured the specific heat of twinned and untwinned single crystals of YBCO. They found that a global fit to  $C(T, H)$  gave a value for the coefficient  $\alpha$  of the  $T^2$  term

in reasonable agreement with expectation, and that the coefficient of the linear- $T$  term could be fit well with a  $H^{1/2}$  dependence, with a prefactor that was also in reasonable agreement with theory. These qualitative conclusions were confirmed on ceramic samples by Wright *et al.* (1999), who further found the expected crossover to a stronger temperature dependence at higher  $T$ . Revaz *et al.* (1998) showed that the anisotropic component of the field-dependent specific heat  $C(T, B\parallel c) - C(T, B\perp c)$  of single crystals of YBCO obeyed a scaling relation predicted for a superconductor with a line of nodes (Simon and Lee, 1997a, 1997b; Volovik, 1997). These results are all consistent with a line of nodes in the superconducting gap in optimally doped YBCO.

### C. Thermal conductivity

An interesting property of a  $d$ -wave gap in two dimensions is that quasiparticle transport should be independent of scattering rate as  $T \rightarrow 0$  (Lee, 1993; Graf *et al.*, 1996; Durst and Lee, 1999). The thermal conductivity of a  $d$ -wave superconductor should therefore not only be linear in temperature at low temperatures, but should also extrapolate to a universal value at zero temperature that is proportional to the ratio of the quasiparticle velocities normal and tangential to the Fermi surface at the nodes. The universal nature of this zero-temperature thermal conductivity has been demonstrated in YBCO (Taillefer *et al.*, 1997) and BSCCO (Bi-Sr-Ca-Cu-O; Chiao *et al.*, 2000). The absolute value for the zero-temperature extrapolated value has been shown to agree well with the prediction using Fermi-liquid theory and values for the quasiparticle velocities from angle-resolved photoemission measurements in BSCCO (Chiao *et al.*, 2000). Thermal conductivity of YBCO as a function of angle of an in-plane magnetic field relative to the crystal axes is consistent with predominantly  $d$ -wave symmetry, with less than 10%  $s$ -wave component (Aubin *et al.*, 1997).

### D. Angle-resolved photoemission

Angle-resolved photoemission spectroscopy (ARPES) has the advantage of directly investigating the momentum dependence of the gap. The development of this technique for studying pairing symmetry in the cuprates has been hampered by its sensitivity to surface conditions, and by its relatively poor energy resolution comparable to the size of the energy gap. Nevertheless, agreement has been reached that the gap in  $\text{Bi}_2\text{Sr}_2\text{CaCu}_2\text{O}_{8+x}$  (Bi-2212) is largest along the  $\Gamma$ - $M$  directions (parallel to  $a$  or  $b$ ) and smallest along  $\Gamma$ - $Y$  (the diagonal line between them) (Shen *et al.*, 1993; Ma *et al.*, 1995; Shen and Dessau, 1995; Ding, Norman, Campuzano, *et al.*, 1996), as expected for a  $d_{x^2-y^2}$  superconductor. Figure 4 shows a plot of the inferred absolute value of the energy gap as a function of angle on the Fermi surface (solid circles), in comparison with the prediction of a simple  $d$ -wave model (solid line). The agreement is remarkable. However, since ARPES is not

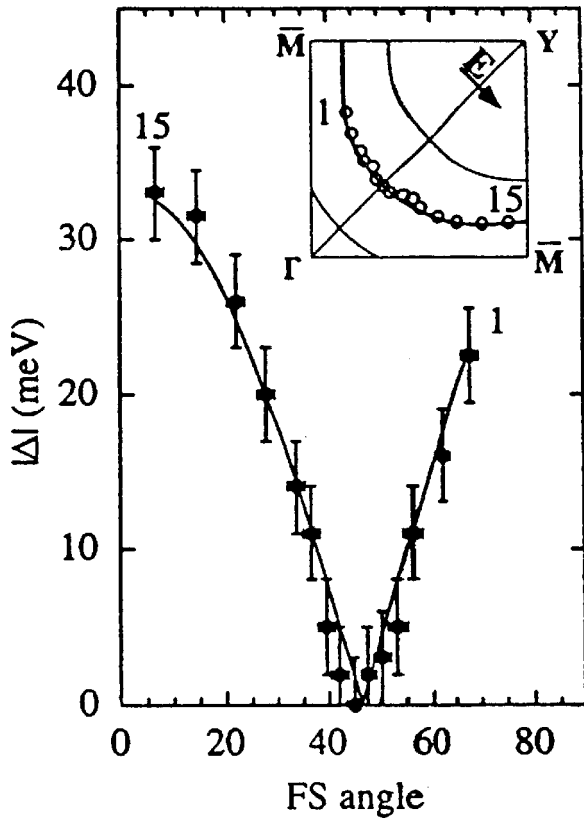


FIG. 4. Energy gap in Bi-2212: ●, measured with ARPES as a function of angle on the Fermi surface; solid curve, with fits to the data using a  $d$ -wave order parameter. Inset indicates the locations of the data points in the Brillouin zone. From Ding, Norman, *et al.* (1996).

phase sensitive, it cannot distinguish between  $d$ -wave and highly anisotropic  $s$ -wave pairing. Ma *et al.* (1995) have reported that the anisotropy in the gap between the  $\Gamma$ - $M$  and  $\Gamma$ - $Y$  directions is strongly temperature dependent, with a maximum anisotropy close to  $T_c$ , in disagreement with a simple  $d$ -wave picture. Liu and Klemm (1994) have cautioned that effects due to surface states in an  $s$ -wave superconductor could mimic a  $d$ -wave gap.

### E. Raman scattering

Raman scattering has the advantage that different symmetry channels of the electronic scattering spectra can be selected by choosing the polarization light vectors appropriately. Devereaux *et al.* (1994, 1995) observed that (1) in contrast to conventional superconductors, there is no well defined gap in the cuprates; (2) the  $B_{1g}$  channel, which transforms like  $x^2 - y^2$ , has a peak at higher energies than the other channels; and (3) the low-frequency ( $\omega$ ) spectrum is proportional to  $\omega^3$  for the  $B_{1g}$  channel, but  $\omega$  for the other channels. They calculated the electronic Raman response in a model with  $d_{x^2-y^2}$  pairing symmetry on a cylindrical Fermi surface, for  $A_{1g}$ ,  $B_{1g}$ , and  $B_{2g}$  polarizations (see Table I) and found good agreement with experiment for BSCCO, YBCO,

and Tl-2201. This view is apparently widely accepted, although Wenger and Käll (1997) found a discrepancy in the absolute intensities of the different symmetry channels using a tight-binding band-structure model, and Jiang and Carbotte (1996) emphasized the role of inelastic scattering. Since Raman scattering is not phase sensitive, it is difficult to distinguish  $d$ -wave symmetry from an anisotropic  $s$ -wave case (Jha, 1996). Strohm and Cardona (1997) proposed a Raman-scattering method to determine the  $s$  component in a  $d+s$  superconductor such as YBCO. Stadlober *et al.* (1995), using Raman scattering, found that the electron-doped cuprate NdCeCuO has an isotropic ( $s$ -wave) gap.

### F. Nuclear magnetic resonance

The advantage of nuclear-magnetic-resonance (NMR) measurements is that they can probe the electronic properties of individual atomic sites on the  $\text{CuO}_2$  sheets of the high-temperature superconductors. Of particular interest is the absence of a Hebel-Slichter peak, an increase in the nuclear relaxation rate  $T_1^{-1}$  near  $T_c$ , for both the Cu and O in-plane sites (see reviews by Pennington and Slichter, 1990; and Walstedt and Warren, 1990). Bulut and Scalapino (1992a, 1992b), using a  $d_{x^2-y^2}$  model with Coulomb correlations, explained this as arising from (a) the weaker quasiparticle density-of-states singularity at the gap edge (compared with an  $s$ -wave BCS gap), (b) the vanishing of the coherence factor for quasiparticle scattering for  $\mathbf{q} \sim (\pi, \pi)$  for a  $d_{x^2-y^2}$  gap, and (c) inelastic-scattering suppression of the peak, which is similar in effect for both  $d$ -wave and  $s$ -wave cases. They found that the temperature dependence of both the Knight shifts and  $T_1^{-1}$  was fit better by a  $d$ -wave than an  $s$ -wave model. Further, they found remarkable agreement between the anisotropy ratio  $(T_1^{-1})_{ab}/(T_1^{-1})_c$  and the transverse nuclear relaxation rate  $T_G^{-1}$  for  $^{63}\text{Cu}(2)$  (Bulut and Scalapino, 1991; Scalapino, 1995) and a  $d$ -wave model. An  $s$ -wave model did not agree with experiment for the last two properties.

### G. Nonlinear Meissner effect

The quasiparticles near the nodes of a  $d$ -wave superconductor give rise to an intrinsic nonlinear dynamic response. Yip and Sauls (1992) suggested that at sufficiently low temperatures this nonlinearity would lead to an increase in the penetration depth proportional to the magnitude of the applied field, with a coefficient that depended on the orientation of the field relative to the nodes. Bidinosti *et al.* (1999) found a linear variation of the penetration depth with field that agreed in magnitude with the prediction of Yip and Sauls (1992), but did not have the correct systematics with temperature and field orientation. Bhattacharya *et al.* (1999a) found no angular dependence to the transverse magnetic moment and concluded that this implied a minimum nonzero gap of at least 2–3 % of the maximum gap amplitude. However, Li *et al.* (1998) and Dahm and Scalapino (1999)

have argued that the linear field dependence can be washed out by impurities and that nonlocal effects will lead to a quadratic dependence on field below a crossover field that is of the same magnitude as  $H_{c1}$ , making the effect unobservable except for situations where the shielding currents flow along the nodes. There is disagreement on whether this crossover field is below (M.-R. Li *et al.*, 1999) or above (Bhattacharya, 1999b) the fields used for the transverse moment measurements. Dahm and Scalapino (1999), following a discussion of Xu, Yip, and Sauls (1995), have proposed that higher-order nonlinear effects may be less sensitive to impurity and nonlocal effects and suggested that they could be studied by harmonic generation or intermodulation effects.

### III. HALF-INTEGER FLUX-QUANTUM EFFECT

Although the symmetry tests outlined above provide evidence that the gap in YBCO and BSCCO is highly anisotropic with a line of nodes, they are both insensitive to the phase of the order parameter and model dependent, making for much controversy (Annett, *et al.*, 1990, 1996; Annett, 1991; Dynes, 1994; Schrieffer, 1994; Müller, 1995). However, recently a new class of phase-sensitive pairing symmetry tests have emerged. These tests are based on two macroscopic quantum coherence phenomena: Josephson tunneling and flux quantization.

#### A. Josephson tunneling

Josephson (1962) first pointed out that it is possible for Cooper pairs to flow through a thin insulating barrier between two superconductors. A schematic drawing of a Josephson tunnel junction is depicted in Fig. 5, showing the tunnel barrier sandwiched between two junction electrodes, with order parameters  $\Delta_i(\mathbf{k}_i) = |\Delta_i|e^{i\varphi_i}$ , where the subscript  $i=L,R$ . The supercurrent  $I_s$ , proportional to the tunneling rate of Cooper pairs through the barrier, was given by Josephson as

$$I_s = I_c \sin \gamma, \quad (19)$$

where  $I_c$  is the Josephson critical current, and  $\gamma$  is the gauge-invariant phase difference<sup>9</sup> at the junction:

$$\gamma = \varphi_L - \varphi_R + \frac{2\pi}{\Phi_0} \int_L^R \mathbf{A} \cdot d\mathbf{l}, \quad (20)$$

where  $\mathbf{A}$  is the vector potential, and  $d\mathbf{l}$  is the element of line integration from the left electrode ( $L$ ) to the right electrode ( $R$ ) across the barrier. The prediction of pair tunneling was almost immediately verified by experiment (Anderson and Rowell, 1963). There is a vast literature on Josephson tunneling and its phenomenology (Barone and Paterno, 1982). For the purpose of our discussion we use the tunneling Hamiltonian approach first

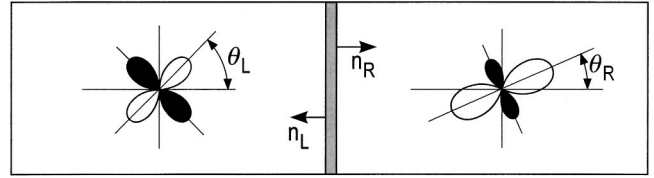


FIG. 5. Schematic diagram of a Josephson junction between a pure  $d_{x^2-y^2}$  superconductor on the left and a superconductor with some admixture of  $s$  in a predominantly  $d_{x^2-y^2}$  state on the right. The gap states are assumed to align with the crystal-line axes, which are rotated by angles  $\theta_L$  and  $\theta_R$  with respect to the junction normals  $\mathbf{n}_L$  and  $\mathbf{n}_R$  on the left- and right-hand sides, respectively.

introduced by Cohen *et al.* (1962). The supercurrent  $I_s$  at zero temperature is given by

$$I_s \propto \sum_{\mathbf{k}, \mathbf{l}} |T_{\mathbf{k}, \mathbf{l}}|^2 \frac{\Delta_L(\mathbf{k})\Delta_R(\mathbf{l})}{E_L(\mathbf{k})E_R(\mathbf{l})} \frac{1}{[E_L(\mathbf{k}) + E_R(\mathbf{l})]} \times \sin(\gamma_L - \gamma_R), \quad (21)$$

where  $T_{\mathbf{k}, \mathbf{l}}$  is the time-reversal-symmetry-invariant tunneling matrix element,  $E_i(\mathbf{k}) = \sqrt{\epsilon_i^2(\mathbf{k}) + \Delta_i^2(\mathbf{k})}$ , and  $\epsilon(\mathbf{k})$  is the one-electron energy. First, Eq. (21) can be used to determine the parity of the superconducting state in cuprates. Pals *et al.* (1977) showed quite generally that the Josephson current vanishes, up to second order in  $T_{\mathbf{k}, \mathbf{l}}$ , in tunnel junctions between spin-singlet (even parity) and -triplet (odd parity) superconductors. This remains true even with paramagnetic impurities in the tunnel barrier. The Josephson effect between triplet and singlet superconductors is nevertheless allowed if there is strong spin-orbit coupling. This is apparently not important in high- $T_c$  cuprate superconductors. Experimentally, pair tunneling exists for Josephson junctions made of a cuprate superconductor and a low- $T_c$  conventional superconductor such as Pb or Nb. Therefore the superconducting state in cuprates, just as in low- $T_c$  conventional superconductors, is that of even-parity spin-singlet pairing.

The Josephson effect also contains information about the magnitude and phase of the order parameters of the superconductors on both sides of the tunnel barrier [Eq. (21)]. In the simplest treatment (Ambegaokar and Baratoff, 1963),  $T_{\mathbf{k}, \mathbf{l}}$  is assumed to be independent of the wave vectors  $\mathbf{k}$  and  $\mathbf{l}$ , which implies an isotropic and uniform tunneling probability, and  $\Delta_{L,R}$  are assumed to be isotropic  $s$ -wave superconductors. The Josephson current as a function of temperature is then

$$I_c(T) = \frac{\pi\Delta(T)}{2eR_n} \tanh\left[\frac{\Delta(T)}{2k_B T}\right], \quad (22)$$

where  $R_n$  is the normal-state tunneling resistance, and  $\Delta_L(T) = \Delta_R(T) = \Delta(T)$  is assumed. Near  $T_c$ , Eq. (22) becomes  $I_c(T) = \pi\Delta^2(T)/4ek_B T_c R_n$  and is proportional to  $1 - T/T_c$  in BCS theory. The Ambegaokar-Baratoff formula [Eq. (22)] for the temperature dependence of  $I_c$  has been confirmed by numerous experiments with low-

<sup>9</sup>See Tinkham (1996), p. 193, for a discussion of the gauge-invariant phase difference in a Josephson junction.

$T_c$   $s$ -wave superconductors (e.g., Fiske, 1964).<sup>10</sup> The magnitude of  $I_c$  obtained in experiments is almost always smaller than that predicted by Eq. (22). Nevertheless, the  $I_c R_n$  product based on Eq. (22) represents an upper bound of junction quality, hence the term Ambegaokar-Baratoff limit.

The concept of Josephson tunneling is not just limited to superconductor-insulator-superconductor ( $SIS$ ) junctions, but has been generalized to all weak-link structures consisting of two superconductors (not necessarily identical) coupled by a small region of depressed order parameter (Likharev, 1979; Tinkham, 1996). Josephson weak links include  $SIS$ ,  $SNS$ , and  $SCS$ , where  $N$  and  $C$  stand for normal metal and constriction, respectively. The weak-link of the junction can be made of two parts as, for example, in  $SINS$  junctions.

In the case of unconventional superconductors with  $d$ -wave pairing symmetry, a wave-vector-independent tunneling matrix would lead to  $I_s \equiv 0$ . There have been several theoretical studies of Josephson tunneling in junctions of  $d$ -wave superconductors (Barash *et al.*, 1995; Bruder *et al.*, 1995; Millis *et al.*, 1988) taking into account the direction dependence of the tunneling matrix element. These studies reveal junction characteristics, in both the supercurrent and quasiparticle tunneling branches, that are different from  $s$ -wave. To use these results to discriminate  $d$ -wave from  $s$ -wave symmetry requires specific knowledge of the sample conditions. For example, the supercurrent  $I_s$  varies near  $T_c$  as  $1 - T/T_c$  or  $(1 - T/T_c)^2$ , depending on the spatial distribution of the order parameter near the tunnel barrier (Barash *et al.*, 1995). However, the  $1 - T/T_c$  dependence is the same as for an  $s$ -wave tunnel junction (Ambegaokar and Baratoff, 1963). Furthermore, all the theoretical studies discussed here implicitly assume that the junction interface is smooth and uniform—a condition that is far from reality. All these make quantitative comparison between theory and experiment for testing pairing symmetry practically impossible.

The phase-sensitive tests described below probe sign changes in the pair critical currents  $I_c$ , not their magnitudes, avoiding this difficulty. Making use of the directional dependence of the pair wave function, sign changes in  $I_c$  can be systematically examined, providing a powerful tool for studying the internal symmetry of Cooper pairs. Sign changes in  $I_c$  due to pairing symmetry are arbitrary for a particular junction, since an arbitrary phase can always be added to either side of the junction. However, the signs of the critical currents in a closed ring of superconductors interrupted by Josephson weak links can always be assigned self-consistently. Counting these sign changes provides a convenient way to determine if a particular geometry is frustrated. For the purposes of this review, a frustrated geometry is one that, in the absence of an externally applied field, has a local maximum in its free energy with zero circulating supercurrent [see, for example, Eq. (36)]. A negative

pair-tunneling critical current  $I_c$  can be thought of (for counting purposes) as a phase shift of  $\pi$  at the junction interface [ $I_s = -|I_c| \sin \gamma = |I_c| \sin(\gamma + \pi)$ ].<sup>11</sup> Such  $\pi$  phase shifts were theoretically predicted between Josephson junctions involving unconventional superconductors such as heavy-fermion superconducting systems (Geshkenbein and Larkin, 1986; Geshkenbein *et al.*, 1987) and cuprate superconductors (Sigrist and Rice, 1992). In addition, it has been suggested that a  $\pi$  phase shift can be realized within a junction by mechanisms unrelated to pairing symmetry such as spin-flip scattering by magnetic impurities (Bulaevskii *et al.*, 1977) or indirect electron tunneling (Spivak and Kivelson, 1991). This second type of phase shift has never been observed experimentally. Historically, the term  $\pi$  junction has been used to describe both the situation in which phase shifts within the superconductor are caused by pairing symmetry, and the situation in which phase shifts within a single Josephson junction are caused by the tunneling mechanism. We shall restrict our use of the term  $\pi$  junction to the latter. However, a superconducting ring with an odd number of  $\pi$  shifts is frustrated, and will show the special effects described below, independent of whether the  $\pi$  shifts result from symmetry or tunneling mechanism effects. Such frustrated rings will be referred to as  $\pi$  rings, independent of the mechanism for the  $\pi$  phase shifts.

For the present purpose, we use the Ginzburg-Landau formalism (Geshkenbein and Larkin, 1986; Yip *et al.*, 1990; Walker and Luettmmer-Strathmann, 1996a). For more details and early work, see reviews by Annett (1991) and Sigrist and Ueda (1991). This approach assumes that the order parameter is small enough (as happens close to  $T_c$ ) to expand the free energy of the Josephson junction as a power series in the order parameter. This is not expected to be a problem, as discussed in the Introduction. Since we are merely interested in the sign of the critical current in the phase-sensitive experiments, the experimental outcome will not be compromised unless there is a second phase transition below  $T_c$ .

In a tetragonal cuprate superconductor with  $C_{4v}$  point-group symmetry, the candidate pair states correspond to one-dimensional irreducible representations:  $A_{1g}$  ( $s$  wave),  $A_{2g}$  ( $g$  wave),  $B_{1g}$  ( $d_{x^2-y^2}$  wave), and  $B_{2g}(d_{xy})$  [i.e.,  $l_j=1$  in Eq. (7); see Fig. 3]. The Ginzburg-Landau free-energy functionals for the junction electrodes on both sides of the tunnel barrier are of the same general form. Hence qualitatively similar thermodynamic properties, regardless of the electrodes' pairing symmetry and its directional dependence, are to

<sup>10</sup>See, however, Overhauser (1999).

<sup>11</sup>This assumes the supercurrent-phase relation is sinusoidal. The possibility of a nonsinusoidal current-phase relationship in the high- $T_c$  superconductors has been studied theoretically (Yip, 1995; Agassi and Cullen, 1996). Recently, there have been a number of experimental studies on this topic in conjunction with high- $T_c$  Josephson junctions (Il'ichev *et al.*, 1998, 1999a, 1999b).

TABLE III. Basis functions  $\chi(\mathbf{n})$  for a Josephson-junction electrode with tetragonal crystal symmetry.

Irreducible representation	$A_{1g}$ $s$	$A_{2g}$ $g$	$B_{1g}$ $d_{x^2-y^2}$	$B_{2g}$ $d_{xy}$
Basis function $\chi(\mathbf{n})$	1	$n_x n_y (n_x^2 - n_y^2)$	$n_x^2 - n_y^2$	$n_x n_y$

be expected. It is the coupling term in the total free energy that contains information about the order-parameter symmetry of the junction.

The free energy per unit area of Josephson coupling between two superconducting electrodes with order parameters  $\psi_L$  and  $\psi_R$  (see Fig. 5) can be described as (see Walker and Luettmmer-Strathmann, 1996a, for example)

$$F_J = W \int ds [\psi_L \psi_R^* e^{i(2\pi/\Phi_0) \int_{LA}^R d\mathbf{l} \cdot \mathbf{A}} + \text{c.c.}], \quad (23)$$

where  $W$  is a measure of the Josephson coupling strength, and the integral is over the junction interface. The exponential multiplier ensures that the Josephson interaction energy  $F_J$  is gauge invariant, as it should be for any observable physical quantity. As required by global gauge invariance,  $F_J$  must be expanded in integral powers of  $\psi_L \psi_R^*$  and its complex conjugates. Thus Eq. (23) represents the lowest-order term in the expansion (Yip *et al.*, 1990). By minimizing the total free energy with respect to  $\psi_L$  and  $\psi_R$ , the Josephson current density  $J_s$ , flowing perpendicular to the junction interface from superconductor  $L$  to  $R$ , is given by (Sigrist and Rice, 1995)

$$J_s = t_{L,R} \chi_L(\mathbf{n}) \chi_R(\mathbf{n}) |\eta_L| |\eta_R| \sin \gamma = J_c \sin \gamma, \quad (24)$$

where  $J_c$  is the critical current density,  $\chi_{L,R}$ , the basis function, is related to the gap function  $\Delta(\mathbf{k})$  through Eq. (7),  $\Delta_{L,R}(\mathbf{n}) = \eta_{L,R}(\mathbf{n}) \chi_{L,R}(\mathbf{n})$ ,  $\mathbf{n}$  is the unit vector normal to the junction interface,  $\eta_{L,R}(\mathbf{n}) = |\eta_{L,R}| e^{i\varphi_{L,R}}$ , and  $\gamma$  is the gauge-invariant phase difference as defined in Eq. (20). The quantity  $t_{L,R}$  is a constant characteristic of a given junction configuration and is closely related to the tunneling matrix element in Eq. (21). The basis functions  $\chi(\mathbf{n})$  for a Josephson-junction electrode with tetragonal crystal symmetry (point group  $C_{4v}$ ), are listed in Table III, where  $n_x, n_y$  are the projections of the unit vector  $\mathbf{n}$  onto the crystallographic axes  $\mathbf{x}$  and  $\mathbf{y}$ , respectively.

Both the sign and the magnitude of the critical current  $I_c$  of a Josephson junction made with at least one non- $s$ -wave superconductor depend sensitively on the gap function symmetry and the relative orientation of the junction electrodes [Eq. (24) and Table III]. It is the directional dependence of the sign changes in the  $I_c$ 's that has been used for phase-sensitive tests of pairing symmetry.

More specifically, for Josephson junctions between two  $d$ -wave superconductors  $\chi(\mathbf{n}) = n_x^2 - n_y^2$ , Eq. (24) reduces to the well-known Sigrist and Rice (1992) formula

$$J_s = A_s (n_x^2 - n_y^2)_L (n_x^2 - n_y^2)_R \sin \gamma \quad (25)$$

or, in terms of  $\theta_L, \theta_R$ , the angles of the crystallographic axes with respect to the interface

$$J_s = A_s \cos(2\theta_L) \cos(2\theta_R) \sin \gamma, \quad (\text{clean}), \quad (26)$$

where  $A_s$  is a constant characteristic of the junction. It should be emphasized that, in the derivation of the Sigrist-Rice formula, it is implicitly assumed that the junction interface is uniform and smooth. Furthermore, if the tunnel barrier is relatively thick compared to the BCS coherence length,  $\xi \sim 15 \text{ \AA}$ , only the pair-tunneling process perpendicular to the junction interface needs to be considered. In real Josephson junctions, especially those made with cuprates, the electron wave vector normal to the junction interface can be significantly distorted by interface roughness, oxygen deficiency, strain, etc. In particular, it is established experimentally that cuprate grain-boundary junctions have inhomogeneous and meandering junction interfaces that depend on the fabrication conditions (Moeckly *et al.*, 1993, 1994; Antognazza *et al.*, 1995; D. J. Miller *et al.*, 1995; Tafuri *et al.*, 1999). In the opposite limit, a maximum-disorder formula for the Josephson current can be derived (Tsuei *et al.*, 1994) by allowing a broad distribution of angular deviations at the tunnel barrier and taking into account the fact that, due to the fourfold symmetry of  $\text{CuO}_2$  planes, the maximum angle of deviation is  $\pi/4$ :

$$J_s = A_s \cos 2(\theta_L + \theta_R) \sin \gamma, \quad (\text{dirty}). \quad (27)$$

The fact that Eq. (27) is significantly different from Eq. (26) underscores the importance of considering the effects of disorder at the junction interface in using Josephson tunneling for a determination of pairing symmetry. It is also clear that a series expansion of trigonometric functions of  $\theta_{L,R}$  is needed for a general description of the angular dependence of the Josephson current. Such an expression was obtained by Walker and Luettmmer-Strathmann (1996a) by writing the Ginzburg-Landau free energy of Josephson coupling in the form

$$F_J = C(\theta_L, \theta_R) \cos \gamma \quad (28)$$

and by imposing the symmetry requirements for the tetragonal lattice:  $C(\theta_L, \theta_R) = C(\theta_R, \theta_L) = C(-\theta_L, -\theta_R) = C(\theta_L + \pi, \theta_R)$ ; and  $C(\theta_L + \pi/2, \theta_R) = C(\theta_L, \theta_R)$  for  $s$ -wave pairing symmetry,  $C(\theta_L + \pi/2, \theta_R) = -C(\theta_L, \theta_R)$  for  $d$ -wave superconductivity. With these symmetry constraints, a general expression for the supercurrent for a junction between two generalized  $s$ -wave superconductors can be given as

$$J_s^s = \sum_{n,n'} [C_{4n,4n'} \cos(4n\theta_L) \cos(4n'\theta_R) + S_{4n,4n'} \sin(4n\theta_L) \sin(4n'\theta_R)] \sin \gamma, \quad (29)$$

where  $n, n'$  are positive integers including zero. Alternately, Eq. (29) can be rewritten as

$$J_s^s = \{C_{0,0} + C_{4,0} [\cos(4\theta_L) + \cos(4\theta_R)] + \dots\} \sin \gamma. \quad (30)$$

For a Josephson junction between  $d$ -wave superconductors,

$$J_s^d = \{C_{4n+2,4n'+2} \cos[(4n+2)\theta_L] \cos[(4n'+2)\theta_R] + S_{4n+2,4n'+2} \sin[(4n+2)\theta_L] \sin[(4n'+2)\theta_R]\} \times \sin \gamma, \quad (31)$$

which can be rewritten as

$$J_s^d = \{C_{2,2} \cos(2\theta_L) \cos(2\theta_R) + S_{2,2} \sin(2\theta_L) \sin(2\theta_R) + \dots\} \sin \gamma. \quad (32)$$

It is interesting to note that, in Eq. (32), the first term is just the Sigrist-Rice clean-limit formula [Eq. (26)]. If  $S_{2,2} = -C_{2,2}$ , the sum of the first two terms leads to the dirty-limit formula [Eq. (27)].

## B. Flux quantization in a superconducting ring

The most striking effect associated with sign changes in the critical current, suggested by Bulaevskii *et al.* (1977), Geshkenbein and Larkin (1986), and Sigrist and Rice (1992), is that a superconducting ring containing an odd number of  $\pi$  shifts will (under certain conditions) spontaneously generate a magnetic field with half of the conventional flux quantization.<sup>12</sup>

The flux quantization of a superconducting ring with self-inductance  $L$  can be expressed (based on the fundamental requirement of single-valuedness of the macroscopic pair wave function) by

$$\Phi_a + I_s L + \frac{\Phi_o}{2\pi} \sum_{ij} \gamma_{ij} = n \Phi_o. \quad (33)$$

The supercurrent circulating in the ring is given by

$$I_s = I_c^{ij}(\theta_i, \theta_j) \sin \gamma_{ij}, \quad (34)$$

where  $I_c^{ij}(\theta_i, \theta_j)$  is the critical current of the junction between superconducting electrodes  $i$  and  $j$ , and  $\theta_i$  and  $\theta_j$  are the corresponding angles of the crystallographic axes with respect to the junction interface. The gauge-invariant phase difference across the junction  $\gamma_{ij}$  is defined as before [Eq. (20)]. Flux quantization of a multiply connected superconductor represents one of the most fundamental demonstrations of macroscopic phase coherence (i.e., off-diagonal long-range order) in the superconducting state (Yang, 1962). The condition of flux quantization as expressed by Eq. (33) is robust and valid for a superconducting ring with any pairing symmetry. For a ring with an odd number of sign changes in the circulating supercurrent  $I_s$ , it is sufficient to consider the case in which only one critical current is negative (say,  $I_c^{12} = -|I_c^{12}|$ ). Then  $I_s = |I_c^{12}| \sin(\gamma_{12} + \pi)$ . In the absence of an external field,  $\Phi_a = 0$ ,  $n = 0$  for the ground state, the combined conditions of Eqs. (33) and (34) lead to (Tsuei *et al.*, 1994)

<sup>12</sup>Volovik and Mineev (1976), in a discussion of vortices in He<sub>3</sub>, pointed out that an unconventional order parameter can lead to a vortex quantization with half of the conventional magnitude.

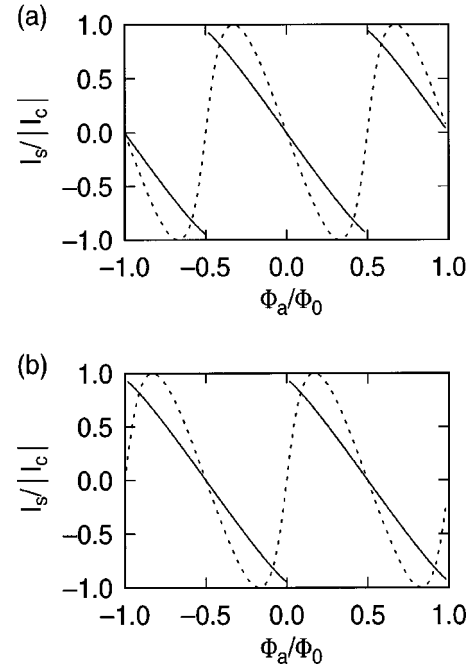


FIG. 6. Minimum-energy solution of Eq. (36) for  $I_s = (\Phi - \Phi_a)/L$  as a function of the externally applied flux  $\Phi_a/\Phi_0$ : (a) for a zero ring; (b) for a  $\pi$  ring. Dashed line,  $\gamma = 2\pi L I_c/\Phi_0 = 0.5$ ; solid line,  $\gamma = 2.0$ . For small applied fields and  $\gamma < 1$ , the shielding currents oppose the applied flux for the zero ring (diamagnetic shielding) and are aligned with the applied flux for the  $\pi$  ring (paramagnetic shielding). For  $\gamma > 1$ , the  $\pi$  ring has spontaneous magnetization with the same sign as small externally applied fields.

$$I_s = \frac{\pi}{2\pi \left( \frac{L}{\Phi_0} \right) + \frac{1}{|I_c^{12}|} + \frac{1}{I_c^{23}} + \dots} \approx \frac{\Phi_0}{2L}, \quad (35)$$

provided that  $|I_c^{12}|L \gg \Phi_0, \dots, |I_c^{ij}|L \gg \Phi_0$ . The ground state of a superconducting ring containing an odd number of sign changes ( $\pi$  ring) has a spontaneous magnetization of a half magnetic-flux quantum (i.e.,  $I_s L \approx (1/2)\Phi_0$ ) when the external field is zero. If the ring contains an even number of  $\pi$  shifts, including no  $\pi$  shifts at all (zero ring),  $I_s = 0$  in the ground state, and the magnetic-flux state has the standard integral flux quantization.

Alternately, the magnetic flux  $\Phi$  through a ring with one Josephson junction can be studied by considering the free energy:

$$U(\Phi, \Phi_a) = \frac{\Phi_0^2}{2L} \left\{ \left( \frac{\Phi - \Phi_a}{\Phi_0} \right)^2 - \left( \frac{L|I_c|}{\pi\Phi_0} \right) \times \cos \left( \frac{2\pi}{\Phi_0} \Phi + \varphi \right) \right\}, \quad (36)$$

where  $\varphi = 0, \pi$  for a zero ring and a  $\pi$  ring, respectively.

The ground state of the single-junction ring can be obtained by minimizing  $U(\Phi, \Phi_a)$  to obtain  $\Phi$  as a function of  $\Phi_a$  (Sigrist and Rice, 1992; Fig. 6). Plots of the free energy vs  $\Phi$  at  $\Phi_a = 0$  (Fig. 7) show that the zero ring has a ladder of metastable states centered at the

ground state  $\Phi=0$ , while the  $\pi$  ring has a ladder of states shifted by  $\Phi_0/2$  from those of the 0 state, centered on a doubly degenerate ground state with (in the limit  $|I_c|L \gg \Phi_0$ )  $\pm \Phi_0/2$  spontaneous magnetization.

In short, in the limit  $|I_c|L \gg \Phi_0$ ,

$$\Phi = n\Phi_0 \quad \text{for } N \text{ even (0 ring)} \quad (37)$$

and

$$\Phi = \left(n + \frac{1}{2}\right)\Phi_0 \quad \text{for } N \text{ odd } (\pi \text{ ring}), \quad (38)$$

where  $N$  is an integer. The last, *half-integer flux-quantum effect*,<sup>13</sup> is in striking contrast to the *integer flux-quantum effect* observed by Gough *et al.* (1987).

### C. Paramagnetic Meissner effect

Conventional superconductors generally tend to expel a small external magnetic field upon cooling into the superconducting state. This ‘‘Meissner effect’’ leads to complete or (due to remnant trapped flux, e.g., in ceramic samples composed of grains and voids) partial diamagnetism. Therefore it came as a surprise when a paramagnetic signal was observed in ceramic  $\text{Bi}_2\text{Sr}_2\text{CaCu}_2\text{O}_8$  (Svedlindh *et al.*, 1989; Braunisch *et al.*, 1992, 1993; Heinzel, 1993; Niskanen, 1994; Shrivastava, 1994). The origin of this effect has been controversial. Braunisch *et al.* (1992, 1993) and Kusmartsev (1992) proposed that some form of spontaneous orbital currents was responsible, giving rise to magnetic moments that could be aligned by the magnetic field. This proposal for spontaneous orbital currents (the Wohleben effect) in turn led Sigrist and Rice (1992, 1995) to propose that an intrinsic  $d_{x^2-y^2}$  symmetry of the superconducting state would naturally lead to frustrated Josephson-junction circuits ( $\pi$  rings) in a ceramic sample where randomly oriented grains contact each other. The origin of this explanation for paramagnetic shielding can be understood from Fig. 6: if  $2\pi LI_c/\Phi_0 < 1$ , a zero ring has an induced flux with the

<sup>13</sup>Spontaneous magnetization upon entering the superconducting state was historically the first-discussed aspect (Bulaevski *et al.*, 1977), and is arguably the most striking aspect of the physics of superconducting samples in a frustrated geometry. For the sake of simplicity, we have confined the above discussion to a ring geometry. In this geometry the spontaneous magnetization for a frustrated ring can be less than  $\Phi_0/2$  if  $LI_c$  is comparable to  $\Phi_0$  or if there is broken time-reversal symmetry. However, to date, symmetry tests on the widest variety of the cuprates (Table IV) have been performed in a blanket film geometry (Sec. IV.C.4). In this geometry, the total magnetic field spontaneously generated in the sample must be *exactly*  $\Phi_0/2$  for a frustrated sample, in the absence of broken time-reversal symmetry, independent of the strength of the Josephson coupling across the grain boundaries. Further, to date there is no evidence for broken time-reversal symmetry from tricrystal or thin-film SQUID magnetometry experiments in any of the cuprates, at any temperature (Sec. IV.E.3). Therefore we use the term ‘‘half-integer flux-quantum effect’’ generically in this review.

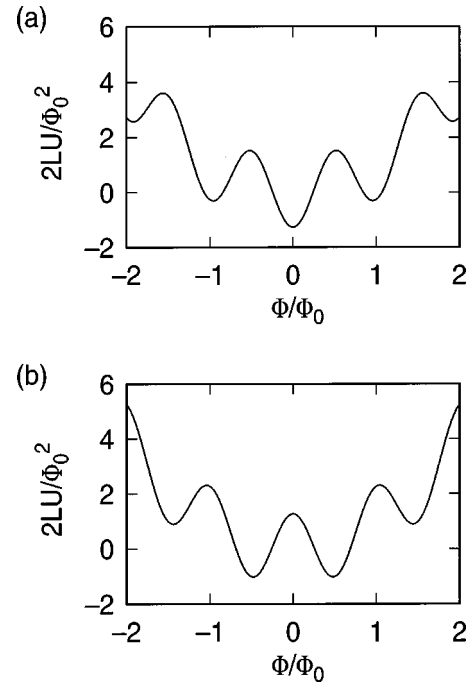


FIG. 7. Free energy of a superconducting ring with a single junction in different configurations, with zero external applied field [Eq. (36)]: (a) zero ring; (b)  $\pi$  ring. Here  $\gamma = 2\pi LI_c/\Phi_0 = 5$ .

opposite sign to the applied flux for small applied fields (diamagnetic shielding), but a  $\pi$  ring has an induced flux with the same sign as the applied flux (paramagnetic shielding). Further, if  $2\pi LI_c/\Phi_0 > 1$ , then the  $\pi$  ring exhibits spontaneous magnetization that is larger than the applied flux for small applied fields. The paramagnetic shielding in these samples has been associated with anomalies in other properties (Khomskii, 1994; Sigrist and Rice, 1995), including microwave absorption (Braunisch *et al.*, 1992; Knauf, 1998), second harmonics in the magnetic susceptibility (Heinzel *et al.*, 1993), and noise in the magnetization (Magnusson *et al.*, 1997), which can also be understood in terms of the magnetic properties of superconducting  $\pi$  rings (Khomskii, 1994; Sigrist and Rice, 1995).

However, paramagnetic shielding has also been observed in bulk Nb (Thompson *et al.*, 1995; Kostić *et al.*, 1996; Pöst *et al.*, 1998) and Al disks (Geim *et al.*, 1998). Both are presumably conventional  $s$ -wave superconductors. This has been taken as evidence against the interpretation of the Wohleben effect in terms of intrinsic superconducting  $\pi$  rings (Kostić *et al.*, 1996; Geim *et al.*, 1998). For large Nb disks it has been suggested that, due to sample inhomogeneity, during the cooling process the surface region nucleates superconductivity before the bulk, so that magnetic flux in the sample is compressed and creates an enhanced magnetization (Koshelev and Larkin, 1995; Obhukov, 1998). For small disks, flux captured at the third (surface) critical field inside the superconducting sheath compresses into a smaller volume, allowing extra flux to penetrate at the surface (Moschalkov *et al.*, 1997; Geim *et al.*, 1998). A small

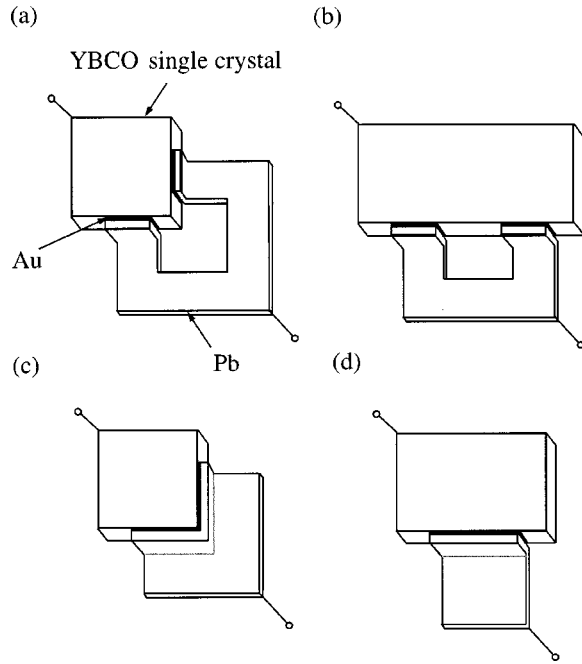


FIG. 8. Experimental geometry used for the experiments of Wollman *et al.* (1993, 1995): (a) corner SQUID configuration; (b) edge SQUID configuration; (c) corner junction; and (d) edge junction.

paramagnetic contribution to the total shielding has also been observed in Nb Josephson-junction arrays, and modeled using a conventional resistively shunted junction model (Barbara *et al.*, 1999).

Sigrist and Rice (1997) argued that the paramagnetic Meissner effects observed in conventional superconductors are qualitatively different from those in granular BSCCO, both in terms of the size of the effect, which is much larger in granular BSCCO, and in terms of its time dependence, which is metastable in Al disks (Geim *et al.*, 1998) and Nb films (Terentiev *et al.*, 1999), but not in BSCCO granular samples. Scanning SQUID microscope images of the magnetic-flux distribution in a granular BSCCO sample exhibiting a large Wohleben effect showed a large polarization of the distribution of the magnetic fluxes at zero externally applied field, indicating that spontaneous magnetization, as opposed to flux-focusing effects, are indeed responsible for the paramagnetic signal (Kirtley, Mota, *et al.*, 1998).

The origin of the paramagnetic Meissner effect in granular BSCCO samples is now of reduced interest, at least in terms of a test of the pairing symmetry of the cuprate superconductors, since such tests are now routinely performed in controlled geometries. Nevertheless, it appears that the debate over this very interesting effect will continue for some time.

#### IV. PHASE-SENSITIVE TESTS OF PAIRING SYMMETRY

A number of phase-sensitive experimental techniques have been developed in recent years to determine the symmetry of the pair state in cuprate superconductors (for early reviews see Scalapino, 1995; Van Harlingen,

1995; Annett *et al.*, 1996). A common feature of these symmetry experiments is that instead of relying on the quantitative magnitude of the Josephson current, they seek a qualitative signature of unconventional superconductivity: sign changes in the Josephson critical current  $I_c$ .

##### A. SQUID interferometry

Wollman *et al.* (1993) did the first phase-sensitive test of pairing symmetry in a controlled geometry, based on quantum interference effects in a YBCO-Pb dc SQUID. In the “corner SQUID” geometry,<sup>14</sup> Fig. 8(a), Josephson weak links were made between Pb thin films and two orthogonally oriented  $ac$ - (or  $bc$ -) plane faces of single crystals of YBCO. If YBCO is a  $d$ -wave superconductor, there should be a  $\pi$  phase shift between weak links<sup>15</sup> on adjacent faces of the crystal. Wollman *et al.* (1993) tested for this phase shift by measuring the SQUID critical current as a function of  $\Phi_a$ , the externally applied magnetic flux through the SQUID. The critical current of the SQUID is the maximum of

$$I_s = I_a \sin \gamma_a + I_b \sin \gamma_b, \quad (39)$$

where  $I_a$  ( $I_b$ ) and  $\gamma_a$  ( $\gamma_b$ ) are the critical currents and phases of the  $a$  ( $b$ ) junctions, respectively. This maximum must be calculated subject to the constraint that the phase be single valued [Eq. (33)]:

$$2\pi n = \gamma_a - \gamma_b + \varphi + 2\pi \left( \frac{I_a L_a}{\Phi_0} - \frac{I_b L_b}{\Phi_0} + \frac{\Phi_a}{\Phi_0} \right), \quad (40)$$

where  $L_a$  and  $L_b$  are the effective self-inductances of the two arms of the ring, and  $\varphi = 0$  or  $\pi$  for a zero ring or a  $\pi$  ring, respectively. This results in a roughly sinusoidal dependence of  $I_c$  on  $\Phi_a$ . If the self-inductances are small, or if the self-inductances and the junction critical currents are symmetric, then  $I_c$  has a maximum at  $\Phi_a = 0$  for a zero ring, but minimum at  $\Phi_a = 0$  for a  $\pi$  ring. In the experiments of Wollman *et al.* (1993), the junction  $I_c$ 's and  $L$ 's were not necessarily balanced, leading to shifts in the  $I_c$  vs  $\Phi_a$  characteristics. This effect was corrected for by measurements at several values of the dc applied current through the SQUID. This was possible because of noise rounding of the current-voltage characteristics of these SQUID's. The phase shift was then plotted as a function of dc current through the SQUID,

<sup>14</sup>This experimental geometry was suggested independently by Sigrist and Rice (1992).

<sup>15</sup>The weak links of Wollman *et al.* (1993) were nominally of the SNS type, since they had no intentional insulating layer. However, their current densities were three orders of magnitude smaller than, for example, typical Pb-Cu-Pb superconducting-normal-superconducting junctions (Clarke, 1966). They were therefore probably more like tunnel contacts. Annett *et al.* (1996) have argued that it is plausible that the pair transfer matrix  $T_{k,1}$  [Eq. (21)] is strongly peaked in the forward direction for both SNS and tunneling weak links, making the Sigrist-Rice clean relation [Eq. (26)] applicable.

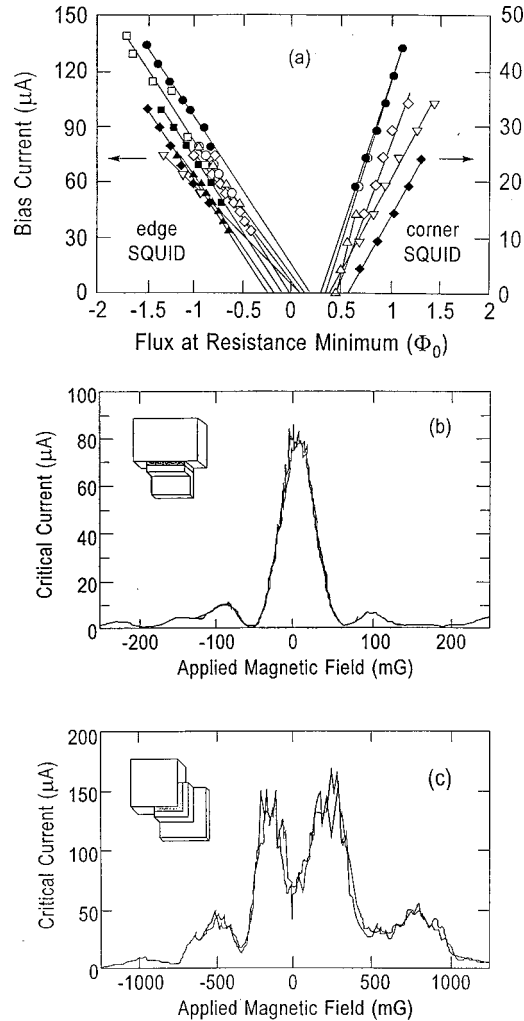


FIG. 9. Summary of the experimental results of Wollman *et al.* (1993, 1995): (a) Extrapolation of the measured SQUID resistance minimum vs flux to zero-bias current for a corner SQUID and an edge SQUID on the same crystal. Each curve represents a different cooldown of the sample; (b) Measured critical current vs applied magnetic field for an “edge” junction and (c) for a “corner” junction.

and then extrapolated to zero current to infer the intrinsic phase shift. These experiments were then repeated with “edge SQUID’s,” Fig. 8(b), with two junctions on the same  $ac$  (or  $bc$ ) face of the crystal. Wollman *et al.* (1993) found that the intercepts for the “corner SQUID’s” varied from  $0.3$  to  $0.6\Phi_0$ , while those for the “edge SQUID’s” centered around zero [Fig. 9(a)].

The SQUID experiments of Wollman *et al.* (1993) had a number of complicating factors in their interpretation. First, there was the question of twinning effects. Since YBCO has an orthorhombic crystal structure, it might be expected that the lobe of the presumed  $d_{x^2-y^2}$  symmetry pairing function with one sign is associated with a particular crystalline direction. Since YBCO crystals normally grow heavily twinned, this would mean that any face of the crystal not intersecting with the  $c$  axis would have both  $a$  and  $b$  crystalline directions normal to it, and therefore an admixture of positive and negative phases. This would tend to randomize the phases that

these experiments depend on. The fact that these experiments on highly twinned crystals, the IBM experiments (Tsuei *et al.*, 1994), and Maryland experiments (Mathai *et al.*, 1995) on highly twinned thin films, and experiments on detwinned crystals (Brawner and Ott, 1994; Van Harlingen, 1995), gave consistent results indicates that the  $d_{x^2-y^2}$  component of the order parameter has the same phase across twin boundaries.

Another issue was the linear extrapolation in dc current used by Wollman *et al.* (1993). The validity of this extrapolation has been called into question (Mathai *et al.*, 1995). Careful analysis of this problem (Hinaus *et al.*, 1996) shows that the linear extrapolation used by Wollman *et al.* (1993) can be problematic if the asymmetry of the SQUID depends on its critical current, and that this problem can be overcome by exploiting the time-reversal invariance of the SQUID equations. However, some of the SQUID’s in the experiments of Wollman *et al.* (1993) were apparently relatively symmetric and could be measured at very low critical currents [e.g., the open diamonds in Fig. 9(a)], so that little correction for self-field effects was required. These symmetric SQUID’s gave results consistent, with little correction from extrapolations, with those from the asymmetric SQUID’s. In retrospect, this justifies the extrapolation procedure.

Another objection that has been raised to these SQUID experiments was that they compared SQUID’s with corners with SQUID’s without corners [as in Figs. 8(a) and (b)]. It is well known that flux-trapping, demagnetization, and field-focusing effects can be strongly dependent on the sample geometry. Klemm (1994) presented arguments that the  $\pi$  phase shifts seen between the “corner” and “edge” SQUID’s could result simply from the differences in their geometries, even for  $s$ -wave cuprate pairing symmetry. Wollman *et al.* (1994) argued against this point of view on a theoretical basis. However, the strongest argument against corners being a decisive influence comes from the results of Tsuei *et al.* (1994), which showed the presence of the half-flux quantum effect in a geometry with no corners.

Finally, the SQUID experiments of Wollman *et al.* (1993) were influenced by the effects of flux trapping. Note, for example, the results of Fig. 9(a). Here, the “edge” and “corner” SQUID’s on the same crystal were cooled repeatedly, with significant differences in both the slopes and the intercepts in the experimental results. The simplest explanation for this is that there were varying amounts of trapped magnetic flux threading through the SQUID area in different cooldowns. Wollman *et al.* (1993) speculated that flux trapping could have occurred in the Pb electrodes leading to the SQUID. Magnetic imaging of the  $ac$  or  $bc$  plane faces of cuprate superconductors (Kirtley, Moler, *et al.*, 1998; Moler *et al.*, 1998) shows that there can be vortices trapped between the planes of the cuprate superconductors, often with opposite senses, even when they are cooled in a very small field. Such trapped vortices could affect the measured-critical-current vs applied-field characteristics of the SQUID’s. However, the fact that Wollman *et al.* (1993)

consistently see a difference between the phase shifts in their “corner” and “edge” SQUID’s indicates that these flux-trapping effects are not sufficiently large to change the qualitative interpretation of these measurements.

A second SQUID interference experiment on single crystals of YBCO was performed by Brawner and Ott (1994). They made a SQUID with two bulk point-contact junctions of niobium, making Josephson weak links on adjoining orthogonal faces of an untwinned YBCO single crystal. Two all-niobium SQUID’s on either side of the sample SQUID were used as controls to measure the relative phase shifts. As with the Wollman *et al.* (1993) experiments, the SQUID’s were asymmetric, so that corrections for self-field effects had to be made. For this Brawner and Ott (1994) measured the dynamic resistance of their SQUID’s as a function of dc applied current and extrapolated their results to zero current. They found consistent phase shifts between their control and sample SQUID’s of  $160 \pm 20^\circ$ , consistent with there being a  $\pi$  phase shift between the components normal to the order parameter on the two faces of the YBCO crystal.

The Brawner and Ott (1994) experiment had the complication of a required correction for self-field effects. Further, the microscopic structure of the weak links was not clear in these experiments. This was an important point, since the experiment depended on there being a difference in the crystal momentum of the order parameter probed on the two faces. Nevertheless, this was an important contribution.

High- $T_c$  SQUID’s made from  $45^\circ$  asymmetric biepitaxial grain boundaries show anomalous dependence of their critical currents on magnetic field. This can be interpreted in terms of  $d$ -wave symmetry, combined with local grain-boundary faceting (Coppeti *et al.*, 1995; Hilgenkamp *et al.*, 1996; Mannhart, Mayer, and Hilgenkamp, 1996). In this type of grain boundary, the node of the presumed  $d_{x^2-y^2}$  order parameter is normal to the average interface on one side of the boundary. Faceting rotates the normal angle slightly, producing alternating positive and negative critical currents along the grain boundary. This is equivalent to having a series of  $\pi$  rings, which spontaneously generate alternating supercurrents, which in turn produce anomalous SQUID interference patterns. This interpretation was supported by scanning SQUID microscope measurements, which imaged the spontaneous magnetization in the grain boundaries (Mannhart, Hilgenkamp, *et al.*, 1996).

Based on the low-inductance SQUID design of Chesca (1999), with spatially distributed junctions, Schulz *et al.* (2000) produced all high- $T_c$  zero- and  $\pi$ -ring SQUID’s using YBCO thin films epitaxially grown on bicrystal and tetracrystal (e.g., Fig. 20 below) SrTiO<sub>3</sub> substrates. These devices, which had the advantages of very small sample volumes (so that flux trapping was not an issue) and small  $I_c L$  products (so that self-field effects were negligible), showed nearly ideal dependences of the critical current on applied field, with a

minimum at zero applied field for the  $\pi$ -ring SQUID, as expected for a  $d$ -wave superconductor in the tetracrystal geometry used.

## B. Single-Josephson-junction modulation

Wollman *et al.* (1993, 1995) performed a set of measurements in a second geometry [Figs. 8(c) and (d)] that were less sensitive than their SQUID experiments to the effects of flux trapping and sample asymmetry. In this geometry, instead of two SNS junctions in a loop, there is a single SNS junction, either at a corner or at an edge of a single YBCO crystal. For junctions with uniform Josephson current density, and in the “short” junction limit where the junction size is much smaller than the Josephson penetration depth, it is expected that the critical current will follow the standard Fraunhofer pattern  $I_c(\Phi) = I_0 |\sin(\pi\Phi/\Phi_0)/(\pi\Phi/\Phi_0)|$  as a function of the flux  $\Phi$  threading the junction, for an “edge” junction with either  $s$ -wave or  $d$ -wave symmetry, and for a “corner” junction with  $s$ -wave symmetry. This pattern has a maximum in the critical current at zero applied field. In contrast, a “corner” junction with  $d$ -wave superconductors of equal current densities on the two faces should show the interference pattern  $I_c(\Phi_0) = I_0 |\sin^2(\pi\Phi/2\Phi_0)/(\pi\Phi/\Phi_0)|$ , with a minimum at zero applied flux. Wollman *et al.* (1993, 1995) reported consistent results of a maximum in the interference pattern for “edge” junctions [Fig. 9(b)], and a minimum for “corner” junctions [Fig. 9(c)], consistent with  $d_{x^2-y^2}$  symmetry. See also Iguchi and Wen (1994).

The interference patterns reported by Wollman *et al.* (1993, 1995) did not agree closely with the ideal expressions above. They attributed this to asymmetries in the current densities in the junctions, and to flux trapping, and they reported good agreement with modeling including these effects (Van Harlingen, 1995). However, interference patterns qualitatively similar to those reported by the Illinois group have been reported for both square (Hyun, Clem, and Finnemore, 1989) and annular (Nappi and Cristiano, 1997; Vernik *et al.*, 1997; Nappi, Cristiano, and Lisitskii, 1998) Josephson junctions with a single vortex trapped in them. The Illinois group reported that symmetric interference patterns, with minima at zero applied field, such as they observe, cannot be reproduced in modeling with an  $s$ -wave superconductor in their geometry. Perhaps the most convincing argument, however, against this possibility is that it seems unlikely that magnetic flux is consistently trapped in the Illinois “corner” junctions in such a way as to mimic  $d$ -wave superconductivity.

Miller, Ying, *et al.* (1995) used frustrated thin-film tricrystal samples to probe the pairing symmetry in YBCO, in an experiment analogous to the “corner” tunnel-junction samples of Wollman *et al.* (1993, 1995). The concept and design of the tricrystal experiments will be discussed in detail in the next section. Miller *et al.* measured the dependence on magnetic field of the critical current of a  $3\text{-}\mu\text{m}$ -wide microbridge spanning the tricrystal point. They found a minimum in the critical cur-

rent at zero applied field, as expected for a  $d$ -wave superconductor in this geometry, in the “short junction” limit [where the width  $W$  of the bridge is much shorter than the Josephson penetration depth  $\lambda_J$  (Owen and Scalapino, 1967)]. They found that junctions in an unfrustrated geometry, or wide junctions ( $L \gg \lambda_J$ ) in a frustrated geometry, showed maxima in their critical currents at zero magnetic field. This agrees with the analysis of Xu, Miller, and Ting (1995), who studied the static properties of one-dimensional  $0-\pi$  Josephson junctions theoretically and found that  $d$ -wave-type interference patterns (with a minimum in  $I_c$  at zero field) can only be obtained for “short” junctions. This analysis was extended to the intermediate range  $L \sim \lambda_J$ , and to asymmetric junctions, with similar conclusions, by Kirtley, Moler, and Scalapino (1997). These results and analyses show that the single-junction interference measurements of Wollman *et al.* (1993, 1995) and Miller, Ying, *et al.* (1995) and the tricrystal magnetometry experiments on half-flux quantum Josephson vortices of Kirtley, Tsuei, Rupp, *et al.* (1996) are complementary, in the sense that the junction interference measurements only show distinctive “ $d$ -wave” interference patterns in a frustrated geometry when the junction width  $L \ll \lambda_J$ , while the magnetometry experiments can only observe spontaneous magnetization of  $\Phi_0/2$  in a frustrated geometry when  $L \gg \lambda_J$ .

### C. Tricrystal and tetracrystal magnetometry

Spontaneous generation of a half-flux quantum at the meeting point of Josephson coupled superconducting crystals with unconventional pairing symmetry (e.g., the heavy-fermion superconductors) in a frustrated geometry was first proposed by Geshkenbein and co-workers (Geshkenbein and Larkin, 1986; Geshkenbein *et al.*, 1987). The first experimental realization of this effect in a controlled geometry was by Tsuei *et al.* (1994).

#### 1. Design and characterization of controlled-orientation multicrystals

The strategy of the multicrystal experiments is to create a multiple-junction ring consisting of deliberately oriented cuprate crystals for defining the direction of the pair wave function. The presence or absence of the half-integer flux-quantum effect in such samples as a function of the sample configuration differentiates between various pairing symmetries. In the first such experiment, tricrystal (100) SrTiO<sub>3</sub> substrates with controlled orientations were designed and fabricated<sup>16</sup> for this purpose. Here,  $c$ -axis-oriented epitaxial cuprate films were deposited and patterned into a ring interrupted by three grain-boundary Josephson junctions. As defined in Fig. 10(a), the misorientation angles  $\alpha_{12}$ ,  $\alpha_{31}$ , and the angle between the grain boundaries  $\beta$  are selected so that the three-junction ring is either a zero ring or a  $\pi$  ring de-

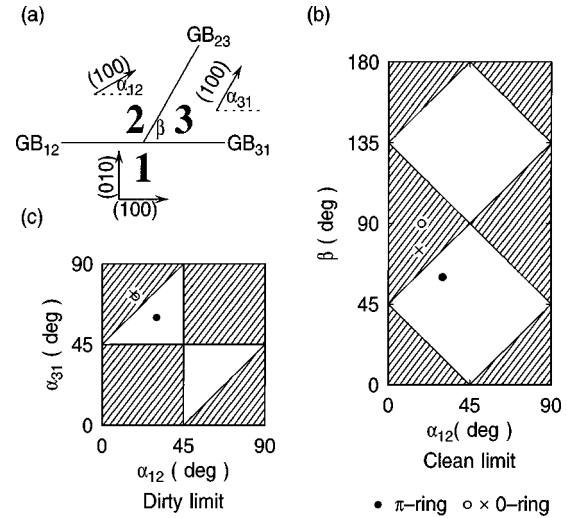


FIG. 10. Design parameters for zero and  $\pi$  rings: (a) Tricrystal geometry; (b),(c) regions of the design parameters that give zero and  $\pi$  rings in the (b) clean and (c) dirty limits. Shaded areas, zero rings; open areas,  $\pi$  rings. ●, the design point for the frustrated three-junction ring samples [Fig. 16(a)]; ○, ×, the design points for the unfrustrated three-junction ring samples [see Figs. 16(b) and (c), respectively].

pending on the symmetry of an assumed pair state. For example, it can be shown using the Sigrist-Rice (clean) formula, Eq. (26), that the three-junction ring is a  $\pi$  ring if  $\cos 2(\alpha_{12} + \beta)\cos 2(\alpha_{12} - \beta)$  is negative (assuming for simplicity that  $\alpha_{12} = \pi/2 - \alpha_{31}$ ). In Fig. 10(b), the design parameters ( $\alpha_{12}, \beta$ ) corresponding to a  $\pi$ -ring design are plotted as open areas; those for the zero ring are shaded. As discussed in Sec. III.A, it is important to take disorder effects into consideration by also satisfying the maximum-disorder formula [Eq. (27); Tsuei *et al.*, 1994]. It can be shown that in this limit the three-junction ring is a  $\pi$  ring if  $\cos(2\alpha_{12})\cos(2\alpha_{31})\cos(\alpha_{12} - \alpha_{31})$  is negative [Fig. 10(c)].

The tricrystal design parameters for the  $d_{x^2-y^2}$  frustrated geometry were chosen as  $\alpha_{12} = 30^\circ$ ,  $\alpha_{31} = 60^\circ$ , and  $\beta = 60^\circ$ , corresponding to the solid circle in Figs. 10(b) and (c). With this tricrystal design, if the cuprate superconductor being tested is indeed a  $d$ -wave superconductor, the half-integer flux-quantum effect should be observed in both the clean and dirty limits, and therefore presumably also in the conditions of the actual junction, which must be somewhere in between.

In the tricrystal experiment of Tsuei *et al.* (1994), an epitaxial YBCO film (1200 Å thick) was deposited using laser ablation on a tricrystal (100) SrTiO<sub>3</sub> substrate with the configuration shown in Fig. 11. The YBCO film had a sharp zero-resistance transition temperature of 90.7 K. X-ray-diffraction measurements on YBCO and other cuprates indicated single-phase, high-quality  $c$ -axis epitaxial film growth. In-plane scanning x-ray-diffraction and electron backscattering measurements on the substrate and the YBCO film showed strong in-plane alignment in the tricrystal cuprate film, with misorientation angles at each grain boundary within  $4^\circ$  of the intended design angle. After blanket film deposition, rings (48  $\mu$ m

<sup>16</sup>The tricrystal and tetracrystal SrTiO<sub>3</sub> substrates were manufactured at Shinkosha Co., Tokyo.

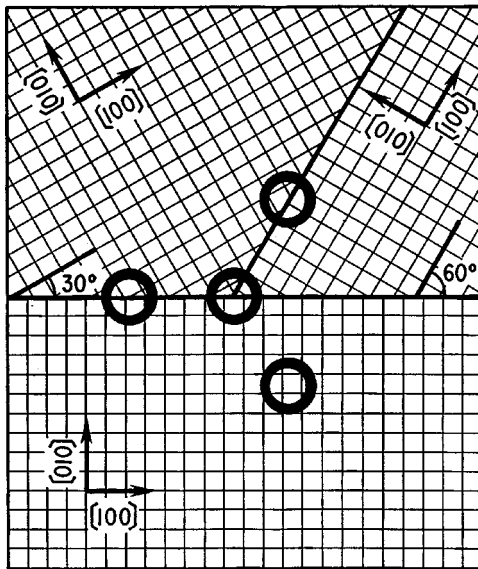


FIG. 11. Experimental configuration for the  $\pi$ -ring tricrystal experiment of Tsuei *et al.* (1994). The central, three-junction ring is a  $\pi$  ring, which should show half-integer flux quantization for a  $d_{x^2-y^2}$  superconductor, and the two-junction rings and zero-junction ring are zero rings, which should show integer flux quantization, independent of the pairing symmetry.

in inner diameter,  $10\ \mu\text{m}$  in width) were patterned by a standard ion-milling photolithographic technique. In addition to the three-junction ring located at the tricrystal meeting point, two two-junction rings and one ring with no junction were also made as controls (see Fig. 11). The control rings are in the zero-ring configuration and should exhibit the standard integer flux quantization. Current-voltage measurements on test microbridges ( $25\ \mu\text{m}$  long and  $10\ \mu\text{m}$  wide) perpendicular to each of the three grain boundaries indicated that (1) electrical resistance as a function of temperature,  $R(T)$ , showed typical features of a grain-boundary weak-link junction; (2) the  $I$ - $V$  curve displayed typical resistively shunted Josephson-junction characteristics; and (3) the values of the critical current for all three junctions agreed within 20% ( $I_c \approx 1.8\ \text{mA}$ ). Since the estimated self-inductance of the ring  $L$  was  $100\ \text{pH}$ , the  $I_c L$  product was about  $100\Phi_0$ , easily satisfying the condition  $I_c L \gg \Phi_0$  for observing the half-integer flux quantization.

## 2. Magnetic-flux imaging

A high-resolution scanning SQUID microscope (Kirtley, Ketchen, *et al.*, 1995) was used to directly measure the magnetic flux threading through the superconducting cuprate rings in the tricrystal magnetometry experiments. The SQUID's used for these experiments were low- $T_c$  Nb-AlO<sub>x</sub>-Nb trilayer SQUID's, fabricated using the planarized, all-refractory technology for superconductivity (PARTS) process (Ketchen *et al.*, 1991; Fig. 12), with SQUID noise about  $2 \times 10^{-6}\Phi_0/\text{Hz}^{1/2}$ .

Since the pickup loops in these SQUID's were photolithographically patterned with well-shielded leads (Fig. 12), it was possible to quantitatively model the magnetic

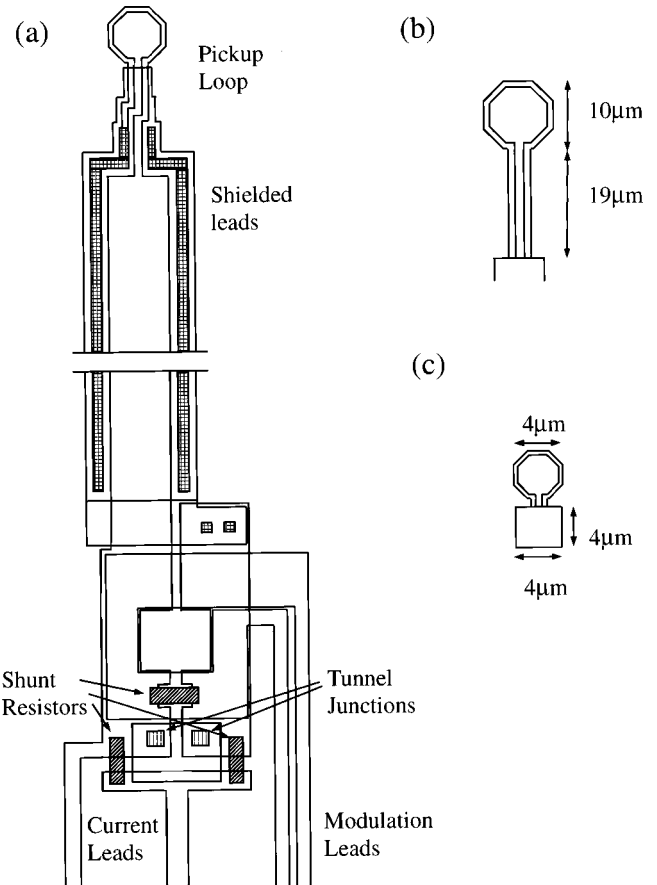


FIG. 12. Schematic diagram (not to scale) of an IBM SQUID magnetometer and effective pickup areas: (a) SQUID magnetometer with an integrated, shielded pickup loop; (b) effective pickup area of the first-generation IBM integrated pickup loop SQUID's; (c) effective pickup area of the second-generation IBM integrated pickup loop SQUID's.

fields imaged by them. In this modeling, the finite width of the lines making up the loop were accounted for by taking the effective loop pickup area as the geometric mean area  $\pi r_{in} r_{out}$  (Ketchen *et al.*, 1985). Two generations of SQUID pickup loops were used for these experiments. The first [Fig. 12(b)] had octagonal pickup loops  $10\ \mu\text{m}$  in diameter (center to center) with leads  $1.2\ \mu\text{m}$  wide, spaced by  $2.4\ \mu\text{m}$ . This loop was modeled as an octagonal pickup area  $9.9\ \mu\text{m}$  in diameter, with an additional slot area  $19\ \mu\text{m}$  long and  $2.4\ \mu\text{m}$  wide. The second-generation loop [Fig. 12(c)] had better shielded leads, with minimum linewidths and spacings of  $0.8\ \mu\text{m}$ . These loops were modeled with effective pickup areas, each of which was the sum of the loop area itself plus an additional area from the shielding of the leads close to the loop, to account for flux-focusing effects. As an example, the smallest of these loops [Fig. 12(c)], with a  $4\text{-}\mu\text{m}$ -diameter octagonal pickup loop, was modeled as an octagonal area  $3.9\ \mu\text{m}$  in diameter, with an additional area  $4\ \mu\text{m}$  by  $4\ \mu\text{m}$ , from which one-third of the flux was added to the ring flux.

Figure 13 shows a scanning SQUID microscope image of a three-junction YBCO ring in the original tricrystal magnetometry experiments (Tsuei *et al.*, 1994). The

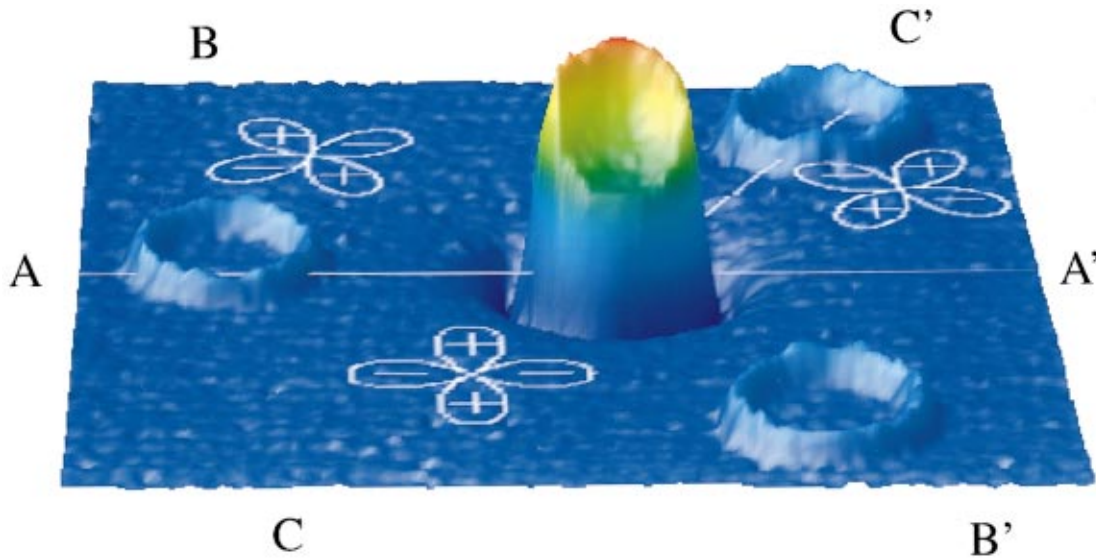


FIG. 13. Three-dimensional rendering of a scanning SQUID microscope image of a thin-film YBCO tricrystal ring sample, cooled and imaged in nominally zero magnetic field. The outer control rings have no flux in them; the central three-junction ring has half of a superconducting quantum of flux spontaneously generated in it [Color].

sample was cooled to 4.2 K and imaged in a magnetic field estimated to be less than  $0.4 \mu\text{T}$ . The interpretation of this image is that the three outer control rings have no magnetic flux trapped in them, but that the central three-junction ring has  $\Phi_0/2$  total flux in it. The control rings are visible due to a slight change in the inductance of the SQUID when it passes over the superconducting rings.

Four different techniques were used to determine the amount of flux in the rings in these experiments (Fig. 14). The first was to calculate directly the SQUID signal for a given flux magnitude in the rings. Since the width of the rings is comparable to the  $10\text{-}\mu\text{m}$  diameter of the pickup loops used to image these samples, the currents in these rings can be modeled as infinitely narrow lines of current. The mutual inductance  $M(\vec{\rho})$  between a pickup loop tilted at an angle  $\theta$  from the sample  $x$ - $y$  plane in the  $x$ - $z$  plane and a circular wire of radius  $R$  at the origin can be written as

$$M(\vec{\rho}) = \frac{\mu_0 R}{4\pi} \int dx dy \int_0^{2\pi} d\phi \frac{\cos \theta (R - y \sin \phi - x \cos \phi) - \sin \theta (z \cos \phi)}{(x^2 + y^2 + z^2 - 2xR \cos \phi - 2yR \sin \phi)^{3/2}}, \quad (41)$$

where the integral  $dx dy$  is over the plane of the pickup loop, and the vector  $\vec{\rho}$  specifies the displacement of the pickup loop with respect to the ring in the  $x$ - $y$  plane.

Numerical integration of Eq. (41), using the pickup loop geometry of Fig. 12(b), a tilt angle of  $20^\circ$ , and a distance between the pickup loop center and the point of contact of the SQUID substrate with the sample surface of  $10 \mu\text{m}$ , gives a mutual inductance of  $2.4 \text{ pH}$  between the pickup loop and one of the rings when the pickup loop is centered above the ring. The ring inductance was calculated to be  $99 \pm 5 \text{ pH}$ . This means that

the fields induced by the pickup loop in the ring are a small perturbation of the self-fields induced by the circulating currents in the rings. A given flux  $\Phi$  threading a superconducting ring with self-inductance  $L$  induces a

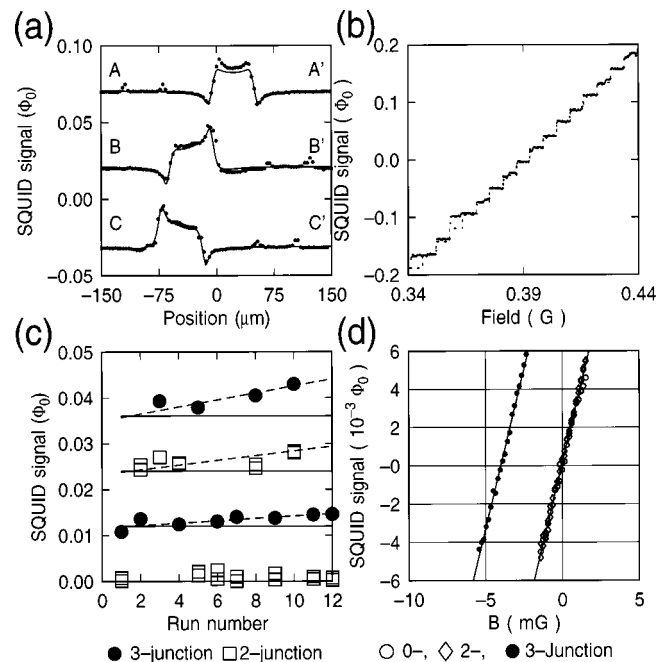


FIG. 14. Four techniques for demonstrating the half integer flux-quantum effect in tricrystal ring samples: (a) Direct calculation, assuming the central ring has  $\Phi_0/2 = h/4e$  flux in it. (b) Observation of the change in the SQUID signal as individual vortices enter the three-junction ring, with the pickup loop centered on the ring. (c) Measurements of the absolute values of the pickup loop flux when it is directly above the zero-junction ring minus that above  $\square$ , the two-junction ring and  $\bullet$ , the three-junction ring, for a number of cooldowns. (d) Measurements of the SQUID signal directly above the rings, as a function of externally applied field.

circulating current  $I_r = \Phi/L$  around the ring, which in turn induces a flux  $\Phi_s(\vec{\rho}) = M(\vec{\rho})\Phi/L$  in the pickup loop.

The solid circles in Fig. 14(a) represent cross sections through the image of Fig. 13 as indicated by the contrasting lines in this image. The solid lines are numerical integrations of Eq. (41), assuming there is  $\Phi = h/4e = \Phi_0/2$  total flux in the central, three-junction ring, and no flux in the other rings. The asymmetry in the ring images results from the tilt of the pickup loop relative to the substrate, as well as the asymmetric pickup area from the unshielded section of the leads. Allowing the total flux in the three-junction ring to be a fitting parameter gives  $\Phi = 0.57 \pm 0.1\Phi_0$ , using a doubling of the best-fit  $\chi^2$  as a criterion for assigning statistical errors.

A second method for calibrating the response of the SQUID pickup loop to flux trapped in the rings was to position the pickup loops directly above the center of a particular ring and measure the SQUID output as a function of externally applied field. An example is shown in Fig. 14(b) for the case of a three-junction ring. In this figure a linear background, measured by placing the loop over the center of the zero-junction control ring, was subtracted out. At low fields stepwise admission of flux into the ring leads to a staircase pattern, with progressively smaller steps, until over a small intermediate-field range, shown for increasing fields in Fig. 14(b), single flux quanta are admitted. The heights of the single flux-quantum steps in this field region, derived by fitting the data with a linear staircase (dashed line), are  $\Delta\Phi_s = 0.0237\Phi_0$ . This is in good agreement with the calculated value of  $\Delta\Phi_s = M(0)\Phi_0/L = (0.025 \pm 0.003)\Phi_0$ . Twelve repetitions of this measurement, including measurements of both the two-junction and three-junction rings, gave values of  $M(0)\Phi_0/L = (0.028 \pm 0.005)\Phi_0$ . The average for eight different cooldowns of the absolute value of the SQUID pickup loop signal above the three-junction ring was  $(1.33 \pm 0.13) \times 10^{-2}\Phi_0$ , different from that above the zero-junction ring when the three-junction ring was in its lowest allowed flux state. Using the calibration above, this meant that the three-junction ring had  $0.46 \pm 0.09\Phi_0$  in its lowest allowed flux state.

A third method for calibrating the flux in the tricrystal ring samples was to cool the sample a number of times under slightly different field conditions. Figure 14(c) shows the results from 12 cooldowns of a YBCO ring sample, plotted as the absolute value of the difference between the SQUID loop flux in the centers of the two-junction or three-junction rings, and the zero-junction control ring. The solid lines are the expected values for the flux difference calculated from Eq. (41).  $\Delta\Phi$  always fell close to  $(N+1/2)\Phi_0$  for the three-junction rings, and  $N\Phi_0$  for the two-junction rings (where  $N$  is an integer). The upward drift to the data as a function of run number was associated with tip wear. The dashed lines in Fig. 14(c) include a correction for this tip wear and agree well with the data.

A fourth method (called magnetic-field titration) for calibrating the amount of flux in the rings (Kirtley,

Tsuei, *et al.*, 1995) is illustrated in Fig. 14(d). This figure shows the SQUID sensor signal at the center of the ring, relative to the signal outside the ring, for all of the rings as a function of field applied by a coil surrounding the microscope. The coil was calibrated by replacing the sample with a large-area pickup loop SQUID magnetometer. For this experiment, the sample was cooled in sufficiently low field that none of the rings had flux, except for the three-junction ring, which contained  $\Phi_0/2$  spontaneously generated flux. As an external field was applied, the rings screened the field with a circulating supercurrent until a critical field, typically  $\sim 5 \mu\text{T}$ , was exceeded, at which point flux entered the rings through the grain boundaries. In the absence of flux penetration, the SQUID difference signal went to zero when there was as much field inside the ring as outside the ring. Therefore the difference in flux through the rings was just the difference in applied field required to make the signal go to zero, times the effective area of the ring. The effective area of the rings was calibrated by cooling the zero-junction ring in different flux states, assuming that it had integer flux quantization. This gave an effective area of  $2572 \pm 53 \mu\text{m}^2$ , in good agreement with the geometric mean area of  $2564 \mu\text{m}^2$ . Using this effective area, the three-junction ring had  $0.490 \pm 0.015\Phi_0$  more flux threading through it than the zero-junction or two-junction rings. Further, the difference in flux between any of the other rings was  $|\Phi| < 0.01\Phi_0$ .

One can use the technique of magnetic-field titration to gain a better understanding of the magnetic-flux quantum states of the cuprate rings. For example, in the tricrystal experiments with YBCO (Kirtley, Tsuei, *et al.*, 1995) and Tl-2201 (Tsuei *et al.*, 1996), the applied flux needed to nullify the SQUID difference signal in the three-junction ring was always found to be within 3% of  $1/2\Phi_0$ . This implies that the gauge-invariant phase shift as defined in Eq. (20) is very close to  $\pi$ , in turn suggesting that there is no significant time-reversal symmetry breaking. Such a mixed pair state (e.g.,  $d+is$ ) would lead to a phase shift  $0 < \varphi < \pi$  and also a fractional flux quantum  $x\Phi_0$  with  $0 < x < 1/2$  (Walker and Luettmers-Strathmann, 1996a; Sigrist, 1998). In the tricrystal experiment with Tl-2201 (Tsuei *et al.*, 1996), in which the  $I_c L$  product is low, the amount of spontaneously generated flux through the ring was indeed noticeably smaller than  $\frac{1}{2}\Phi_0$  ( $x \sim 0.3$ ). This can be understood by considering the free energy [Eq. (36)] of a  $\pi$  ring ( $\varphi = \pi$ ). The ground-state flux  $\Phi_m$  of the ring can be calculated by minimizing the free energy  $U(\Phi, \Phi_a)$  as a function of applied flux  $\Phi_a$ . This calculation indicates that fractional vortices arising from low- $I_c$   $\pi$  rings are possible (Fig. 15) and do not necessarily imply an order parameter with broken time-reversal symmetry.

### 3. Nature of the observed half-integer flux quantization

A series of tricrystal experiments with various geometrical configurations was performed to clarify the origin of the observed half-integer flux-quantum effect in the three-junction ring. Only the  $d_{x^2-y^2}$  frustrated con-

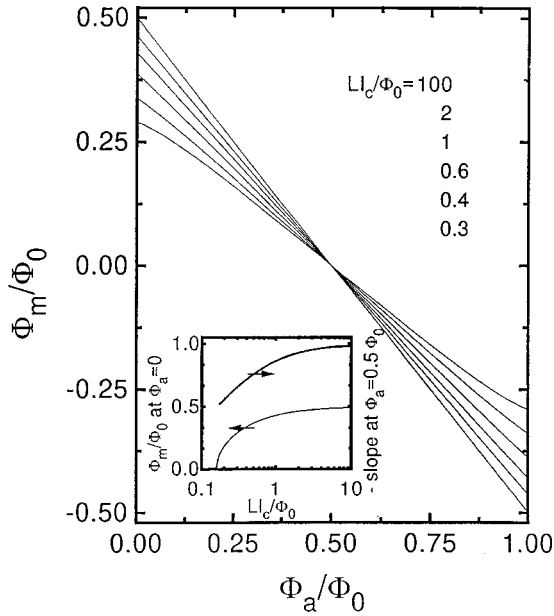


FIG. 15. Calculated ground-state flux  $\Phi_m$  for a  $\pi$  ring as a function of externally applied flux  $\Phi_a$ , for different values of  $\lambda_L/\Phi_0$ . Inset,  $\Phi_m$  and  $d\Phi_m/d\Phi_a$  at  $\Phi_a=0$ .

figuration showed the half-integer flux-quantum effect (Fig. 16). As expected, the tricrystal experiments displayed in Figs. 16(b) and (c) (Kirtley, Tsuei, *et al.*, 1995; Tsuei, Kirtley, *et al.*, 1995) corresponded to zero ring configurations [i.e., shaded areas in Figs. 10(b) and (c)]. The absence of the half-integer flux-quantum effect in these two tricrystal experiments has ruled out any symmetry-independent mechanisms (Bulaevskii *et al.*, 1977; Spivak and Kivelson, 1991) as the cause of the  $\pi$  phase shift. In addition, the tricrystal shown in Fig. 16(c) rules out even-parity  $g$ -wave pairing symmetry with order parameter varying as  $(\cos k_x + \cos k_y)$ .

If the half-integer flux-quantum effect is due to the symmetry of the superconducting pairing, then it should not depend on the macroscopic geometry of the sample. Figure 17 shows the results of a set of experiments to test for the effects of sample geometry. Panel (a) is a scanning SQUID microscope image of a YBCO ring sample as described above. Panel (b) is an image of a sample with photolithographically patterned disks. Panel (c) is an image of a YBCO tricrystal sample with no photolithographic processing of the film. In cases (b) and (c), the supercurrents flowing around the tricrystal point take the form of a Josephson vortex, with total flux  $\Phi_0/2$ . Therefore the observation of spontaneous magnetization of  $\Phi_0/2$  is independent of macroscopic sample configuration, as long as it is in a frustrated geometry.

#### 4. Integer and half-integer Josephson vortices

Figure 18 shows images of several different types of vortices trapped in an unpatterned YBCO film on a tricrystal with a  $d_{x^2-y^2}$   $\pi$ -ring geometry (Kirtley, Tsuei, *et al.*, 1996). Contour lines have been placed on the data at 0.1, 0.3, 0.5, 0.7, and 0.9 of the full-scale amplitudes. The dots in Fig. 19 are cross sections through the images

of Fig. 18 as indicated by the contrasting lines and letters in this figure. The solid lines in Fig. 19 are modeling as follows:

The magnetic induction in vacuum at a distance  $r$  away from the center of a superconducting bulk vortex, in the limit  $r \gg \lambda_L, t$ , where  $\lambda_L$  is the London penetration depth and  $t$  is the film thickness, is given by (Pearl, 1966; Chang, 1992; Kogan, 1993)

$$\vec{B}(\vec{r}) = (\Phi_0/2\pi)\vec{r}/|\vec{r}|^3. \quad (42)$$

The effective pickup area of the 4- $\mu\text{m}$ -diameter octagonal pickup loop used for these measurements was modeled as outlined in Fig. 12(c). The extra pickup area from the shielding of the leads produces slight “tails” in the images directly below the vortices. The solid lines  $AA'$  and  $BB'$  in Fig. 19 are fits to the data, using the fields of Eq. (42), integrating over the pickup loop area, with an angle of  $10^\circ$  between the plane of the loop and the sample surface plane, using the height of the loop as a fitting parameter. The effective height is  $1.8 \mu\text{m}$ . The height estimated from the sensor geometry is  $0.7 \mu\text{m}$ . This discrepancy is most likely due to our use of a bulk model to describe the fields from a vortex trapped in a thin film. The effective height determined from fitting the bulk vortices fixes the height for the rest of the modeling of the Josephson vortices.

The grain boundaries making up the tricrystal point can be modeled as wedges of superconductors, meeting at the tricrystal line ( $x=0, y=0, z$ ). The phase shift  $\phi(r_i)$  across the  $i$ th grain boundary is described by the sine-Gordon equation (Owen and Scalapino, 1967; Clem and Coffey, 1990),

$$\nabla^2 \phi(r_i) = \sin[\phi(r_i) + \varphi(r_i)]/\lambda_{Ji}^2, \quad (43)$$

where  $r_i$  is the position along the  $i$ th grain boundary, and  $\varphi$  is zero everywhere for a conventional superconductor, but can be either zero or  $\pi$  for an unconventional superconductor.  $\phi(r_i)$  is related to the current flowing perpendicular to the grain boundaries by the Josephson relation  $J_{i\perp} = J_{ci} \sin[\phi(r_i) + \varphi(r_i)]$ . The solution to Eq. (43), which describes a  $h/2e$  Josephson vortex [ $\varphi(r_i)=0$  everywhere], centered about  $r_i=0$  along a single grain boundary, is

$$\phi(r_i) = 4 \tan^{-1}(e^{r_i/\lambda_{Ji}}). \quad (44)$$

The solution to Eq. (43) for a  $h/4e$  half-vortex with  $\varphi(r_i)=0$ ,  $r_i < 0$  and  $\varphi(r_i)=\pi$ ,  $r_i > 0$  is (Xu, Yip, and Sauls, 1995)

$$\begin{aligned} \phi(x) &= 4 \tan^{-1}[(\sqrt{2}-1)e^{r_i/\lambda_{Ji}}] & r_i < 0, \\ & 4 \tan^{-1}[(\sqrt{2}+1)e^{r_i/\lambda_{Ji}}] - \pi & r_i > 0. \end{aligned} \quad (45)$$

The general expression for the phase  $\phi$  at the tricrystal point is complicated, if the grain boundaries have differ-

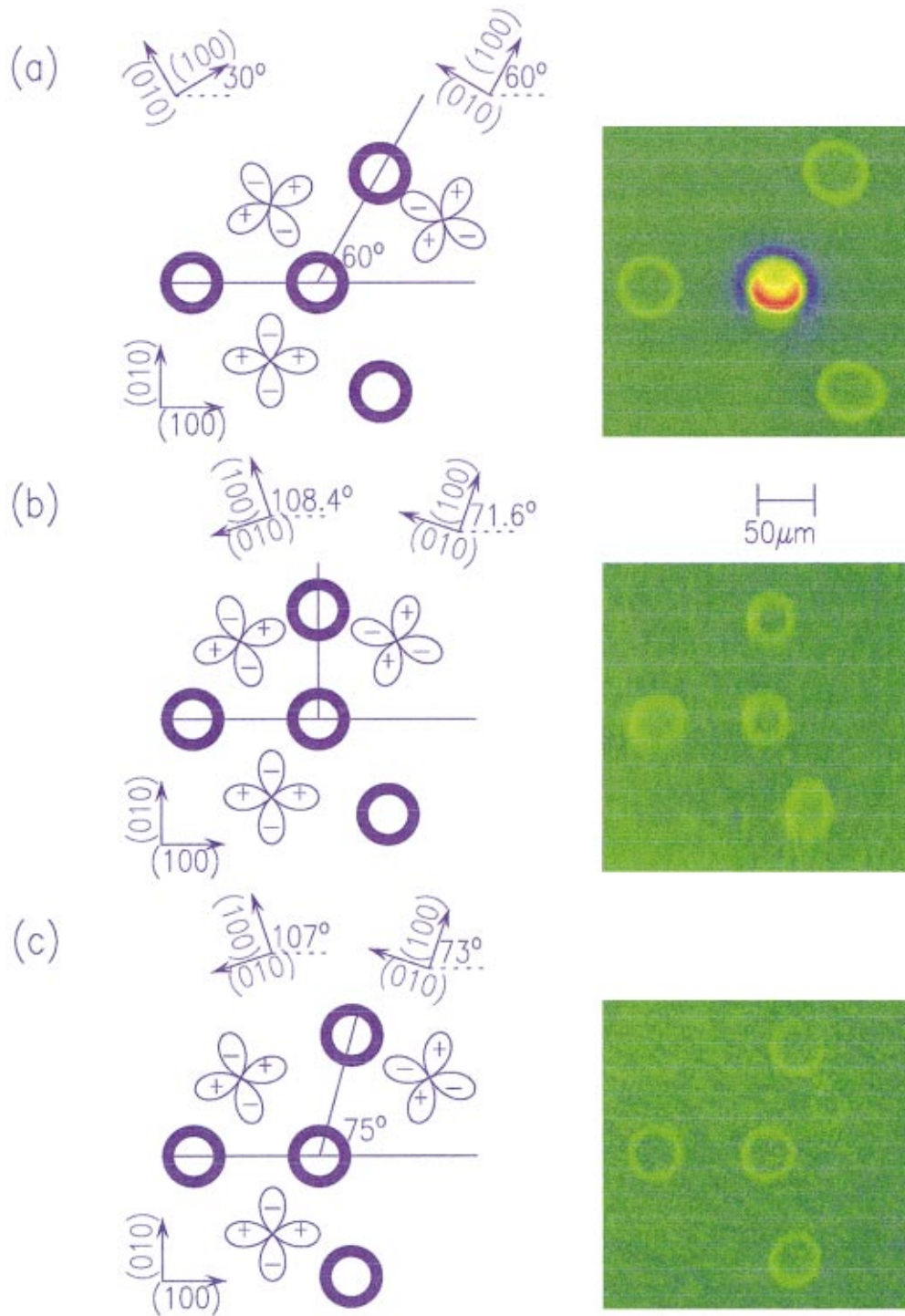


FIG. 16. Three different  $\text{SrTiO}_3$  tricrystal geometries and scanning SQUID images of YBCO ring samples fabricated on these substrates. The central, three-branch junction ring in (a) should be a  $\pi$  ring for  $d_{x^2-y^2}$  pairing. It shows spontaneous generation of a half integer flux quantum when cooled in zero field, while the surrounding, control rings show no trapped flux. The three-branch junction ring in (b) should be a zero-ring for any pairing symmetry. The fact that it does not show spontaneous magnetization rules out a symmetry-independent mechanism for the half-integer flux-quantum effect in these rings. The three-branch junction ring in (c) is designed to be a zero-ring for  $d_{x^2-y^2}$  pairing symmetry, but a  $\pi$  ring for extended  $s$ -wave pairing. This result rules out simple extended  $s$ -wave pairing in YBCO [Color].

ent supercurrent densities, but the magnetic flux per unit length in the  $i$ th branch of the vortex can be written as

$$\frac{d\Phi(r_i)}{dr_i} = \frac{\Phi_0}{2\pi} \frac{d\phi}{dr_i} = \frac{\Phi_0}{2\pi} \frac{-4a_i}{\lambda_{Ji}} \frac{e^{-r_i/\lambda_{Ji}}}{1 + a_i^2 e^{-2r_i/\lambda_{Ji}}}, \quad (46)$$

where in this case  $r_i=0$  for all grain boundaries at the tricrystal point, and  $r_i$  is restricted to values greater than zero. Inside the superconductors, the London theory gives  $\vec{\nabla}^2 \vec{B} = \vec{B}/\lambda_L^2$ . Using London theory to describe the

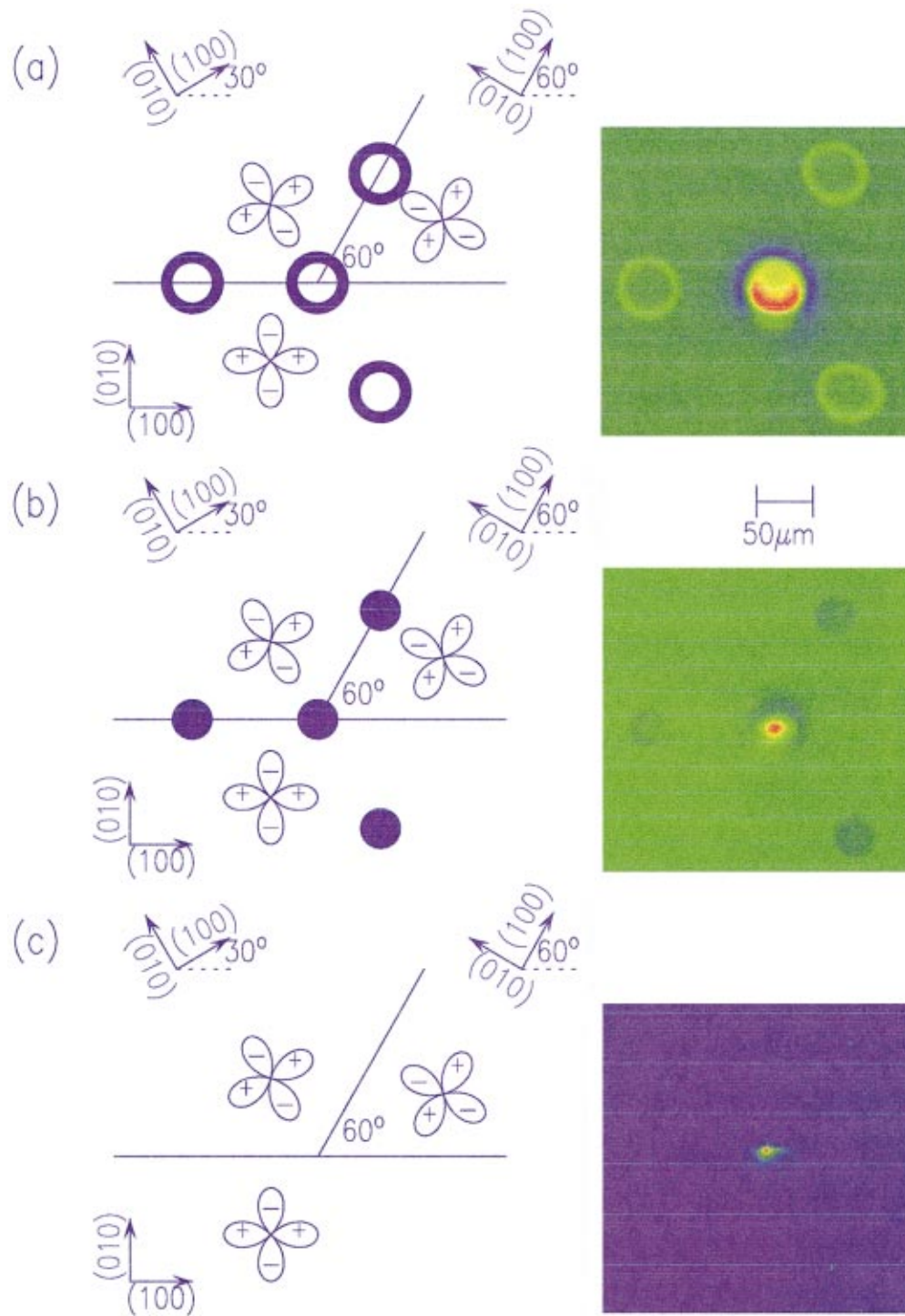


FIG. 17. Scanning SQUID microscope images of three thin-film samples of YBCO epitaxially grown on tricrystal substrates designed to show the half-integer flux-quantum effect for  $d_{x^2-y^2}$  superconductors: (a) a sample photolithographically patterned into four rings with inner diameter  $48 \mu\text{m}$  and width  $10 \mu\text{m}$ ; (b) a similar sample, but this time patterned into disks with the same outside diameter; (c) a sample with no photolithographic patterning. The sample of panel (a) was imaged with a  $10\text{-}\mu\text{m}$ -diameter octagonal pickup loop; sample (b) was imaged with a  $10\text{-}\mu\text{m}$ -diameter octagonal pickup loop; and sample (c) was imaged with a  $4\text{-}\mu\text{m}$ -diameter octagonal pickup loop. In all cases there was a half flux quantum of total flux spontaneously generated at the tricrystal point, but the spatial distributions of supercurrent are different [Color].

field inside a superconductor is strictly valid only if no current flows through the sample boundary. This is a reasonable approximation if  $\lambda_L \ll \lambda_J$ . Neglecting the derivative parallel to the grain boundaries in the Laplacian leads to

$$B_z(r_i, r_\perp) = \frac{\Phi_0 a_i}{\pi \lambda_L \lambda_{Ji}} \frac{e^{-r_i/\lambda_{Ji}}}{1 + a_i^2 e^{-2r_i/\lambda_{Ji}}} e^{-|r_{i\perp}|/\lambda_L}, \quad (47)$$

where  $r_{i\perp}$  is the perpendicular distance from the  $i$ th

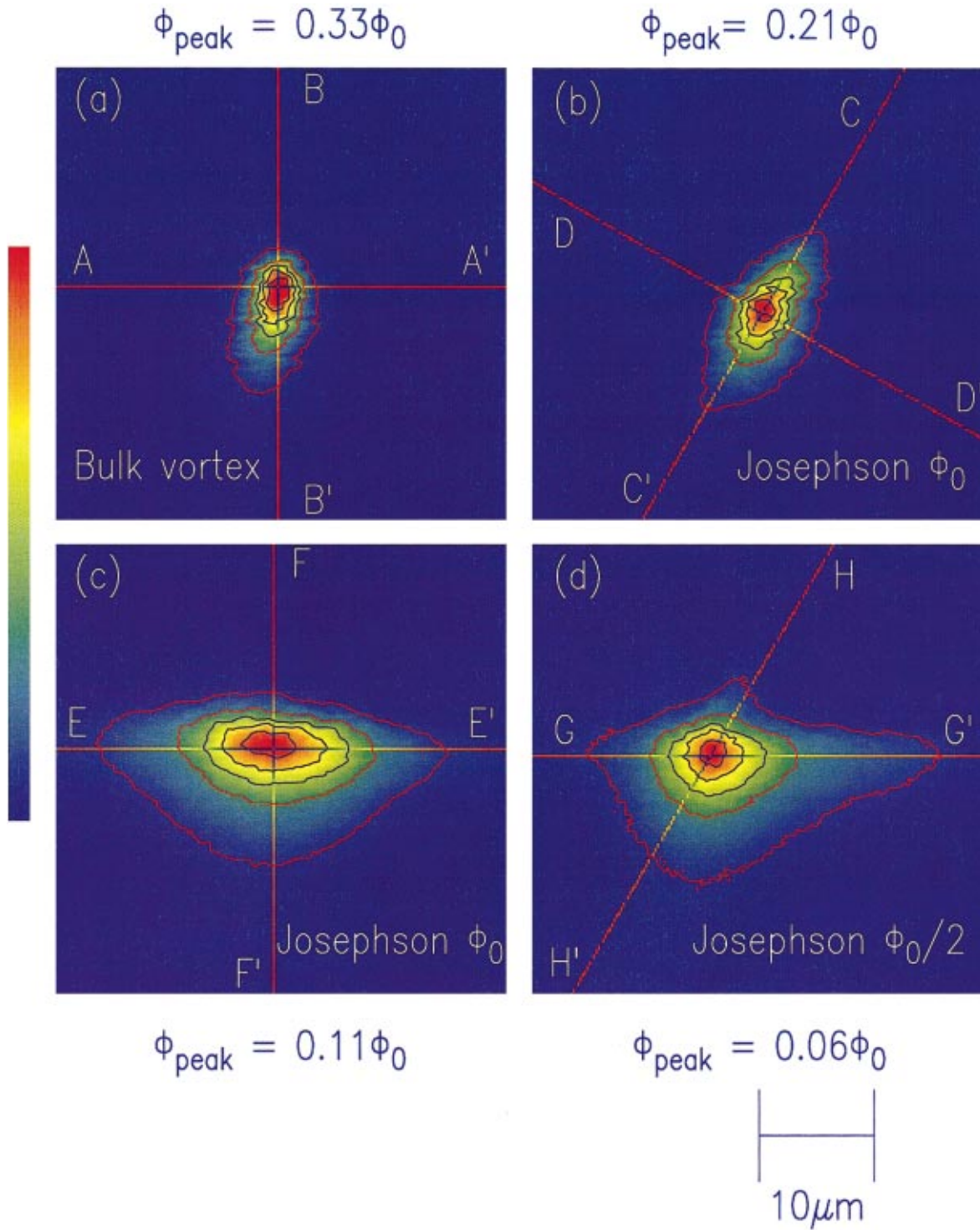


FIG. 18. Images of several types of vortex trapped in a YBCO film on a tricrystal SrTiO<sub>3</sub> substrate designed to generate the half-flux-quantum effect in a  $d_{x^2-y^2}$  superconductor: (a) a bulk vortex; (b) a Josephson vortex trapped on the diagonal grain boundary; (c) a Josephson vortex trapped on the horizontal grain boundary; (d) a half-quantum Josephson vortex trapped at the tricrystal point [Color].

grain boundary. A Josephson vortex with  $h/2e$  total flux in it, and with a single penetration depth, has

$$B_z(r_i, r_{i\perp}) = (\Phi_0/2\pi\lambda_L\lambda_J)\text{sech}(r_i/\lambda_J)e^{-|r_{i\perp}|/\lambda_L}. \quad (48)$$

For the tricrystal, the  $a_i$ 's are normalization constants determined by two conditions: First, the condition that

the magnetic induction at the tricrystal point varies smoothly implies that  $a_i/[\lambda_{Ji}(1+a_i^2)]$  is the same for each grain boundary. Second, the total flux at the tricrystal point is given by  $\Phi = \sum_i(\Phi_0/2\pi)4 \tan^{-1}(a_i) = \Phi_0/2$ .

Once the fields at the surface of the grain boundary

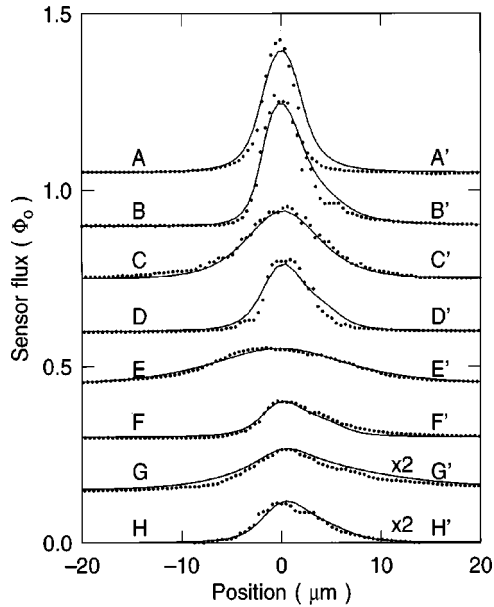


FIG. 19. Cross sections through the vortex images of Fig. 18 as indicated by the contrasting lines and letters: experimental cross sections; solid lines, fits to these data as described in the text, assuming that the bulk vortex and Josephson vortices along the grain boundaries have  $h/2e$  of total flux in them, and the vortex at the tricrystal point has  $h/4e$  total flux.

are calculated, the magnetic inductions at a height  $z$  above the surface are determined by noting that, for magnetic inductions derived from a two-dimensional current distribution,

$$b_z(k_x, k_y, z) = \exp(-\sqrt{k_x^2 + k_y^2}z) b_z(k_x, k_y, 0), \quad (49)$$

where  $b_z$  is the two-dimensional Fourier transform of the field  $B_z(\vec{r})$ , and  $k_x$  and  $k_y$  are the wave vectors in the  $x$  and  $y$  directions, respectively (Roth *et al.*, 1988). As for the bulk vortex, the fields at a height  $z$  above the sample were integrated over the pickup loop geometry to obtain the SQUID flux as a function of scanning position.

The solid lines  $CC' - FF'$  in Fig. 19 are fits of the model above to the data, with  $\lambda_L = 150$  nm and using the Josephson penetration depth  $\lambda_J$  as the only fitting parameter. This gave  $\lambda_J = 5.0 \pm 0.5 \mu\text{m}$  for the Josephson vortices along the horizontal grain boundary, while  $\lambda_J = 2.2 \pm 0.5 \mu\text{m}$  along the diagonal grain boundary. The lines  $GG'$  and  $HH'$  in Fig. 19 are fits to the half-vortex at the tricrystal point, using the three Josephson penetration depths as fitting parameters. The best fit, holding the total flux at  $h/4e$ , occurs for  $\lambda_J = 4.2 \mu\text{m}$  for the horizontal grain boundary to the left of the tricrystal point,  $\lambda_J = 8.2 \mu\text{m}$  to the right of the tricrystal point, and  $\lambda_J = 2.0 \mu\text{m}$  for the diagonal grain boundary. This modeling is simplified in that it neglects the effects of overlapping of fields from different grain boundaries close to the tricrystal point, and it does not take into account modifications to the fields due to the finite thickness of the cuprate films. However, it does allow the conclusion that the spontaneous magnetization at the tricrystal point has approximately  $\Phi_0/2$  total flux in it. Further,

values for the Josephson penetration depth can be obtained from such fits. Similar experiments imaging inter-layer vortices have allowed direct, local measurements of the  $c$ -axis penetration depths in a number of cuprate superconductors (Kirtley, Moler, *et al.*, 1998; Moler *et al.*, 1998; Tsvetkov *et al.*, 1998).

The advantage of the tricrystal magnetometry experiments is that they allow the half-integer flux-quantum effect to be directly imaged, in its ground state, with a tunable geometry to ensure that the pairing symmetry is being probed. Since no currents are applied externally, there are no complications associated with self-field effects. The tricrystal ring samples have very small sample volumes, so that flux trapping is highly unlikely. Any flux trapping that occurs is imaged with high sensitivity. The disadvantage of these experiments is that they use grain-boundary junctions, which have fairly rough interfaces. However, care was taken to account for this interface roughness. Further, these experiments were extremely reproducible: dozens of samples were made and measured in hundreds of cooldowns. All tricrystal or tetracrystal samples that had sufficiently high supercurrent densities across the grain boundaries ( $\lambda_J < 50 \mu\text{m}$ ) gave results (producing either zero or  $\pi$  rings) that were as expected for predominantly  $d$ -wave pairing symmetry.

##### 5. Evidence for pure $d$ -wave pairing symmetry

The phase-sensitive pairing symmetry tests described above yielded convincing evidence for a predominantly  $d$ -wave order parameter. However, none of these experiments could rule out a  $d+s$  mixed pair state. In an orthorhombic superconductor such as YBCO,  $s$ -wave and  $d$ -wave spin-singlet pairings correspond to the same irreducible representation (i.e.,  $A_{1g}$ ) of the point group  $C_{2v}$ . A mixing of  $s$ - and  $d$ -wave order parameters is therefore allowed. Based on such a group-theoretic symmetry argument and the results of Josephson-junction measurements on untwinned YBCO single crystals, it is concluded that  $s+d$  pairing mixing is an unavoidable consequence of orthorhombicity (Walker and Luettmers-Strathmann, 1996a; Béal-Monod, 1998). The observation of a finite  $c$ -axis supercurrent in YBCO/Pb junctions (Sun *et al.*, 1994) also supports a  $d+s$  mixed pair state.

The order parameter  $\Delta(\mathbf{k})$  of a  $d+s$  superconductor should transform as  $d(k_x^2 - k_y^2) + s(k_x^2 + k_y^2)$  to reflect the underlying crystal lattice symmetry, where  $s$  and  $d$  are the amounts of  $s$ -wave and  $d$ -wave subcomponents. Node lines ( $\Delta=0$ ) in the gap function, given by  $k_y = \pm[(d+s)/(d-s)]^{(1/2)}k_x$ , exist, provided that  $d/s \geq 1$ . The slope of the node lines deviates from that of pure  $d$ -wave  $k_x = \pm k_y$ , the diagonals for the Brillouin zone, depending on the degree of  $s$  admixture. The Pb-YBCO corner SQUID (or single-Josephson-junction) interference experiments rely only on a sign change of the order parameter between the  $a$  and  $b$  faces of the YBCO single crystal, and therefore can not discriminate pure  $d$ -wave from  $d+s$  pair states as long as  $d/s \geq 1$ . In principle, the tricrystal experiments with YBCO and Tl-2201 are capable of locating the nodes on the Fermi surface

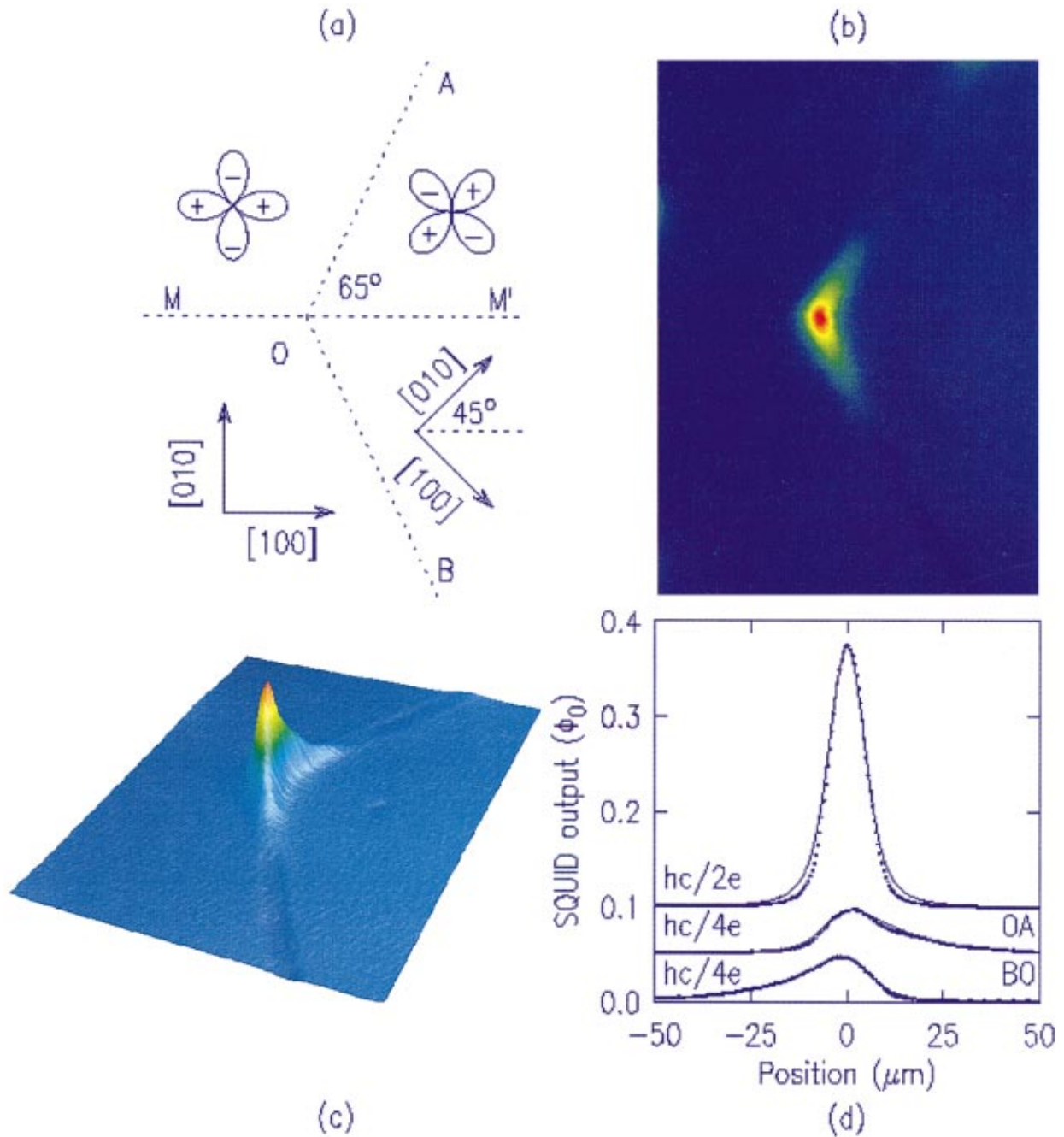


FIG. 20. Tetragonal  $\text{Tl}_2\text{Ba}_2\text{CuO}_{6+\delta}$ : (a) Tetracystal geometry; (b) scanning SQUID microscope image of a film of Tl-2201 epitaxially grown on a  $\text{SrTiO}_3$  substrate with the geometry of (a), cooled in nominally zero field, and imaged at 4.2 K with an  $8.2\text{-}\mu\text{m}$ -square pickup loop; (c) three-dimensional rendering of the data of Fig. 20(b); (d) cross sections through a bulk Abrikosov vortex and through the half-vortex of Figs. 20(b) and (c), along the directions indicated in Fig. 20(a); ●, experimental data; solid lines, modeling, assuming the Abrikosov vortex has  $h/2e$  flux trapped in it, and the vortex at the tetracystal point has  $h/4e$  flux [Color].

of a  $(d+s)$ -wave superconductor. However, this would require a systematic series of tricrystal experiments based on a detailed model describing the complex process of pair tunneling across a realistic grain-boundary junction. Failing that, basic symmetry arguments can nevertheless be made for a pure  $d$ -wave pair state in certain cuprates.

#### a. Tetragonal $\text{Tl}_2\text{Ba}_2\text{CuO}_{6+\delta}$

A tetracystal flux-imaging experiment with tetragonal Tl-2201 films (Tsuei, Kirtley, *et al.*, 1997) was carried out using a geometrical configuration shown in Fig. 20(a), based on a suggestion by Walker and Luettmers-Strathmann (1996a). The original proposal consisted of a ring containing two  $c$ -axis-oriented tetragonal cuprate

grains rotated about the  $c$  axis by an angle of  $\pi/4$  with respect to each other. The symmetrical placement of the two grain-boundary junctions in the ring assured that for a pair state with  $d_{x^2-y^2}$  or  $d_{xy}$  symmetry the supercurrents across the two junctions were equal in magnitude but opposite in sign, resulting in a  $\pi$  ring. For  $s$ -wave or  $g$ -wave ( $A_{1g}$  and  $A_{2g}$  irreducible representation, respectively), there is no sign reversal, and the ring should show the standard integer flux quantization. It is extremely difficult to make a bicrystal SrTiO<sub>3</sub> substrate with the required  $\pi/4$ -rotated wedge as well as two identical grain boundaries that are smooth and free of microscopic voids. To overcome these difficulties, two bicrystals were fused along the dividing line MM' in Fig. 20(a) to achieve the desired bicrystal wedge configuration. Also shown in Fig. 20(a) are the polar plots of the assumed  $d_{x^2-y^2}$  gap function aligned with the crystallographic axes of the SrTiO<sub>3</sub> substrate. For a  $d_{x^2-y^2}$  or  $d_{xy}$  pair state, the built-in reflection symmetry with respect to the line MOM' ensures that the Josephson currents across the grain boundaries  $OA$  and  $OB$  are related by

$$(I_s)_{OA} = -(I_s)_{OB}. \quad (50)$$

This conclusion can also be reached by considering the general formula for the supercurrent of a Josephson junction between two  $d$ -wave superconductors [Eq. (32); Walker and Luettmmer-Strathmann, 1996a]:

$$I_s \propto C_{2,2} \cos(2\theta_1) \cos(2\theta_2) + S_{2,2} \sin(2\theta_1) \sin(2\theta_2) + \dots \quad (51)$$

As required by the reflection symmetry of the experiment, the angles  $\theta_1$  and  $\theta_2$  are given by

$$\theta_1 = \begin{pmatrix} +\alpha \\ -\alpha \end{pmatrix}, \quad \theta_2 = \begin{pmatrix} \pi/4 - \alpha \\ \pi/4 + \alpha \end{pmatrix} \quad (52)$$

for grain-boundary junctions ( $OA$ ), respectively.

When this reflection symmetry operation is applied to Eq. (51), every term changes its sign, reducing to Eq. (50). Shown in Fig. 20(b) is the scanning SQUID image of an epitaxial Tl-2201 film ( $T_c = 83$  K) on the tetracrystal SrTiO<sub>3</sub> substrate [Fig. 20(a)]. A three-dimensional presentation of the data in Fig. 20(b) is shown in Fig. 20(c). The results of detailed modeling (Kirtley, Tsuei, Rupp, *et al.*, 1996) of the image data are presented in Fig. 20(d). The total flux at the wedge point is  $\Phi_0/2$ . The fact that the half-flux quantum is the only vortex in a relatively large area suggests that it is spontaneously generated, as expected. Due to its importance to the symmetry argument, the tetragonal crystal structure of the single-phase Tl-2201 epitaxial films used in the experiment was confirmed by using micro-Raman spectroscopy, x-ray diffraction, bright-field imaging transmission electron microscopy, selected-area electron diffraction, and convergent-beam electron diffraction (Ren *et al.*, 1996; C. A. Wang *et al.*, 1996).

As emphasized earlier, the superconducting order parameter should transform like the symmetry of the underlying crystal lattice. For a tetragonal superconductor with point group  $C_{4v}$  as in Tl-2201,  $s$ -wave and  $d$ -wave pair states correspond to two distinctly different irreducible representations,  $A_{1g}$  and  $B_{1g}$ , respectively. From a group-theoretic point of view, no admixture of  $s$  and  $d$  is allowed. Furthermore, the conclusion about the sign change in the Josephson current is based on a rigorous symmetry argument and does not depend on any model describing pair tunneling. Therefore the observation of the half-integer flux-quantum effect in the tetracystal geometry represents model-independent evidence for pure  $d_{x^2-y^2}$  pairing symmetry.

#### b. Orthorhombic Bi<sub>2</sub>Sr<sub>2</sub>CaCu<sub>2</sub>O<sub>8+δ</sub>

The Bi-2212 superconducting system is probably one of the most-investigated members of the cuprate family, due to its importance in fundamental studies and practical applications. Early pairing symmetry studies on Bi-2212 using techniques such as quasiparticle tunneling spectroscopy and angle-resolved photoemission spectroscopy (ARPES) yielded controversial results. The early tunneling experiments were plagued by problems with junction quality and various spurious effects (for a review, see Hasegawa and Kitazawa, 1991).

However, as discussed in Sec. II.D, ARPES studies on gap anisotropy yielded important evidence suggesting  $d$ -wave pairing symmetry in Bi-2212 (Shen *et al.*, 1993; Ding, Norman, Compuzano, *et al.*, 1996; Ding, Norman, Mochiku, *et al.*, 1996), although ARPES lacks phase sensitivity and therefore cannot distinguish between  $d$ -wave and highly anisotropic  $s$ -wave pairing. A tricrystal flux-imaging experiment with Bi-2212 (Kirtley, Tsuei, Raffy, *et al.*, 1996) proved that the order parameter has sign changes that are indeed consistent with  $d$ -wave pairing symmetry. Shown in Figs. 21(b) and (c) are scanning SQUID microscope images of a  $c$ -axis-oriented Bi-2212 film deposited on a tricrystal SrTiO<sub>3</sub> substrate designed for testing  $d$ -wave pairing symmetry. From these figures, one can see that, at an ambient field of  $0.4 \mu\text{T}$ , vortices are found in the grains (Abrikosov vortices) and along the grain boundaries (Josephson vortices). The vortices at the grain boundaries can be used to locate the tricrystal meeting point, where a relatively weak vortex is observed. When the tricrystal sample is cooled in a nominally zero magnetic field, only the vortex at the tricrystal point remains, suggesting that it is spontaneously generated. Detailed modeling of flux-imaging data shows that the vortex at the tricrystal point has a total flux of  $\Phi_0/2$ , while all others correspond to single vortices with full flux quantum  $\Phi_0$  [Fig. 21(d)]. The results of ARPES and the tricrystal experiment combined lead to the conclusion that, if Bi-2212 has a  $d+s$  mixed pair state, the  $s$ -wave component must be very small.

Based on symmetry arguments, one can go one step further by suggesting that the orthorhombic Bi-2212 is a pure  $d$ -wave superconductor (Tsuei and Kirtley, 1998) just like its tetragonal counterpart Tl-2201. The crystal

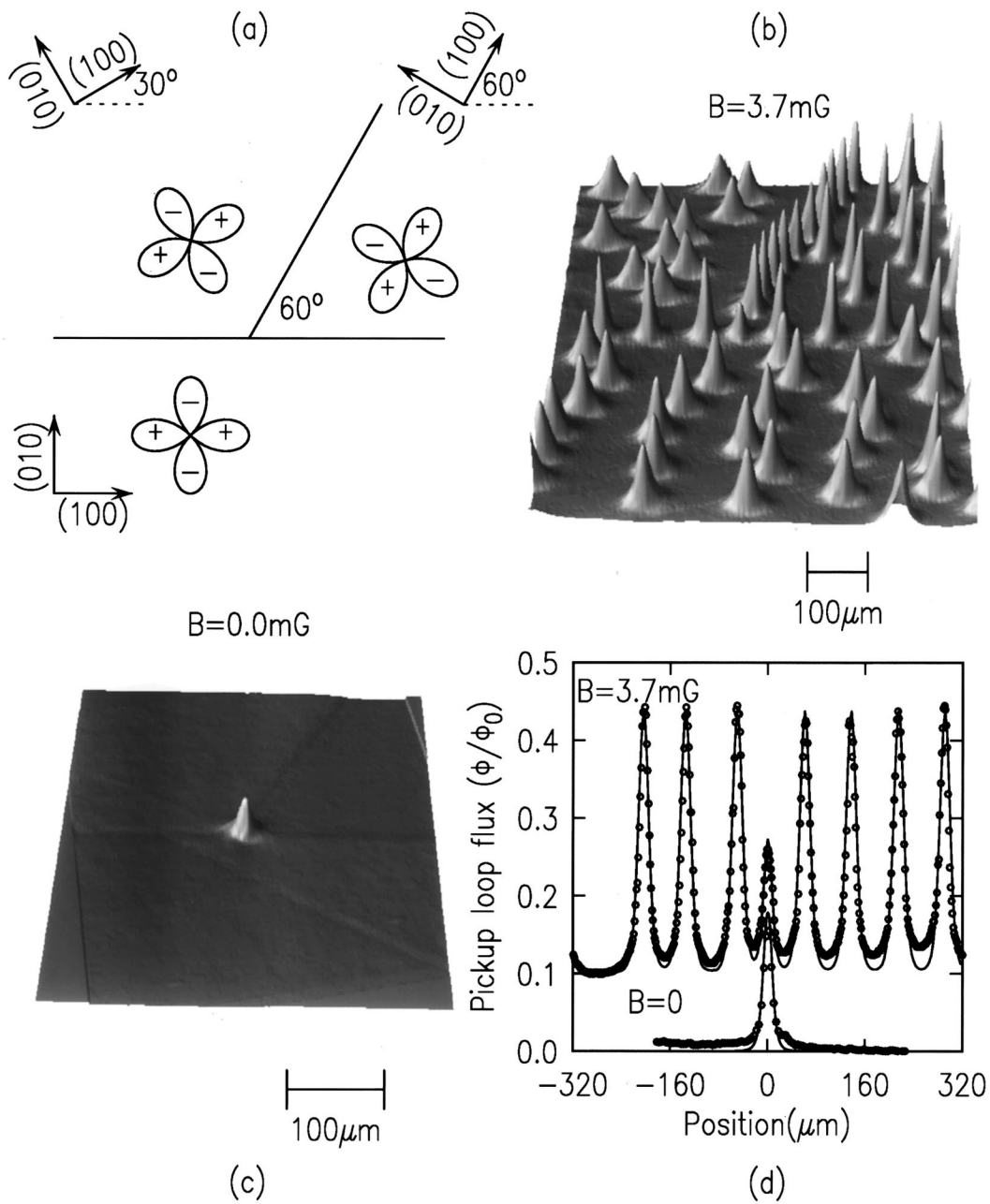


FIG. 21. Scanning SQUID microscope data on Bi-2212: (a) tricrystal geometry, including polar plots of assumed  $d_{x^2-y^2}$  order parameters aligned along the crystalline axes; (b) scanning SQUID microscope image of  $640 \times 640 \mu\text{m}^2$  area of an epitaxial film of Bi-2212 on a SrTiO<sub>3</sub> trisubstrate with the geometry of Fig. 21(a), cooled in a field of  $0.4 \mu\text{T}$ , and imaged at  $4.2 \text{ K}$  with an  $8.2\text{-}\mu\text{m}$ -square pickup loop; (c)  $400 \times 400 \mu\text{m}^2$  image of the same sample, cooled in nominal zero field; (d) comparison of horizontal cross sections through the images (b) and (c) with modeling assuming that all vortices have  $\Phi_0$  of flux, except at the tricrystal point, which has  $\Phi_0/2$  flux spontaneously generated.

structure of Bi-2212 is orthorhombic as a result of an incommensurate lattice modulation with a periodicity of  $\sim 4.7b$  ( $b = 5.41 \text{ \AA}$ , the lattice constant) along the  $b$ -axis direction (for reviews, see Beyers and Shaw, 1988; Chen, 1992). This microstructural feature leads to a reduced Brillouin zone that is rotated by exactly  $\pi/4$  with respect to that of the orthorhombic YBCO. The inequivalent axes for orthorhombic anisotropy coincide with the node lines (Fig. 22) established by the ARPES measurements. From group-theoretic considerations,  $s$ -wave and

$d_{x^2-y^2}$ -wave pair states correspond to two distinct irreducible representations (i.e.,  $A_{1g}$  and  $B_{1g}$ , respectively) and therefore are not allowed to mix (Annett *et al.*, 1996). Based on this symmetry consideration, one is led to the conclusion that the  $s$ -wave component of the order parameter in Bi-2212 should be vanishingly small. This assertion is apparently supported by zero (Durosy *et al.*, 1996; Sinha and Ng, 1998a) or nearly zero (Mössle and Kleiner, 1999)  $c$ -axis pair tunneling in this nominally orthorhombic superconducting system.

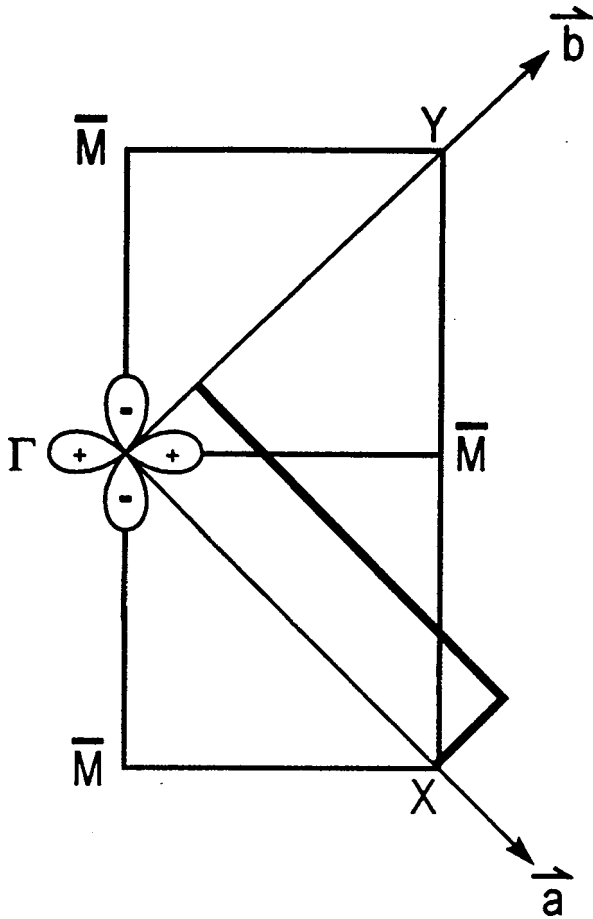


FIG. 22. Brillouin zone for Bi-2212. The reduced zone as a result of incommensurate superlattice modulation (along the  $b$  direction) is outlined schematically. The orientation of the  $d_{x^2-y^2}$ -wave polar plots is established by the ARPES data.

#### D. Thin-film SQUID magnetometry

Mathai *et al.* (1995) performed tests of pairing symmetry in YBCO with thin-film YBCO-Pb (sample) SQUID's. They imaged the magnetic flux in these SQUID's as a function of externally applied magnetic field, using a scanning SQUID microscope with a low- $T_c$  Nb-Pb (sensor) SQUID. The YBCO films were epitaxially grown on (100)  $\text{LaAlO}_3$  substrates by pulsed laser deposition. They were then patterned, a thin layer of Ag was deposited, annealed, cleaned by ion milling, and a thin Pb (In 5% at.wt) film was deposited to form SQUID's. In the experiments of Mathai *et al.* (1995) the sample SQUID's had either a "corner" or "edge" configuration, in analogy with the experiments of Wollman *et al.* (1993) [see, for example, Figs. 8(a) and (b)]. Also in analogy with the experiments of Wollman *et al.* (1993), the "corner" SQUID's should be  $\pi$  rings if YBCO is a  $d$ -wave superconductor, while the "edge" SQUID's should be zero rings, independent of the superconducting pairing symmetry. The YBCO-Pb sample SQUID's were washers, with  $50\text{-}\mu\text{m}$  inner-side length, and  $250\text{-}\mu\text{m}$  outer-side length. They had a self-inductance of about 75 pH, and a  $\beta = 2\pi LI_c / \Phi_0 \sim 1$ . This relatively small  $\beta$  value meant that the spontaneous

flux and circulating supercurrents at zero external field (see Fig. 15) generated by the  $\pi$ -ring SQUID's were quite small. Further, there was a large mutual inductance between the sample and sensor SQUID's. Therefore the influence of the Nb-Pb sensor SQUID on the YBCO-Pb sample SQUID screening currents had to be corrected for in these measurements.

Rather than measuring the amplitudes of the spontaneous flux at zero applied field, Mathai *et al.* measured the superconducting phase shift in their rings with a clever trick: the dependence of the screening currents in the YBCO-Pb sample SQUID's was measured as a function of externally applied field, tracing out a number of branches, each branch corresponding to a different number of vortices in the YBCO-Pb sample SQUID. The measurements were then repeated with the leads to the Nb-Pb sensor SQUID and the external magnet reversed. This was equivalent to a time-reversal operation. If time-reversal-symmetry invariance is satisfied, and if the YBCO-Pb sample SQUID shielding current branches are labeled with the integers  $n$ , a zero ring will map under time reversal onto a branch  $n'$  with  $\Delta n = n - n'$  an even integer, while a  $\pi$  ring will have  $\Delta n$  odd. Mathai *et al.* (1995) found that the "corner" SQUID's had  $\Delta n$  odd while the "edge" SQUID's had  $\Delta n$  even, as expected for  $d$ -wave superconductivity. Further,  $\Delta n$  was close to an integer for both types of sample SQUID's, implying that time-reversal invariance was closely satisfied. Mathai *et al.* (1995) estimated that the time-reversal-symmetry-breaking component of the pairing order parameter was less than 5%, in agreement with the conclusions drawn by Kirtley, Tsuei, *et al.* (1995) from "magnetic titration" of tricrystal rings, as described in Sec. IV.C.2. These experiments had the advantages that they directly imaged trapped flux, so that its influence could be avoided; and they allowed a phase shift of  $\pi$  to be measured self-consistently using just the "corner" SQUID, without reference to the "edge" SQUID.

Later work by Gim *et al.* (1997) tested geometries intermediate between the "corner" SQUID and "edge" SQUID in an attempt to determine the momentum dependence of the phase shift in the order parameter. In these SQUID's one of the junction normals was parallel to the YBCO  $b$  axis, while the other was at an angle  $\theta$  relative to the  $a$  axis. If YBCO were a pure  $d$ -wave superconductor, these SQUID's would be expected to have a zero phase shift for  $0 < \theta < 45^\circ$  and a  $\pi$  phase shift for  $45^\circ < \theta < 90^\circ$ . The results of these experiments were complicated by interface roughness introduced by the etching process used. However, the authors concluded that the angular dependence of the phase of the order parameter follows  $d_{x^2-y^2}$  symmetry, although it was necessary to understand the details of the junction fabrication process to reach this conclusion.

#### E. Universality of $d$ -wave superconductivity

The phase-sensitive pairing symmetry experiments described above have provided clear evidence for a pre-

dominantly  $d$ -wave pair state in several cuprate superconductors; but is it universal? There exists considerable theoretical work suggesting that the stability of the  $d$ -wave pair state depends on the details of the electronic band structure as well as the pairing potential (Wheatley and Xiang, 1993; Dagotto, 1994; O'Donovan and Carbotte, 1995a, 1995b; Koltenbah and Joynt, 1997; T. Sakai *et al.*, 1997; Wysokinski, 1997; Varelogiannis, 1998a, 1998b). Given both  $s$ -wave and  $d$ -wave pairing channels, the general conclusion of these studies is that pairing symmetry is a function of band filling and certain band parameters. Based on the  $t$ - $t'$ - $J$  model, with  $t'/t \geq -0.4$ , the  $d$ -wave pair state prevails in a doping range centered around half-filling of the band, and  $s$ -wave-like pairing is more stable in the under- and over-doped regimes (Wheatley and Xiang, 1993; O'Donovan and Carbotte, 1995a; Koltenbah and Joynt, 1997). There are some Raman data on Bi-2212 and Tl-2201 as a function of oxygen content suggesting that the gap is  $d$  wave near optimal doping and isotropic in the overdoped range (Kendziora *et al.*, 1996). Like many other indirect symmetry experiments, such an interpretation of the results is controversial. For an alternative point of view, see Hewitt *et al.* (1997).

It has been suggested that as the temperature decreases below a certain characteristic value, a pure  $d$ -wave pair state is not stable against the formation of mixed pair states such as  $d_{x^2-y^2} + is$  or  $d_{x^2-y^2} + id_{xy}$  (Kotliar, 1988; Laughlin, 1994, 1998; Liu *et al.*, 1997; Ghosh and Adhikari, 1998a, 1998b; Zhu *et al.*, 1998; Zhu and Ting, 1998). Due to the coupling between the two subcomponents of the order parameter, the mixed pair state is fully gapped, much like that in an  $s$ -wave superconductor (Ghosh and Adhikari, 1998a, 1998b). The power-law temperature dependence of observables such as specific heat, thermal conductivity, and penetration depth characteristic of  $d$ -wave superconductors reverts to the exponential behavior typical of  $s$ -wave superconductors. Measurements of the penetration depth of Zn-substituted LSCO (Karpínska *et al.*, 2000) shows that it retains a  $T^2$  dependence, indicative of  $d$ -wave pairing in the presence of scattering, until  $T_c$  is suppressed to zero. This argues against an admixture of  $s$ -wave pairing at any  $T_c$ . There has been a report of a temperature-dependent pair state with broken time-reversal symmetry (i.e.,  $d_{x^2-y^2} + is$  state) in YBCO near  $T_c$  (Koren *et al.*, 1998). The gap anisotropy in Bi-2212 measured by ARPES also suggests a temperature-dependent two-component order parameter with only a  $d_{x^2-y^2}$  symmetry component near  $T_c$  and both  $s$ - and  $d$ -wave components at lower temperatures (Ma *et al.*, 1995). Furthermore, there is thermal transport evidence suggesting that a phase transition from a pure  $d_{x^2-y^2}$ -wave state into states of broken time-reversal symmetry such as  $d + is$  or  $d_{x^2-y^2} + id_{xy}$  can be induced in Bi-2212 at low temperatures by magnetic field (Krishana *et al.*, 1997) or by magnetic impurities (Movshovich *et al.*, 1998). However, there are new experiments (Aubin *et al.*, 1998, 1999; Krishana *et al.*, 1998) and calculations

(Anderson, 1998) indicating that the interpretation of the original experiments is much more involved.

In view of these interesting but controversial results, it is worthwhile to examine the universality issue by performing phase-sensitive symmetry experiments with different superconducting cuprate systems, and as a function of composition (doping) and temperature for a given cuprate system.

### 1. Hole-doped cuprates

As shown in Table IV, evidence for predominantly  $d$ -wave pairing has been found in all the hole-doped cuprate superconductors tested using phase-sensitive methods. This is generally consistent with the numerical studies of band structure which address the form of pairing symmetry. As mentioned above, the  $d$ -wave channel is favored near half-filling. More phase-sensitive symmetry experiments are needed in the under- and overdoped regimes to fully test the universality issue. The interpretation of symmetry experiments with twinned YBCO single crystals or films depends on the exact nature of the twin boundaries (Annett *et al.*, 1996; Walker, 1996). However, phase-sensitive experiments with a tetragonal cuprate superconductor such as Tl-2201 (Tsuei *et al.*, 1996, 1997) and untwinned YBCO samples (Wollman *et al.*, 1993; Brawner and Ott, 1994) make such complications irrelevant. The fact that a  $d$ -wave signature has been consistently and reproducibly observed in both orthorhombic and tetragonal cuprates argues strongly that the twin boundaries in YBCO have odd reflection symmetry (Walker, 1996). The  $d$ -wave component of the order parameter continues across the twin boundary, whereas the  $s$ -wave counterpart changes its sign. An even-reflection twin boundary corresponds to a predominantly  $s$ -wave pair state, which is not observed in any of the YBCO experiments listed in Table IV.

### 2. Electron-doped cuprates

Non-phase-sensitive symmetry tests have been contradictory in the electron-doped cuprate superconductors  $\text{Nd}_{1.85}\text{Ce}_{0.15}\text{CuO}_{4-\delta}$  (NCCO) and  $\text{Pr}_{1.85}\text{Ce}_{0.15}\text{CuO}_{4-\delta}$  (PCCO). For example, the in-plane penetration depth  $\lambda_{ab}(T)$  in NCCO has been fit both with an exponential temperature dependence (Wu *et al.*, 1993; Andreone *et al.*, 1994; Anlage *et al.*, 1994; Alff *et al.*, 1999), indicating  $s$ -wave symmetry, and a power-law dependence (Kokales *et al.*, 2000; Prozorov *et al.*, 2000), indicating a symmetry with a line of nodes. The penetration depth measurements in these materials are complicated by the fact that they likely have large impurity scattering, which tends to change  $\lambda_{ab}(T)$  from a  $T$  to a  $T^2$  temperature dependence in a superconductor with a line of nodes (Annett *et al.*, 1991; Hirschfeld and Goldenfeld, 1993), and by the paramagnetism of  $\text{Nd}^{3+}$  ions in NCCO (Cooper, 1996). Similarly, penetration depth measurements of PCCO have been interpreted as indicating either an  $s$ -wave (Alff *et al.*, 1999) or non- $s$ -wave (Kokales *et al.*, 2000; Prozorov *et al.*, 2000) pairing symmetry. Quasiparticle tunneling measurements in NCCO (Huang *et al.*,

TABLE IV. Summary of phase-sensitive tests of cuprate pairing symmetry. All these experiments indicate dominant  $d$ -wave pairing.

Cuprate systems	$T_c(K)$	Comments	References	
YBa <sub>2</sub> Cu <sub>3</sub> O <sub>7-<math>\delta</math></sub> (YBCO)	91	Orthorhombic crystal structure with space group $Pmmm$ , two layers of CuO <sub>2</sub> per unit cell, point group $C_{2v}$ in the CuO <sub>2</sub> plane.	YBCO single crystals, Pb-YBCO SQUID interferometry $c$ -axis oriented epitaxial films, tricrystal magnetometry single crystals, Nb-YBCO SQUID interferometry, Nb point contacts single crystals, Pb-YBCO corner junction, magnetic field modulation of the critical current thin-film YBCO-Pb SQUID interferometry, applied magnetic field and bias current reversed magnetic field modulation in YBCO tricrystal junctions	Wollman <i>et al.</i> (1993) Tsuei <i>et al.</i> (1994) Brawner and Ott (1994) Wollman <i>et al.</i> (1995) Mathai <i>et al.</i> (1995) J. H. Miller, Jr. <i>et al.</i> (1995)
GdBa <sub>2</sub> Cu <sub>3</sub> O <sub>7-<math>\delta</math></sub> (GBCO)	95	Isomorphic with YBCO, antiferromagnetic ordering ( $T_N \approx 2.2$ K), tricrystal direct magnetic-flux imaging		Tsuei and Kirtley (1997)
Tl <sub>2</sub> Ba <sub>2</sub> CuO <sub>6+<math>\delta</math></sub> (Tl-2201)	82	Tetragonal crystal structure with space group $I4/mmm$ , single layer of CuO <sub>2</sub> per unit cell, point group $C_{4v}$ , optimally doped, tricrystal magnetometry		Tsuei <i>et al.</i> (1996)
Bi <sub>2</sub> Sr <sub>2</sub> CaCu <sub>2</sub> O <sub>8+<math>\delta</math></sub> (Bi-2212)	80	Orthorhombic crystal structure, space group $Fmmm$ , bilayers of CuO <sub>2</sub> per unit cell, optimally doped films Tricrystal magnetometry		Kirtley, Tsuei, Raffy, <i>et al.</i> (1996)
Nd <sub>1.85</sub> Ce <sub>0.15</sub> CuO <sub>4-<math>\delta</math></sub> (NCCO)	23	Electron-doped, $c$ -axis oriented thick epitaxial films, tricrystal magnetometry		Tsuei and Kirtley (2000)
Pr <sub>1.85</sub> Ce <sub>0.15</sub> CuO <sub>4-<math>\delta</math></sub> (PCCO)	22	Electron-doped, $c$ -axis-oriented thick epitaxial films, tricrystal magnetometry		Tsuei and Kirtley (2000)

1990) indicate  $s$ -wave symmetry, as does the absence of a zero-bias conductance peak in tunneling (Ekin *et al.*, 1997; Alff, Beck, *et al.*, 1998; Kashiwaya *et al.*, 1998). However, zero-bias conductance peaks can be suppressed by disorder effects, as demonstrated in ion-irradiated YBCO/Pb junctions (Aprili *et al.*, 1998). Although the  $I_c R_n$  values of NCCO/Pb junctions are found to be finite (0.5–6  $\mu$ V; Woods *et al.*, 1999), they are much smaller than the Ambegaokar-Baratoff limit, an indication of an appreciable non- $s$ -wave component.

These contradictory results underscore the need for a phase-sensitive experiment. Recently Tsuei and Kirtley (2000) performed tricrystal pairing symmetry experiments on NCCO and PCCO. These experiments are made difficult by the very small supercurrent densities across the grain boundaries in these materials (Hilgenkamp and Mannhart, 1999; Schoop *et al.*, 1999). Nevertheless, Tsuei and Kirtley (2000) were able to show that

samples in a geometry designed to be frustrated for a  $d$ -wave superconductor spontaneously generated a half-integer Josephson vortex at the tricrystal point upon cooling in zero field. Control samples in two other geometries, designed to be unfrustrated for a  $d$ -wave superconductor, did not show the half-integer flux-quantum effect. These results indicate that both NCCO and PCCO are  $d$ -wave superconductors.

The electron-doped superconductors are different from their hole-doped counterparts in many ways. For example, the hole doped cuprates such as YBCO and LSCO have apical oxygens; the electron doped cuprates do not. Superconductivity in the electron-doped cuprate systems occurs in a very narrow doping range [ $0.14 \leq x \leq 0.17$  for NCCO (Tokura *et al.*, 1989) and  $0.13 \leq x \leq 0.2$  for PCCO (Takagi *et al.*, 1989; Peng *et al.*, 1997)]; in the hole-doped LSCO system the range is broader ( $0.05 \leq x \leq 0.3$ ). The highest  $T_c$  values in the hole-doped

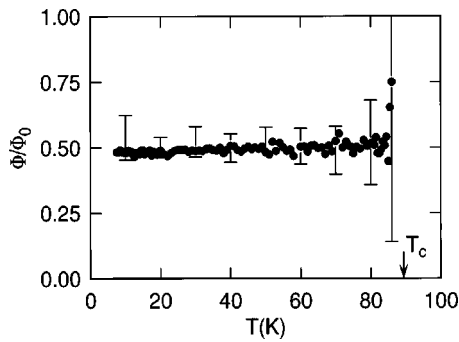


FIG. 23. Best-fit values for the total magnetic flux spontaneously generated at the tricrystal point of a YBCO thin-film sample in a tricrystal geometry designed to be frustrated for a  $d_{x^2-y^2}$  superconductor, as a function of temperature. To within the experimental uncertainties, the total flux is  $\Phi_0/2$  from 0.5 K to  $T_c \sim 90$  K. This indicates that  $d$ -wave pairing symmetry dominates at all temperatures, with little (if any) imaginary component, in YBCO.

cuprates are over five times those in the highest- $T_c$  electron-doped cuprates. In optimally doped YBCO and LSCO the in-plane resistivity increases linearly with temperature over a wide range (Takagi *et al.*, 1992), with small or nearly zero extrapolated values at zero temperature; in PCCO and NCCO ( $x=0.15$ ) the in-plane resistivity is approximately quadratic in temperature, with a relatively large residual resistivity (Tsuei *et al.*, 1989; Peng *et al.*, 1997). Photoemission spectroscopy studies show  $\text{CuO}_2$ -plane-derived flat energy bands near the Fermi surface of the high- $T_c$  hole-doped cuprates such as YBCO (Abrikosov *et al.*, 1993) and BSCCO (Dessau *et al.*, 1993), but not within 300 meV of the Fermi surface of NCCO (King *et al.*, 1993). That both appear to have  $d$ -wave pairing symmetry in spite of these differences indicates that  $d$ -wave pairing is central to the mechanism of superconductivity in the cuprate superconductors.

### 3. Temperature dependence of the $\Phi_0/2$ effect

The universality of  $d$ -wave pairing symmetry can also be considered by investigating the temperature dependence of the half-integer flux-quantum effect. Kirtley, Tsuei, and Moler (1999) used a variable-sample-temperature scanning SQUID microscope (Kirtley, Tsuei, Moler, *et al.*, 1999) to measure the total spontaneous flux at the tricrystal point of a YBCO thin film in a frustrated tricrystal geometry as a function of temperature. They found (Fig. 23) that the half-integer flux-quantum effect at the tricrystal meeting point persists from  $T=0.5$  K through  $T_c$  ( $\sim 90$  K) with no change in total flux ( $\Phi_0/2$ ). This implies that  $d$ -wave pairing symmetry dominates in this cuprate, with no observable time-reversal symmetry breaking, over the entire temperature range.

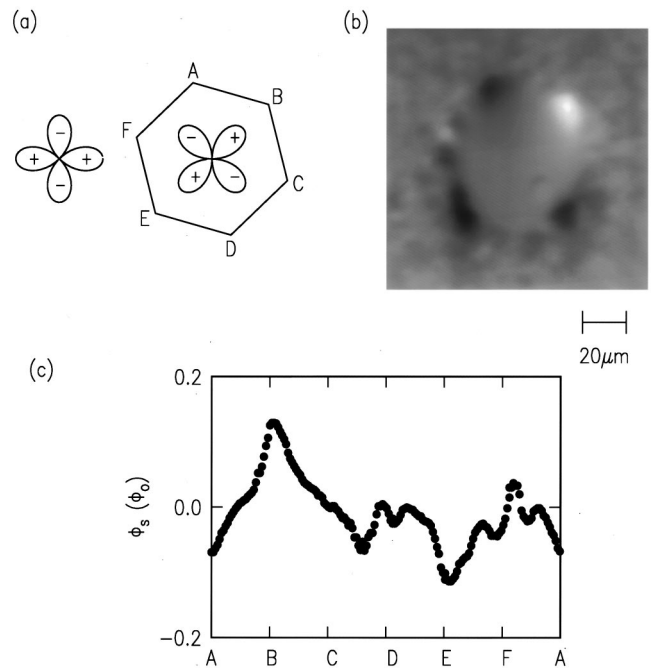


FIG. 24. Data from the samples of Chaudhari and Lin: (a) schematic diagram of the biepitaxial grain-boundary hexagon samples of Chaudhari and Lin; (b) scanning SQUID microscope image of one of these samples; (c) cross section through the data along the hexagonal grain boundary of the scanning SQUID microscope image of (b).

## V. RELATED SYMMETRY-SENSITIVE EXPERIMENTS

### A. Biepitaxial grain-boundary experiments

An experiment that played an important role in the early debate on pairing symmetry was that of Chaudhari and Lin (1994). It is well established that grain boundaries in thin cuprate films act as Josephson weak links (Dimos *et al.*, 1990). Chaudhari and Lin used samples with seeding layers to grow hexagon-shaped grain boundaries in YBCO with  $45^\circ$  rotations of the crystalline orientations inside the hexagons relative to outside the hexagons [Char *et al.*, 1991; Fig. 24(a)]. Using the Sigrist and Rice (1992) formulas for the supercurrent density across the grain boundaries as a function of crystalline orientations [Eq. (26)], they argued that a  $d$ -wave superconductor would have cancellation of the Josephson supercurrents across various edges between the insides and the outsides of the hexagons, leading to an average supercurrent over the entire hexagon of zero. Instead they found that the supercurrent was finite. Moreover, when they removed successive adjacent edges of the hexagon by laser ablation, they found that the total supercurrent was linear in the number of edges, independent of their orientations. They interpreted this as evidence for  $s$ -wave superconductivity.

However, Millis (1994) analyzed the Chaudhari-Lin experiment and found that if the magnitude of the Josephson coupling is strong, but with spatially varying sign, then local vortices will appear to relieve the frustration. This will reduce the cancellation between edges

with critical currents of opposite signs. This argument is similar to that of Xu, Miller, and Ting (1995; Sec. IV.B). The Josephson penetration depth in the Chaudhari-Lin samples was about 6 microns, much shorter than the face length of 500  $\mu\text{m}$ . Therefore there should be no cancellation of the critical currents from the various faces of the hexagons in these experiments, even if the samples were perfectly ordered.

Further, magnetic imaging of these samples shows that these samples are not well ordered magnetically. Figure 24(b) shows a scanning SQUID microscope image of a smaller hexagon, 36  $\mu\text{m}$  in length along each section, fabricated using the same technology as the Chaudhari-Lin samples. The sample was cooled and imaged in nominally zero field, as indicated by the fact that there are no bulk Abrikosov vortices evident in the image, and the flux trapped in the hexagonal grain boundary is on average zero. Figure 24(c) shows a cross section around the perimeter of the hexagonal grain boundary of the scanning SQUID microscope image [Fig. 24(b)]. Magnetic flux is spontaneously generated in the grain boundaries with no apparent order. An analysis of SQUID microscope images of a number of similar grain boundaries by Kirtley, Chaudhari, *et al.* (1995) shows that the total flux in the grain boundary is quantized in units of the superconducting flux quantum  $\Phi_0$ , but that the spatial distribution of this flux is random. This random magnetic ordering is most likely due to a combination of grain-boundary interface roughness and the relatively small critical current densities in these 45° misorientation grain boundaries (Copetti, 1995; Hilgenkamp, Mannhart, and Mayer, 1996; Mannhart, Mayer, and Hilgenkamp, 1996).

## B. *c*-axis pair tunneling

### 1. Tunneling into conventional superconductors

The phase-sensitive symmetry tests described so far all rely on Josephson tunneling parallel to the  $\text{CuO}_2$  planes. In the following, we shall review a series of *c*-axis (perpendicular to the  $\text{CuO}_2$  planes) pair-tunneling experiments.

In the crystal structure of YBCO, the inequivalence in the lattice constants along the *a* and *b* directions in the  $\text{CuO}_2$  planes is about 2%. The effects of orthorhombicity on the normal-state and superconducting properties are well documented in the literature. Significant anisotropy exists in the in-plane resistivity ( $\rho_a/\rho_b \sim 2$ ) and the London penetration depth ( $\lambda_a/\lambda_b \sim 1.5$ ; see, for example, Basov *et al.*, 1995; Sun *et al.*, 1995). From the  $\lambda_a/\lambda_b$  ratio, a large anisotropy in the superfluid density  $(n_s)_b/(n_s)_a = \lambda_a^2/\lambda_b^2 \geq 2$  can be inferred. Since the  $\text{CuO}_2$  plane of YBCO is characterized by a rectangular  $\text{CuO}_2$  lattice with point-group symmetry  $C_{2v}$ , the *s*-wave and *d*-wave pairing symmetries correspond to the same irreducible representation ( $A_{1g}$ ). Therefore *s*+*d* pairing mixing is allowed. Now that the predominance of *d*-wave pairing in YBCO has been established, the issue is the magnitude of the *s*-wave component in such a

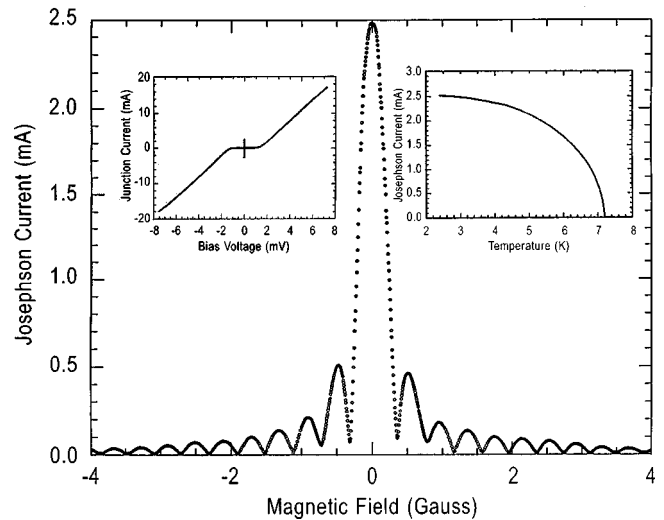


FIG. 25. Experimental data on *c*-axis tunneling from single-crystal YBCO into Pb: Left inset, current-voltage characteristic, showing little leakage current and finite supercurrent. Right inset, Josephson critical current vs temperature. Main figure, Josephson critical current as a function of field applied parallel to the plane of the junction, showing a high-quality interference pattern. Adapted from Sun *et al.* (1994).

mixed pair state. A study of *c*-axis Josephson pair tunneling between a cuprate (such as YBCO) and an *s*-wave superconductor (such as Pb) represents an ideal way to determine the extent of the *d*+*s* admixture. Since the *d*-wave order parameter has lobes equal in area but opposite in sign, the net *c*-axis supercurrent  $I_c$  should be zero [see Eq. (21)], if YBCO were a pure *d*-wave superconductor. Therefore the observation of a finite *c*-axis Josephson current signals the existence of *d*+*s* mixed pairing. The normal-state junction resistance  $R_n$  can also be readily measured. The  $T=0$  K  $I_c R_n$  product for a Josephson junction between two *s*-wave superconductors was given by Anderson (1964):

$$I_c R_n = \frac{\pi \Delta_1 \Delta_2}{e(\Delta_1 + \Delta_2)} K \left( \left| \frac{\Delta_1 - \Delta_2}{\Delta_1 + \Delta_2} \right| \right), \quad (53)$$

where  $\Delta_1$  and  $\Delta_2$  are the BCS energy gaps of the junction electrodes, and  $K$  is the complete elliptic integral. Equation (53) reduces to the Ambegaokar-Baratoff formula [Eq. (22)], for  $\Delta_1 = \Delta_2 = \Delta$ , yielding  $I_c R_n = \pi \Delta / 2e$ . In principle, the ratio of  $I_c R_n$  determined experimentally in a *c*-axis tunneling experiment to that predicted theoretically by Eq. (53) can be a measure of the extent of the *d*+*s* admixture. In practice this is not so straightforward.

Sun *et al.* (1994) reported evidence for *c*-axis Josephson coupling between a low- $T_c$  *s*-wave superconductor (Pb) and a high- $T_c$  cuprate superconductor (YBCO). The *I*-*V* characteristics of a Pb/YBCO *c*-axis planar junction showed extremely low leakage current below the Pb gap ( $\sim 1.4$  meV), linearity at high bias, and a finite pair-tunneling current at zero-bias voltage (Fig. 25, left inset). The temperature dependence of the Joseph-

son critical current demonstrated conventional Josephson-junction behavior (Fig. 25, right inset). These results indicate that single-step, elastic tunneling dominates in these junctions. The variation of the critical current with applied in-plane magnetic field at 1.3 K shows a deeply modulated Fraunhofer pattern (Fig. 25), suggesting highly uniform current distribution. Sun *et al.* (1996) later provided additional evidence from *ab*-edge junctions that the previously observed *c*-axis pair tunneling was indeed along the *c* direction as a result of *c*-axis Josephson coupling, and not due to some in-plane tunneling. The values of the  $I_c R_n$  product were found to be between 0.1 meV and 1 meV in these experiments, the latter being about 20% of the *A-B* limit for the all-*s*-wave case. Kleiner *et al.* (1996) observed microwave-induced steps on the *I-V* curves of the *c*-axis YBCO/Pb tunnel junctions at voltages that were multiples of  $hf/2e$  ( $f$  is the frequency of the applied microwaves), instead of  $hf/4e$ , suggesting that the observed *c*-axis tunneling is first order. According to a theory by Tanaka (1994), second-order *c*-axis pair tunneling is possible for a junction between *s*-wave and pure *d*-wave superconductors. In this case, the standard Josephson current-phase relation, Eq. (19), is replaced by  $I_s = I_s^0 \sin(2\gamma)$ .

YBCO/Pb *c*-axis pair tunneling was also studied using *c*-axis-oriented epitaxial YBCO films (Katz *et al.*, 1995; Lesueur *et al.*, 1997). In these experiments, the high-quality Josephson-tunnel-junction characteristics displayed in Fig. 25 were reproduced, except that the  $I_c R_n$  product was one to two orders of magnitude smaller than obtained on single-crystal YBCO/Pb junctions (Sun *et al.*, 1994). Moreover, *c*-axis pair tunneling was observed in epitaxial film YBCO/Pb low-leakage tunnel junctions by Kwo *et al.* in 1990. A typical  $I_c R_n$  product of  $\sim 0.5$  mV was observed. However, these results were not considered in the context of pairing symmetry at that time.

As a consequence of its orthorhombic crystal symmetry, a YBCO sample is usually twinned unless it is specially treated. The twin boundaries in YBCO run at  $45^\circ$  with respect to the major crystallographic axes *a* and *b*. The two crystal lattice domains on each side of a twin boundary are related via a mirror reflection symmetry (see Fig. 26). Most of the YBCO samples studied in the *c*-axis tunneling experiments were twinned. In polycrystalline YBCO, the spacing between parallel twins can be as small as 10 nm (Beyers and Shaw, 1988; Shaw *et al.*, 1989). To understand the effect of twinning on *c*-axis pair tunneling in such heavily twinned samples, it is extremely important to know how the order parameter varies across a single twin boundary in a YBCO single crystal. As discussed above, there are two alternatives in YBCO (Annett *et al.*, 1996; Walker, 1996; Walker and Luettmmer-Strathmann, 1996b): (1) the *d*-wave component of the order parameter changes sign across the twin boundary, whereas the sign of the *s*-wave component remains unchanged; or (2) the converse.

As discussed earlier, option (1) implies an *s*-wave-dominant order parameter (Walker and Luettmmer-Strathmann, 1996b) and has been ruled out by

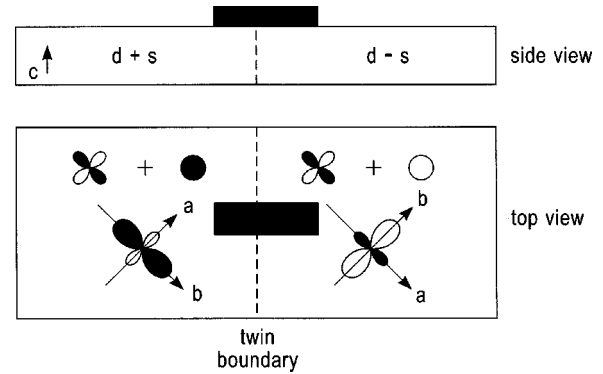


FIG. 26. Experimental geometry for *c*-axis tunneling into a conventional superconductor (Pb) from single-crystal YBCO, with the junction spanning a single twin boundary. YBCO is an orthorhombic superconductor with an admixture of *d*-wave and *s*-wave pairing symmetries. The diagram shows the  $d_{x^2-y^2}$  components with the same phase across the twin boundary, but the *s*-wave component with opposite signs across the twin boundary. There is therefore a change in sign of the net *c*-axis coupling across the twin boundary. Adapted from Kouznetsov *et al.* (1997).

the phase-sensitive symmetry experiments listed in Table IV. Kouznetsov *et al.* (1997) demonstrated the sign reversal of the *s*-wave component across the twin boundary in a study of a *c*-axis Josephson tunnel junction that straddled a single YBCO twin boundary. In Fig. 26, the polar plots of the gap function in the twins (top view) represent the mirror reflection symmetry across the twin boundary (dotted line). Only the *s*-wave component changes its sign across the twin boundary. As a result, the signs of the *c*-axis supercurrent switch across the twin boundary. This is analogous to the Pb/YBCO corner junction (Wollman *et al.*, 1993, 1995). When a magnetic field  $B$  is applied parallel to the twin boundary, the field variation of the critical current  $I_c(B)$  should show a Fraunhofer pattern with the maximum critical current peak shifted to the field value corresponding to a half flux quantum. Furthermore, as the angle  $\phi$  between the direction of  $B$  and the twin boundary varies from  $0$  to  $90^\circ$ , the Fraunhofer pattern  $I_c(B)$  should gradually recover its standard form. This is as observed (Fig. 27). These results provide strong evidence for a *d*-wave-dominant ( $d+s$ ) mixed pairing state in YBCO and for a sign reversal of the *s*-wave component across the twin boundary.

The determination of the magnitude of the *s*-wave component is, however, much more difficult and inconclusive. The results of various  $I_c R_n$  product measurements reported so far vary by three orders of magnitude, from  $\sim 1$  mV to a few  $\mu\text{V}$ . However, rough systematics are discernible. The values of  $I_c R_n$  are 1–1.3 mV for untwinned YBCO crystals (Kleiner *et al.*, 1996), and 0.3–0.9 mV for twinned crystals (Sun *et al.*, 1994). Kleiner *et al.* (1996) also report  $I_c R_n$  values of 0.2, 0.3, and 0.09 mV for twinned crystals. Compared with the all-*s*-wave Ambegaokar-Baratoff limit ( $\sim 5$  mV), these

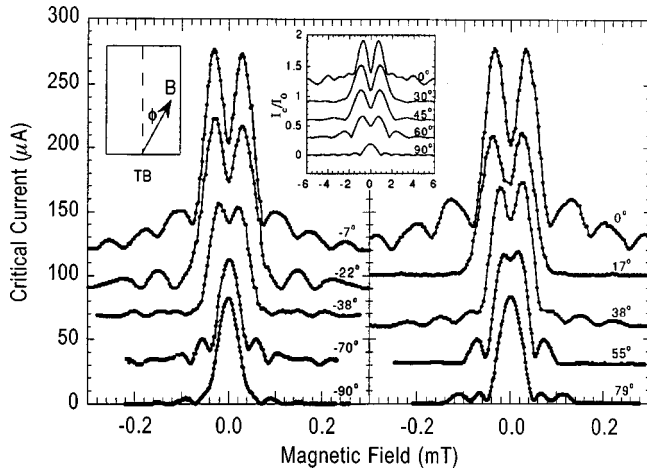


FIG. 27. Josephson interference patterns from the sample of Fig. 26, with the magnetic field in the plane of the junction, as a function of field angle relative to the twin boundary. These characteristics are consistent with the pairing phases as diagrammed in Fig. 26. Inset, results from modeling. Adapted from Kouznetsov *et al.* (1997).

results suggest as much as a 20%  $s$ -wave component in the  $d+s$  admixture.<sup>17</sup>

The  $c$ -axis tunneling experiment of Kouznetsov *et al.* (1997) demonstrated that the tunneling current changes sign across a twin boundary. Depending on the relative abundance of the two kinds of domains separated by the twin boundary, the  $I_c R_n$  products of twinned (tw) and untwinned (untw) junctions should be related by the following expression (O'Donovan *et al.*, 1997):

$$I_c R_n^{tw} = \left| \frac{n-m}{n+m} \right| I_c R_n^{untw}, \quad (54)$$

where  $n/m$  is the ratio of the two twin domains.

The fact that the  $I_c R_n$  values for twinned junctions are not much smaller than those for untwinned ones suggests that volume fractions of the two domains are quite different ( $n \gg m$ ) for the twinned samples measured. It is important to determine experimentally the  $n/m$  ratio for each junction and correlate this with its  $I_c R_n$  value.

In junctions made of heavily twinned films, the  $I_c R_n$  product should be nearly zero as a result of equal abundance of the two twin domains (i.e.,  $n = m$ ). Indeed, the values of  $I_c R_n$  for the thin-film junctions are small but not zero. Katz *et al.* (1995) report  $I_c R_n$  values of 1–40  $\mu\text{V}$ . An  $I_c R_n$  of  $\sim 5 \mu\text{V}$  was obtained by Lesueur *et al.* (1997) for all *in situ* thin-film junctions with or without

an Ag buffer layer in the junction. Judging from the  $I$ - $V$  characteristics and Fraunhofer patterns, the quality of some thin-film junctions is comparable to that of junctions made on single crystals. Low  $I_c R_n$  values are also observed in  $c$ -axis Bi-2212/Pb and Nd<sub>1.85</sub>Ce<sub>0.15</sub>CuO<sub>4</sub>/Pb junctions. Mössle and Kleiner (1999) report  $I_c R_n$  values of 0.5–8  $\mu\text{V}$  for single-crystal Bi-2212/Pb junctions, independent of  $I_c$ , and  $T_c$  of the Bi-2212 crystals used in the tunnel junction. In the case of Bi-2212, the presence of an  $s$ -wave component in the order parameter suggested by the  $c$ -axis tunneling experiment is not compatible with the conclusion of pure  $d$ -wave pairing symmetry based on a group-theoretic argument and the results of a tricrystal experiment and the ARPES measurements described above.

Recently the results of  $I_c R_n$  measurements on various cuprate/Pb tunnel junctions, with the exception of single-crystal junctions made with YBCO (Sun *et al.*, 1994; Kleiner *et al.*, 1996), have given small but finite values. For example,  $I_c R_n$  is about 5  $\mu\text{V}$  for junctions made on YBCO films (Lesueur *et al.*, 1997); 0.5–8  $\mu\text{V}$  for Bi-2212 crystals (Mössle and Kleiner, 1999); and 0.5–6  $\mu\text{V}$  for NCCO films (Woods *et al.*, 1999). The  $I_c R_n$  values in the Bi-2212/Pb junctions are found to be roughly constant, while  $I_c$  and  $R_n$  vary up to three orders of magnitude (Mössle and Kleiner, 1999). In contrast, on average, the  $I_c R_n$  product in the in-plane grain-boundary Josephson weak-link junctions scales with  $R_n^{-1}$  or  $I_c^{-1}$ , as demonstrated by Russek *et al.* (1990) and others (see a review by Prester *et al.*, 1998).

These results can be explained as follows: The relatively large single-crystal YBCO  $I_c R_n$  products may be due to a finite subdominant  $s$  component (allowed in this orthorhombic crystal structure). The  $I_c R_n$  products in thin-film junctions are greatly reduced because of twinning. Small but nonzero  $I_c R_n$  products in tetragonal cuprate superconductors may result from an  $s$ -wave component in a  $d$ -wave superconductor induced, under certain conditions, by spatial inhomogeneities such as surfaces, interfaces, or steps on a surface. The induction of  $s$ -wave pairing in a  $d$ -wave superconductor can be studied by using the Ginzburg-Landau formalism (Joynt, 1990; Volovik, 1993; Alvarez *et al.*, 1996; Bahcall, 1996; Sigrist *et al.*, 1996; Zapotocky *et al.*, 1997) or the Bogoliubov–de Gennes equations (Feder *et al.*, 1997; Martin and Annett, 1998; Zhu and Ting, 1998).

As pointed out by Kouznetsov *et al.* (1997), the observation of nonzero supercurrent in heavily twinned YBCO junctions can be attributed to an additional  $s$ -wave component to the order parameter induced by the presence of the surface, and to a localized time-reversal symmetry-breaking  $d+is$  state (Sigrist *et al.*, 1996; Walker and Luettmmer-Strathmann, 1996b). The  $d+is$  pair state would manifest itself as spontaneously generated fractional flux quanta along the twin boundaries. A search for these effects with a scanning SQUID microscope in a lightly twinned YBCO single crystal was not successful (Moler, Kirtley, *et al.*, 1997), although they could have been below the instrumental sensitivity.

<sup>17</sup>A systematic study of the angular magnetic dependence of the thermal conductivity in a detwinned YBCO single crystal has put an upper limit of 10% on the amount of  $s$ -wave component in the  $d+s$  order parameter (Aubin *et al.*, 1997). A quantitative analysis of directional tunneling and Andreev-reflection measurements on YBCO single crystals indicates a predominantly  $d_{x^2-y^2}$  pairing symmetry, with less than 5%  $s$ -wave component in either the  $d+s$  or  $d+is$  scenario (Wei, Tsuei, *et al.*, 1998; Wei, Yeh, *et al.*, 1998).

## 2. $c$ -axis twist junctions

In principle, a test of pairing symmetry in the cuprate superconductors can be made using junctions with varying misorientation (twist) angle  $\phi$  about the  $c$ -axis direction between two identical cuprate single crystals. If the pair tunneling in the  $c$ -axis direction conserves in-plane momentum, Eq. (21) leads, for a pure  $d$ -wave superconductor, to

$$I_c(\phi) \sim \int_0^{2\pi} \cos(2\theta)\cos(2\theta + \phi)d\theta = \pi \cos \phi. \quad (55)$$

Although some authors have considered the possibility that  $c$ -axis pair transport in the cuprates conserves parallel momentum (Artemenko *et al.*, 1999), both theory (Graf *et al.*, 1993, 1995; Rojo *et al.*, 1993; Hirschfeld *et al.*, 1994, 1997; Abrikosov, 1996; Radtke *et al.*, 1996; Das Sarma, 1998; Klemm, Arnold, *et al.*, 1998), and experiment (Cooper and Gray, 1994; Hosseini *et al.*, 1998) support the view that momentum-non-conserving processes should be included. These latter processes would reduce any sensitivity of the junction critical current to  $\phi$ .

The critical currents of  $c$ -axis twist junctions have been measured in the Bi-Sr-Ca-Cu-O (BSCCO) system. Although early measurements showed a strong dependence of  $I_c$  on  $\phi$  (Tomita *et al.*, 1992; Wang *et al.*, 1994), one group reports no angular dependence (Q. Li *et al.*, 1997, 1999b; Zhu *et al.*, 1998). In fact, this work reports that the twist-boundary critical current density  $J_c$  is the same as that of the bulk in the  $c$ -axis direction. This has been taken as evidence against  $d$ -wave superconductivity in BSCCO (Klemm, Rieck, and Scharnberg, *et al.*, 1998; Q. Li *et al.*, 1999b). However, these experiments were done with macroscopic samples and large currents, such that heating and self-field effects were not negligible. It was not possible to measure Josephson interference patterns, a test of junction uniformity (see, e.g., Fig. 25) in these experiments. Further, it is well known that there is a low intragrain  $J_c$  along the [100] direction due to flux creep in BSCCO. Recently, Q. Li *et al.* (1999a) reported experiments in which they irradiated their twist bicrystals with 2.2-GeV Au ions. This created pinning sites in the bulk of the grains, raising the grain  $J_c$ , but having little influence on the twist boundary  $J_c$ . This brings the behavior of these samples more in line with that of other grain boundaries. In short, experimental difficulties must be resolved, and a full understanding of  $c$ -axis transport in the bulk is required, before critical current measurements on  $c$ -axis twist junctions can provide a test of pairing symmetry in the cuprates.

## VI. IMPLICATIONS OF $d_{x^2-y^2}$ PAIRING SYMMETRY

In many areas of research,  $d_{x^2-y^2}$  pairing symmetry in the cuprates has important implications. We shall briefly discuss a few of them here.

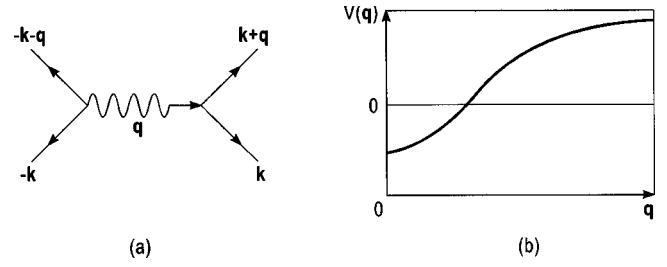


FIG. 28. Examples of the pairing interaction: (a) Graphic representation of the standard BCS pairing;  $\mathbf{q} = \mathbf{k} - \mathbf{k}'$  is the momentum transfer. (b) Schematic representation of the pairing interaction  $V(\mathbf{q})$  constrained by a  $d_{x^2-y^2}$  order parameter. The  $V(\mathbf{q}) = 0$  line is determined by the details of the microscopic pairing mechanism.

### A. Pairing interaction

It has become clear that the established paradigm (Fermi-liquid theory) has to be significantly if not fundamentally altered (Anderson, 1997) in view of the unconventional pairing symmetry, the unprecedentedly high  $T_c$ 's, and the many anomalous normal-state and superconducting properties of the cuprates. In the following discussion, we shall tread on more established ground, keeping in mind the need for and challenge of such a fundamental change. We start with a generalized BCS pairing Hamiltonian:

$$H = \sum_{\mathbf{k}, \sigma} \epsilon(\mathbf{k}) c_{\mathbf{k}\uparrow}^\dagger c_{\mathbf{k}\uparrow} + H_{pairing}, \quad (56)$$

where the one-electron energy dispersion  $\epsilon(\mathbf{k})$  of the quasiparticles in the  $\text{CuO}_2$  band is described by the tight-binding approximation

$$\epsilon(\mathbf{k}) = -2t(\cos k_x + \cos k_y) + 4t' \cos k_x \cos k_y, \quad (57)$$

where  $t$  and  $t'$  are nearest-neighbor and next-nearest-neighbor hopping integrals, respectively.

The pairing interaction  $H_{pairing}$  must be compatible with the underlying point-group symmetry of the Cu-O square/rectangular lattice ( $C_{4v}$  or  $C_{2v}$ ), and can be expressed in terms of the momentum transfer  $\mathbf{k} - \mathbf{k}' = \mathbf{q}$  [see Fig. 28(a)]:

$$H_{pairing} = \sum_{\mathbf{k}, \mathbf{k}', \mathbf{q}} V(\mathbf{q}) c_{\mathbf{k}+\mathbf{q}, \uparrow}^\dagger c_{-\mathbf{k}-\mathbf{q}, \downarrow}^\dagger c_{-\mathbf{k}, \downarrow} c_{\mathbf{k}, \uparrow}. \quad (58)$$

The standard BCS gap equation can be written as

$$\Delta(\mathbf{k}) = - \sum_{\mathbf{k}'} V(\mathbf{k} - \mathbf{k}') \frac{\Delta(\mathbf{k}')}{2E(\mathbf{k}')} \tanh \left[ \frac{E(\mathbf{k}')}{2k_B T} \right], \quad (59)$$

where the quasiparticle energy  $E(\mathbf{k}) = \sqrt{\epsilon^2(\mathbf{k}) + \Delta^2(\mathbf{k})}$ , as defined before. For the case of  $d$ -wave pairing, the  $\mathbf{k}$ -dependent gap potential takes the form

$$\Delta(\mathbf{k}) = \Delta_0(\cos k_x - \cos k_y). \quad (60)$$

The establishment of  $d$ -wave pairing symmetry in high- $T_c$  cuprates does not necessarily specify a high- $T_c$

mechanism. It does impose well-defined constraints on possible models for this mechanism. To be compatible with a  $d$ -wave order parameter [Eq. (60)], the BCS equation, Eq. (59), requires a pairing interaction  $V(\mathbf{k}-\mathbf{k}')=V(\mathbf{q})$  that is relatively attractive for small momentum transfer  $\mathbf{q}$ , and repulsive for large  $\mathbf{q}$  (Bulut and Scalapino, 1996), as shown schematically in Fig. 28(b).

It is both experimentally and theoretically well established that a strong on-site Coulomb repulsion is present in all cuprates. Such a strong electron correlation causes the universally seen Mott transition at near-zero doping (Imada *et al.*, 1998). It is generally believed that the strong on-site Coulomb repulsion rules out simple  $s$ -wave pairing. For pairing interactions of range up to next-nearest neighbor, a strong Coulomb repulsion also rules out all but  $d_{x^2-y^2}$  pairing in models based on a Van Hove singularity<sup>18</sup> in the two-dimensional band structure of the  $\text{CuO}_2$  planes (Tsuei, Newns, *et al.*, 1995). The possibility of stabilizing  $d$ -wave pairing by a Van Hove singularity in the band structure is also discussed by Levin *et al.* (1996). Wheatley and Xiang (1993) studied numerically the relative stability of the generalized  $s$  [ $\Delta(\mathbf{k})=\Delta_0(\cos k_x+\cos k_y)$ ] and  $d_{x^2-y^2}$  pairing channels in a BCS model with only an attractive nearest-neighbor interaction. In the range of parameters where the Van Hove singularity  $T_c$  enhancement is pronounced,  $0 < t/t' < 0.5$  in Eq. (57), the  $d_{x^2-y^2}$  channel is always more stable than the generalized- $s$  one. Similar conclusions have been reached in several Monte Carlo studies (Husslein *et al.*, 1996; Bromly and Newman, 1998).

The possibility of  $d_{x^2-y^2}$  pairing symmetry was first proposed for the cuprates in connection with pairing through the exchange of antiferromagnetic spin fluctuations (Miyake *et al.*, 1986; Scalapino *et al.*, 1986, 1987; Bickers *et al.*, 1987, 1989; Millis *et al.*, 1990; Moriya *et al.*, 1990; Pao and Bickers, 1994). For reviews, see Scalapino

(1995) and Pines (1995). In the spin-fluctuation model for superconductivity, the pairing interaction between charge carriers and spin fluctuations can be described by the  $\mathbf{q}$ -dependent spin susceptibility  $\chi(\mathbf{q})$ :

$$V(\mathbf{k}-\mathbf{k}')=V(\mathbf{q})=g^2\chi(\mathbf{q}), \quad (61)$$

where  $g$  is the coupling strength of a given superconductor. For a nearly antiferromagnetic Fermi-liquid system such as the cuprate superconductors, the function  $\chi(\mathbf{q})$  is sharply peaked at or near  $(\pi, \pi)$  in the Brillouin zone. The pairing interaction represented by Eq. (61) is always repulsive [i.e., the additive constant in  $V(\mathbf{q})$  in Fig. 28(b) corresponds to  $V(0)>0$ ]. When such a pair interaction  $V(\mathbf{q})=g^2\chi(\mathbf{q})$  is entered in the BCS gap equation [Eq. (59)], it naturally leads to a gap with  $d$ -wave symmetry. This is demonstrated by several numerical calculations (Lenck and Carbotte, 1994; O'Donovan and Carbotte, 1995a, 1995b). In the case of ferromagnetic spin fluctuations,  $\chi(\mathbf{q})$  has its maximum at  $\mathbf{q}=0$  (Miyake *et al.*, 1986) and will lead to a  $p$ -wave triplet pairing as in superfluid  $^3\text{He}$  (Anderson and Brinkman, 1973; Levin and Valls, 1983) and possibly in the superconductor  $\text{Sr}_2\text{RuO}_4$  (Rice and Sigrist, 1995). The crucial issue is whether the pairing interaction  $V(\mathbf{q})$  is large enough to support a  $T_c$  of the order of 100 K in the cuprates. These  $T_c$ 's depend sensitively on the phenomenological model used for calculating  $\chi(\mathbf{q}, \omega)$  (Schüttler and Norman, 1996). A  $\chi(\mathbf{q}, \omega)$  based on NMR data on YBCO predicts a  $T_c$  of about 100 K (Millis *et al.*, 1990; Monthoux *et al.*, 1991). However,  $\chi(\mathbf{q}, \omega)$  determined from neutron-scattering data yields a  $T_c \leq 20$  K (Radtke *et al.*, 1992). For a more detailed discussion of this issue, see Schüttler and Norman (1996) and Pines (1995).

All high- $T_c$  cuprate superconductors have a relatively low charge carrier density. As a result the ratio of  $k_B T_c$  to  $E_F$  is about  $10^{-1}-10^{-2}$ , which is  $10^3-10^4$  times larger than conventional superconductors. Therefore Migdal's theorem holds for neither spin-fluctuation nor phonon-mediated superconductivity (Schrieffer, 1994, 1995; Capelluti and Pietronero, 1996; Schüttler and Norman, 1996; Ummarino and Gonnelli, 1997). Specifically for the case of  $d$ -wave antiferromagnetic spin-fluctuation pairing, the breakdown of the Migdal approximation suggests that the strength of the pairing interaction could be significantly reduced when vertex corrections are taken into account (Schrieffer, 1995). However, it has also been argued that vertex corrections could act to enhance  $T_c$  (Monthoux, 1997).

While the spin-fluctuation pairing mechanism leads naturally to an order parameter with  $d_{x^2-y^2}$  symmetry, the conventional BCS electron-phonon pairing interaction gives rise to  $s$ -wave superconductivity. Therefore the relevance of phonons to high- $T_c$  superconductivity is not obvious and is still a topic of great controversy. However, there is much experimental evidence for significant involvement of phonons in the superconducting state of the cuprates (MacFarlane *et al.*, 1987; Thomsen and Cardona, 1989; Thomsen, 1991; Hadjiev *et al.*, 1998). The near-zero oxygen isotope effect at optimal doping

<sup>18</sup>A Van Hove singularity is a peak in the electronic density of states (DOS) due to a saddlelike region in the energy surface upon which an electron (hole) moves. The Van Hove model, which depends on the close proximity of the Van Hove singularity to the Fermi level in the optimally doped cuprates (Markiewicz, 1990, 1992; Tsuei *et al.*, 1990, 1992; Newns *et al.*, 1991, 1994), is built on initial work by Labbe and Bok, 1987; Friedel, 1987, 1989; and Labbe, 1989. The Van Hove model has two parts: (1) The large DOS near a Van Hove singularity can enhance the  $T_c$ , reduce the isotope effect, etc., within the BCS formalism, as observed in cuprate superconductors near optimal doping. (2) The large phase space available for electron-electron scattering at a Van Hove singularity leads to marginal Fermi-liquid behavior (Varma *et al.*, 1989). Several ARPES measurements (Abrikosov *et al.*, 1993; Dessau *et al.*, 1993; Gofron *et al.*, 1994) have firmly established the existence of the Van Hove singularity in YBCO and other high- $T_c$  cuprate superconductors. The unusual flatness of the quasiparticle energy dispersion  $\epsilon(\mathbf{k})$  suggests an extended (one-dimensional) Van Hove singularity, which may be due to strong correlation effects (Levin *et al.*, 1991; Dagotto *et al.*, 1994). For reviews, see Newns *et al.* (1992) and Markiewicz (1997).

(Franck, 1994) suggests a nonphononic pairing mechanism. However, as a function of decreasing doping and  $T_c$ , the isotope exponent increases to values around 0.5, the standard BCS value. Such a doping-dependent isotope effect can be understood in terms of the Van Hove scenario (Tsuei *et al.*, 1990; Newns, *et al.* 1995), and offers strong support for a phonon contribution to high-temperature superconductivity. For details of the phonon isotope effect in strongly correlated systems, see Kim and Tešanović (1993).

In recent years there have been a number of theoretical studies on the importance of electron-phonon coupling in achieving  $d$ -wave superconductivity in the cuprates. For example, phonon-mediated  $d$ -wave superconductivity is found possible in the presence of short-range antiferromagnetic correlations by Lee *et al.* (1995), Kamimura *et al.* (1996), Nazarenko and Dagotto (1996), and others. The breakdown of the Migdal theorem is dealt with by Cappalluti and Pietronero (1996), Zeyher and Kulić (1996), Cappalluti *et al.* (1997), and Ummarino and Gonnelli (1997). There is a general consensus among these authors that electron-phonon coupling to the out-of-plane modes (buckling, and apical oxygen modes) makes the essential contribution to  $d$ -wave superconductivity (Kamimura *et al.*, 1996; Nazarenko and Dagotto, 1996; Sakai, Yoyoka, and Nakamura, 1997; Jepsen *et al.*, 1998). The in-plane (breathing) modes are not effective in making high- $T_c$  superconductivity. This theoretical conclusion finds strong support in a recent observation of the scaling behavior of  $T_c$  and the  $\text{CuO}_2$  plane buckling in a YBCO-type cuprate system (Chmaissem *et al.*, 1999). The importance of small- $\mathbf{q}$  forward-electron-phonon scattering to pairing is emphasized (Santi *et al.*, 1996; Weger *et al.*, 1996; Danylenko *et al.*, 1999). The anomalous isotope effect can also be understood (Nazarenko and Dagotto, 1996; Ummarino and Gonnelli, 1997; Nunner *et al.*, 1999). The Van Hove singularity enhancement of  $T_c$  is also important in these studies (Capelluti and Pietronero, 1996; Nazarenko and Dagotto, 1996; Mierzejewski *et al.*, 1998; Varelogiannis, 1998a).

## B. Quasiparticles in $d$ -wave superconductors

The quasiparticle state in  $d$ -wave superconductors is different from that in  $s$ -wave superconductors (Coffey and Coffey, 1993; Hatsugai and Lee, 1993; Lee, 1993). This difference appears in the vortex contribution to specific heat in the clean limit (Volovik, 1993) and the dirty limit (Kübert and Hirschfeld, 1998a; Senthil *et al.*, 1998; Vishveshwara and Fisher, 2000; see Secs. II.B and II.C); universal heat conduction (Lee, 1993; Taillefer *et al.*, 1997); and around impurities (Hirschfeld and Goldenfeld, 1993; Lee, 1993; Sun and Maki, 1995). Recent scanning tunneling microscopy studies indicate that nonmagnetic impurities on the surface of Bi-2212 induce low-energy excitations in this  $d$ -wave superconductor (Hudson *et al.*, 1999; Yazdani *et al.*, 1999; Pan *et al.*, 2000). These zero-bias quasiparticle states are localized within the coherence length  $\xi$ , consistent with the theo-

retical predictions of Lee (1993) and Salkola *et al.* (1996). The angular distribution of these states relative to the impurity atom observed (Pan *et al.*, 2000) is in good agreement with theoretical predictions (Byers *et al.*, 1993; Salkola *et al.*, 1996) for a  $d$ -wave superconductor. In addition, the nature of the quasiparticle excitations in  $d$ -wave superconductors has been investigated through recent studies using ARPES (Mesot *et al.*, 1999; Valla *et al.*, 1999; Kaminski *et al.*, 2000), magnetic-field dependence of low-temperature thermal conductivity (Ong *et al.*, 1999), and complex conductivity (Corson *et al.*, 2000). Feenstra *et al.* (1997) report a strong enhancement of the recombination time for photoinduced quasiparticles, which they attribute to kinematical constraints near the gap nodes.

## C. Surfaces and interfaces

The physics of surfaces and interfaces of  $d$ -wave superconductors is distinctly different from the  $s$ -wave case. It is predicted that the  $d_{x^2-y^2}$  order parameter in the bulk can be drastically altered at a surface or interface, inducing  $s$ -wave symmetry, time-reversal symmetry breaking, and other effects (Buchholtz *et al.*, 1995a, 1995b; Nagato and Nagai, 1995; Alber *et al.*, 1996; Martin and Annett, 1998). Interface roughness has an important effect on the surface critical field  $H_{c3}$  (Alber *et al.*, 1996; Setty, 1998) and grain-boundary Josephson junctions (Hilgenkamp *et al.*, 1996). In addition, zero-energy (at  $E_F$ ) quasiparticle surface bound states can form due to the  $d_{x^2-y^2}$  symmetry of the gap potential (Hu, 1994).

### 1. Zero-bias conductance peaks

At a [110]-oriented surface of a  $d_{x^2-y^2}$  superconductor, the node line ( $\Delta=0$ ) is perpendicular to the surface. The incident and specularly reflected quasiparticles experience gap potentials of opposite sign. This leads to a new type of Andreev reflection that results from the sign change of the  $k$ -dependent order parameter. It was pointed out by Hu (1994) and others (Yang and Hu, 1994; Buchholtz *et al.*, 1995b; Matsumoto and Shiba, 1995a, 1995b; Tanaka and Kashiwaya, 1995; Xu *et al.*, 1996) that zero-energy bound states can form at the reflecting surface as a consequence of repeated Andreev reflections. These Andreev bound states give rise to a peak in the quasiparticle density of states at the Fermi energy, and should result in a zero-bias conductance peak in the quasiparticle tunneling spectra of cuprate-normal-metal tunnel junctions. Recent observations of zero-bias conductance peaks in different types of tunnel junctions with several cuprate superconductors have been attributed to Andreev surface-bound states. For example a zero-bias conductance peak is found in scanning tunneling microscopy of YBCO (Kashiwaya *et al.*, 1995), in planar tunnel junctions (Covington *et al.*, 1997; Ekin *et al.*, 1997), and in grain-boundary junctions (Alff, Beck, *et al.*, 1998; Alff, Kleefisch, *et al.*, 1998). Zero-bias conductance peaks have also been found in junctions with Tl-2212 (Ekin *et al.*, 1997), Bi-2212 (Alff, Beck,

*et al.*, 1998; Sinha and Ng, 1998b), and  $\text{La}_{1.85}\text{Sr}_{0.15}\text{CuO}_4$  (Alff, Beck, *et al.*, 1998). There are numerous alternate explanations for the observed zero-bias conductance peaks, ranging from superconducting shorts to magnetic interface scattering (Appelbaum, 1966; Anderson, 1966b). For a summary of the various possible origins of zero-bias conductance peaks, see Hu (1998). Before *d*-wave pairing symmetry was established, the zero-bias conductance peak in cuprate junctions was explained in terms of the Appelbaum-Anderson model (see Alff, Kleefisch, *et al.*, 1998; and Hu, 1998).

The areal density of the Andreev bound states is predicted (Yang and Hu, 1994; Buchholtz *et al.*, 1995b; Tanaka and Kashiwaya, 1995) to be maximal on the [110]-oriented surface of a  $d_{x^2-y^2}$  superconductor. This is in agreement with a study of the spatial variation of the zero-bias conductance peak on a (110) YBCO surface (Alff *et al.*, 1997). However, theoretical studies (Yang and Hu, 1994) predict the existence of Andreev bound states on non-(110) surfaces, and various interfaces between cuprate grains. An investigation of the directional tunneling and Andreev reflection on the (100), (110), and (001) surfaces of YBCO single crystals provides further supporting evidence for *d*-wave pairing and mid-gap states (Wei, Yeh, *et al.*, 1998).

In short, the correlation between the observation of zero-bias conductance peaks and the occurrence of *d*-wave pairing in various cuprate superconductors strongly suggests that these zero-bias peaks have their origin in the *d*-wave order parameter.

## 2. Time-reversal symmetry breaking

As discussed earlier, the phase-sensitive symmetry tests have ruled out time-reversal symmetry breaking in the bulk of cuprate superconductors. The situation may be quite different at the surfaces and interfaces of a  $d_{x^2-y^2}$  superconductor. There are many theoretical studies suggesting the existence of pair states with time-reversal symmetry breaking when a *d*-wave superconductor is perturbed by surfaces, interfaces (including grain boundaries and vortex cores), impurities, etc.<sup>19</sup> It has been suggested that a *d*-wave superconductor is intrinsically unstable against the formation of two-component fully gapped order parameters such as  $d_{x^2-y^2} + is$  and  $d_{x^2-y^2} + id_{xy}$  due to the presence of nodes. Note that the nodes in the gap are not removed by forming a *d* + *s* mixed pair state unless  $s \geq d$ .

The predicted time-reversal symmetry breaking should manifest itself in many experiments. For example, it can cause a deviation from the well-established Josephson's sinusoidal current-phase relationship [Eq. (19)]. If Eq. (19) is rewritten as  $I_s = I_c \sin(\gamma - \alpha)$ , the condition of time-reversal symmetry invariance,  $I_s(\gamma) = -I_s(-\gamma)$ , requires  $\alpha = 0$  or  $\pi$ . Any intermediate values

are possible only if the time-reversal symmetry is broken (Yip, 1995; Belzig *et al.*, 1998; see also Sigrist, 1998). Recent current-phase measurements on 45°-misoriented inhomogeneous YBCO grain-boundary junctions found a nearly perfect sinusoidal current-phase relation in the temperature range (60–80 K) studied (Il'ichev *et al.*, 1999a). At low temperatures a possible exception to the above is also reported (Il'ichev *et al.*, 1999b).

Time-reversal symmetry violation should lead to a zero-magnetic-field splitting of the zero-bias conductance peak induced by the Andreev surface bound states (Fogelström *et al.*, 1997; Belzig *et al.*, 1998). Indeed, zero-field splitting of the zero-bias conductance peak in YBCO/I/Cu tunnel junctions was observed below  $\sim 8$  K by Covington *et al.* (1997). Both the zero-field splitting and the field evolution agree with the predictions of Fogelström *et al.* (1997). However, such splitting has not been found in other similar experiments (Ekin *et al.*, 1997). Krupke and Deutscher (1999) conclude the presence of a subdominant *s* or  $d_{xy}$  component out of phase with the  $d_{x^2-y^2}$  component from the field dependence of the zero-bias conductance peak in in-plane (100) YBCO/In junctions. Evidence for broken time-reversal symmetry has been found in spontaneous magnetization in *c*-axis-oriented YBCO films, measured in bulk with a SQUID magnetometer (Carmi *et al.*, 2000), and imaged using a scanning SQUID microscope. In the latter, this magnetization is apparently associated with defects in the films (Tafari and Kirtley, 2000).

## 3. Josephson junctions in *d*-wave superconductors

A tremendous effort has been devoted to the study of Josephson junctions made of high- $T_c$  cuprate superconductors. Here, *d*-wave pairing manifests itself in several junction characteristics that are different from those of all *s*-wave junctions. The Josephson and quasiparticle tunneling are highly directional (see Sec. III.A; also Wei, Yeh, *et al.*, 1998; Nie and Coffey, 1999). The depression of the order parameter at the junction interface plays an important role in determining the  $I_c R_n$  product and other junction properties (Mannhart and Martinoli, 1991; Hilgenkamp and Mannhart, 1997). In grain-boundary junctions, combined effects of faceting and  $d_{x^2-y^2}$  pairing symmetry can partially explain the observed decrease in  $J_c$  with increasing grain-boundary misorientation angle (Hilgenkamp *et al.*, 1996). For other contributing factors, see Gurevich and Pashitskii (1998). For reviews on *d*-wave Josephson junctions, see Kupriyanov and Likharev (1990), Gross (1994), and Prester (1998).

## D. Vortex state

The superconducting cuprates have a large Ginzburg-Landau parameter (i.e.,  $\lambda_{ab}/\xi \sim 100$ ) and are therefore extreme type-II superconductors (Saint-James *et al.*, 1969; de Gennes, 1989; Poole *et al.*, 1995; Tinkham, 1996). As in the conventional low- $T_c$  type-II superconductors, magnetic field above the lower critical field  $H_{c1}$

<sup>19</sup>These include Matsumoto and Shiba, 1995a, 1995b; Kuboki and Sigrist, 1996; Balatsky, 1998; Fogelström and Yip, 1998; Franz and Tešanović, 1998; Laughlin, 1998; Salkola and Schrieffer, 1998; and Sigrist, 1998.

penetrates the bulk as integrally quantized vortices (Abrikosov, 1957). However, it has been proposed that the vortex state in a  $d$ -wave superconductor is significantly different from that in an  $s$ -wave superconductor in three aspects: the structure of the vortex itself, the way in which vortices interact with each other (e.g., the vortex lattice), and the electronic bound states within the vortex (Xu *et al.*, 1996; Maki *et al.*, 1999; Franz and Tešanović, 2000).

Various theoretical studies (Soininen *et al.*, 1994; Berlinsky *et al.*, 1995; Ren *et al.*, 1995; Schopohl and Maki, 1995; Wang and MacDonald, 1995; Ogata, 1999; Han and Lee, 2000) suggest an instability of the  $d$ -wave order parameter, resulting in  $s$ -wave pairing or time-reversal symmetry breaking near the vortex core. Furthermore, the vortex in a  $d$ -wave superconductor can be metallic or insulating and/or ferromagnetic, depending on the doping concentration (see also Zhang, 1997).

Calculations of the structure of the vortex show a slight fourfold distortion from cylindrical symmetry in the vortex core and in the magnetic fields extending away from the core (Morita *et al.*, 1998; Maki *et al.*, 1999). Although decoration experiments at low fields ( $\sim 5$  mT) indicated that the superconducting vortices in YBCO arrange themselves in a conventional hexagonal lattice (Dolan *et al.*, 1989), neutron scattering (Keimer *et al.*, 1994) and scanning tunneling microscope (Maggio-Aprile *et al.*, 1995) experiments at higher fields ( $\sim 1$  T) instead show an oblique lattice with nearly equal lattice vectors spaced by about  $75^\circ$ . Both the structure and the orientation of the vortex lattice are consistent with  $d_{x^2-y^2}$  gap pairing symmetry, although there is disagreement whether the dominant factor is a modification of the vortex core structure (Shiraishi *et al.*, 1999), or longer-range vortex-vortex interactions (Affleck *et al.*, 1997; Kogan *et al.*, 1997). Scanning tunneling microscope measurements indicate that, as opposed to conventional superconductors, which have thousands of bound states in the vortex core (Caroli *et al.*, 1964; Hess *et al.*, 1989), there is only one bound state in YBCO (Karrāi *et al.*, 1992) and possibly none in BSCCO (Maggio-Aprile *et al.*, 1995; Renner *et al.*, 1998). This is consistent with calculations of the quasiparticle spectra around a single vortex for a  $d$ -wave superconductor (Morita *et al.*, 1997, 1998). These calculations further predict low-lying excitations in four diagonal directions, which have no counterpart in  $s$ -wave superconductors.

## VII. CONCLUSIONS

Phase-sensitive symmetry tests, along with evidence from a number of non-phase-sensitive techniques, have combined to provide overwhelming evidence in favor of predominantly  $d$ -wave pairing symmetry in a number of optimally doped cuprates. The consequences of this unconventional pairing have been felt throughout the area of high-temperature superconductivity research. Due to space limitations, only a small fraction of the research work in this area has been discussed in this review.

The identification of  $d$ -wave pairing symmetry is based on very general principles of group theory and the macroscopic quantum coherence phenomena of pair tunneling and flux quantization. Therefore it does not necessarily specify a mechanism for high-temperature superconductivity. It does, however, provide general constraints on possible models. During the last 14 years it has become clear that the solution to this problem should include pairing symmetry, pairing interactions (mediated by spin fluctuations, phonons, or ...) in the presence of strong correlations, the anomalous normal state (see a recent review by Timusk and Statt, 1999), and charge segregation and the stripe phase (Tranquada, 1997). Especially intriguing is the observation of the pseudogap, also with  $d$ -wave-like  $\mathbf{k}$  dependence, in the normal state of many (mostly underdoped) cuprate superconductors (Ding, Norman *et al.*, 1996; Loeser *et al.*, 1996; Shen *et al.*, 1998). The nature of these and other anomalous normal-metal properties and their relationship to  $d$ -wave high- $T_c$  superconductivity is currently of great interest (see Anderson, 1997; Emery *et al.*, 1997). The  $SO(5)$  theory attempts to unify  $d$ -wave superconductivity in the doped cuprates with the antiferromagnetism of the undoped Mott insulators (Zhang, 1997). Given the unconventional superconducting symmetry and the anomalous normal state, the basic issue is whether we should modify or abandon the standard paradigm established during the last 50 years. Obviously, there is no easy solution to the debate of evolution versus revolution.

In the area of pairing symmetry, there are a few remaining issues. The elucidation of pairing symmetry as a function of doping, impurity, temperature, etc. is very important, since it may provide clues to the origin of high-temperature superconductivity. Pairing symmetry tests using the half-flux quantum effect were first proposed for the heavy-fermion superconductors (Geshkenbein *et al.*, 1986, 1987). Such tests have still not been done. In addition, it has been proposed that the organic superconductors such as  $\kappa$ -(BEDT-TTF)<sub>2</sub>(NCS)<sub>2</sub>, which may have unconventional pairing symmetry, are suitable candidates for phase-sensitive tests (Van Harlingen, 1999). Further, phase-sensitive tests should be carried out on possible odd-parity spin-triplet  $p$ -wave superconductors such as Sr<sub>2</sub>RuO<sub>4</sub>.

It is generally believed that the low-lying excitations in a  $d$ -wave gap give rise to damping effects in the electrodynamic response of the cuprates. This could compromise the advantage of a large gap in microwave or terahertz applications, but may not be a severe problem, given the observation of very long quasiparticle lifetimes in the superconducting state by Bonn *et al.* (1992) and Hosseini *et al.* (1999). The depression of the  $d$ -wave order parameter at interfaces such as grain boundaries (Mannhart and Martinoli, 1991) definitely reduces the critical current of some cuprates, but this is not the crucial limiting factor.

Concerning potential applications of  $d$ -wave superconductivity, a novel superconductor-antiferromagnet-superconductor (SAS) Josephson junction has been pro-

posed (Demler *et al.*, 1998; den Hertog *et al.*, 1999), in conjunction with the  $SO(5)$  theory (Zhang, 1997). The recent successful development of all-high- $T_c$   $d$ -wave  $\pi$  SQUID's (Schulz *et al.*, 2000) represents an important step towards the realization of the complementary Josephson-junction devices and circuits proposed by Terzioglu and Beasley (1998). It has been suggested that the bistable magnetic-flux state in a  $\pi$  ring [see Fig. 7(b)] be exploited for quantum computation (Ioffe *et al.*, 1999). Quantum computation (Bennett, 1995; DiVincenzo, 1995; Barenco, 1996; Ekert and Jozsa, 1996) is based on the superposition principle of quantum mechanics and has been proposed as a means for performing certain types of computation much faster than conventional computers. The realization of quantum computation depends on maintaining quantum coherence in the presence of dissipation. Ioffe *et al.* (1999) proposed a device that is a combination of  $s$ -wave and  $d$ -wave Josephson elements, and discussed the decoherence of such devices. The realization of a  $d$ -wave quantum computer would be an exciting outcome of the ideas discussed in this review.

In short, the identification of  $d$ -wave pairing symmetry represents an important step towards a better understanding of high-temperature superconductivity and may lead to novel applications in the future.

#### ACKNOWLEDGMENTS

We would like to thank J. F. Annett, T. Doderer, R. P. Hübener, M. B. Ketchen, R. H. Koch, Z. Z. Li, J. Mannhart, K. A. Moler, D. M. Newns, H. Raffy, J. Z. Sun, M. B. Walker, S. I. Woods, and S. K. Yip for discussion and comments in the process of writing this review.

#### REFERENCES

- Abrikosov, A. A., 1957, *Sov. Phys. JETP* **5**, 1174.  
 Abrikosov, A. A., 1996, *Physica C* **258**, 53.  
 Abrikosov, A. A., J. C. Campuzano, and K. Gofron, 1993, *Physica C* **214**, 73.  
 Affleck, I., M. Franz, and M. H. Sharifzadeh Amin, 1997, *Phys. Rev. B* **55**, R704.  
 Agassi, D., and J. R. Cullen, 1996, *Phys. Rev. B* **54**, 10112.  
 Alber, M., B. Bäuml, R. Ernst, D. Kienle, A. Kopf, and M. Rouchal, 1996, *Phys. Rev. B* **53**, 5863.  
 Alff, L., A. Beck, R. Gross, A. Marx, S. Kleefisch, Th. Bauch, H. Sato, M. Naito, and G. Koren, 1998, *Phys. Rev. B* **58**, 11197.  
 Alff, L., S. Kleefisch, U. Schoop, M. Zittartz, T. Kemen, T. Bauch, A. Marx, and R. Gross, 1998, *Eur. Phys. J. B* **5**, 423.  
 Alff, L., S. Meyer, S. Kleefisch, U. Schoop, A. Marx, H. Sato, M. Naito, and R. Gross, 1999, *Phys. Rev. Lett.* **83**, 2644.  
 Alff, L., H. Takashima, S. Kashiwaya, N. Terada, H. Ihara, Y. Tanaka, M. Koyanagi, and K. Kajimura, 1997, *Phys. Rev. B* **55**, R14757.  
 Allen, P. B., 1990, in *High-Temperature Superconductivity*, edited by J. W. Lynn (Springer, New York), p. 303.  
 Alvarez, J. J. V., G. C. Buscaglia, and C. A. Balseiro, 1996, *Phys. Rev. B* **54**, 16168.  
 Ambegaokar, V., and A. Baratoff, 1963, *Phys. Rev. Lett.* **10**, 456; **11**, 104(E).  
 Andersen, O. K., A. I. Liechtenstein, O. Jepsen, and F. Paulsen, 1995, *J. Phys. Chem. Solids* **56**, 1573.  
 Anderson, P. W., 1964, in *Lectures on the Many-Body Problem*, Vol. 2, edited by E. R. Caianiello (Academic, New York), p. 113.  
 Anderson, P. W., 1966a, *Rev. Mod. Phys.* **38**, 298.  
 Anderson, P. W., 1966b, *Phys. Rev. Lett.* **17**, 95.  
 Anderson, P. W., 1984, *Basic Notions of Condensed-Matter Physics* (Benjamin-Cummings, San Francisco).  
 Anderson, P. W., 1997, *The Theory of Superconductivity in the High- $T_c$  Cuprates* (Princeton University, Princeton, New Jersey).  
 Anderson, P. W., 1998, "Anomalous magnetothermal resistance of high- $T_c$  superconductors: anomalous cyclotron orbits at a Dirac point," e-print, cond-mat/9812063.  
 Anderson, P. W., and W. F. Brinkman, 1973, *Phys. Rev. Lett.* **30**, 1108.  
 Anderson, P. W., and J. M. Rowell, 1963, *Phys. Rev. Lett.* **10**, 230.  
 Andreone, A., A. Cassinese, A. Di Chiara, R. Vaglio, A. Gupta, and E. Sarnelli, 1994, *Phys. Rev. B* **49**, 6392.  
 Anlage, S. M., D. W. Wu, J. Mao, S. N. Mao, X. X. Xi, T. Venkatesan, J. L. Peng, and R. L. Greene, 1994, *Phys. Rev. B* **50**, 523.  
 Annett, J. F., 1991, *Adv. Phys.* **39**, 83.  
 Annett, J. F., N. D. Goldenfeld, and A. J. Leggett, 1996, in *Physical Properties of High-Temperature Superconductors V*, edited by D. M. Ginsberg (World Scientific, Singapore), p. 376.  
 Annett, J. F., N. D. Goldenfeld, and S. R. Renn, 1990, in *Physical Properties of High-Temperature Superconductors II*, edited by D. M. Ginsberg (World Scientific, Singapore), p. 571.  
 Annett, J. F., N. D. Goldenfeld, and S. R. Renn, 1991, *Phys. Rev. B* **43**, 2778.  
 Antognazza, L., B. H. Moeckly, T. H. Geballe, and K. Char, 1995, *Phys. Rev. B* **52**, 4559.  
 Appelbaum, J., 1966, *Phys. Rev. Lett.* **17**, 91.  
 April, M., M. Covington, E. Paroanu, B. Niedermeier, and L. H. Greene, 1998, *Phys. Rev. B* **57**, R8139.  
 Artemenko, S. N., L. N. Bulaevskii, M. P. Maley, and V. M. Vinokur, 1999, *Phys. Rev. B* **59**, 11587.  
 Atkinson, W. A., and J. P. Carbotte, 1995, *Phys. Rev. B* **51**, 16371.  
 Aubin, H., K. Behnia, S. Ooi, and T. Tamegai, 1999, *Phys. Rev. Lett.* **82**, 624.  
 Aubin, H., K. Behnia, S. Ooi, T. Tamegai, K. Krishna, N. P. Ong, Q. Li, G. Gu, and N. Koshizuka, 1998, *Science* **280**, 11.  
 Aubin, H., K. Behnia, M. Ribault, R. Gagnon, and L. Taillefer, 1997, *Phys. Rev. Lett.* **78**, 2624.  
 Bahcall, S. R., 1996, *Phys. Rev. Lett.* **76**, 3634.  
 Balatsky, A. V., 1998, *Phys. Rev. Lett.* **80**, 1972.  
 Barash, Yu. S., A. V. Galaktionov, and A. D. Zaikin, 1995, *Phys. Rev. B* **52**, 665.  
 Barbara, P., F. M. Aroujo-Moreira, A. B. Cawthorne, and C. J. Lobb, 1999, *Phys. Rev. B* **60**, 7489.  
 Barenco, A., 1996, *Contemp. Phys.* **37**, 375.  
 Bardeen, J., L. N. Cooper, and J. R. Schrieffer, 1957, *Phys. Rev.* **108**, 1175.  
 Barone, A., and Paterno, G., 1982, *Physics and Applications of the Josephson Effect* (Wiley, New York).

- Barrett, S. E., D. J. Durand, C. H. Pennington, C. P. Slichter, T. A. Friedman, J. P. Rice, and D. M. Ginsberg, 1990, *Phys. Rev. B* **41**, 6283.
- Basov, D. N., H. A. Mook, B. Dabrowski, and T. Timusk, 1995, *Phys. Rev. B* **52**, R13141.
- Béal-Monod, M. T., 1998, *Phys. Rev. B* **58**, 8830.
- Bednorz, J. G., and K. A. Müller, 1986, *Z. Phys. B* **64**, 189.
- Belzig, W., C. Bruder, and M. Sigrist, 1998, *Phys. Rev. Lett.* **80**, 4285.
- Bennett, C. H., 1995, *Phys. Today* **48**(10), 24.
- Berlinsky, A. J., A. L. Fetter, M. Franz, C. Kallin, and P. I. Soininen, 1995, *Phys. Rev. Lett.* **75**, 2200.
- Beyers, R., and T. M. Shaw, 1988, in *Solid State Physics*, Vol. 42, edited by H. Ehrenreich and D. Turnbull (Academic, San Diego), p. 135.
- Bhattacharya, A., I. Zutic, O. T. Valls, A. M. Goldman, U. Welp, and B. Veal, 1999a, *Phys. Rev. Lett.* **82**, 3132.
- Bhattacharya, A., I. Zutic, O. T. Valls, A. M. Goldman, U. Welp, and B. Veal, 1999b, *Phys. Rev. Lett.* **83**, 887.
- Bickers, N. E., D. J. Scalapino, and R. T. Scalettar, 1987, *Int. J. Mod. Phys. B* **1**, 687.
- Bickers, N. E., D. J. Scalapino, and S. R. White, 1989, *Phys. Rev. Lett.* **62**, 961.
- Bidinosti, C. P., W. N. Hardy, D. A. Bonn, and Ruixing Liang, 1999, *Phys. Rev. Lett.* **83**, 3277.
- Blount, E. I., 1985, *Phys. Rev. B* **32**, 2935.
- Bonn, D. A., P. Dosanjh, R. Liang, and W. N. Hardy, 1992, *Phys. Rev. Lett.* **68**, 2390.
- Bonn, D. A., and W. N. Hardy, 1996, in *Physical Properties of High-Temperature Superconductors*, Vol. 5, edited by D. M. Ginsberg (World Scientific, Singapore).
- Braunisch, W., N. Knauf, G. Bauer, A. Kock, A. Becker, B. Freitag, A. Grütz, V. Kataev, S. Neuhausen, B. Roden, D. Khomskii, and D. Wohlleben, 1993, *Phys. Rev. B* **48**, 4030.
- Braunisch, W., N. Knauf, V. Kateev, S. Neuhausen, A. Grütz, A. Koch, B. Roden, D. Khomskii, and D. Wohlleben, 1992, *Phys. Rev. Lett.* **68**, 1908.
- Brawner, D. A., and H. R. Ott, 1994, *Phys. Rev. B* **50**, 6530.
- Bromley, S. T., and D. J. Newman, 1998, *Physica C* **297**, 294.
- Bruder, C., A. Van Otterlo, and G. T. Zimanyi, 1995, *Phys. Rev. B* **51**, 12904.
- Buchholtz, L. J., M. Palumbo, D. Rainer, and J. A. Sauls, 1995a, *J. Low Temp. Phys.* **101**, 1079.
- Buchholtz, L. J., M. Palumbo, D. Rainer, and J. A. Sauls, 1995b, *J. Low Temp. Phys.* **101**, 1099.
- Bulaevskii, L. N., V. V. Kuzii, and A. A. Sobyenin, 1977, *JETP Lett.* **25**, 290.
- Bulut, N., and D. J. Scalapino, 1991, *Phys. Rev. Lett.* **67**, 2898.
- Bulut, N., and D. J. Scalapino, 1992a, *Phys. Rev. Lett.* **68**, 706.
- Bulut, N., and D. J. Scalapino, 1992b, *Phys. Rev. B* **45**, 2371.
- Bulut, N., and D. J. Scalapino, 1996, *Phys. Rev. B* **54**, 14971.
- Byers, J. M., M. E. Flatte, and D. J. Scalapino, 1993, *Phys. Rev. Lett.* **71**, 3363.
- Cappelluti, E., C. Grimaldi, and L. Pietronero, 1997, *J. Supercond.* **10**, 397.
- Cappelluti, E., and L. Pietronero, 1996, *Europhys. Lett.* **36**, 619.
- Carmi, R., R. Polturak, G. Koren, and A. Auerbach, 2000, "Appearance of spontaneous macroscopic magnetization at the superconducting transition of YBCO," e-print, cond-mat/0001050.
- Caroli, C., P. G. de Gennes, and J. Matricon, 1964, *Phys. Lett.* **9**, 307.
- Chang, A. M., H. D. Hallen, H. F. Hess, H. L. Kao, J. Kwo, A. Sudbo, and T. Y. Chang, 1992, *Europhys. Lett.* **20**, 645.
- Char, K., M. S. Colclough, S. M. Garrison, N. Newman, and G. Zaharchuk, 1991, *Appl. Phys. Lett.* **59**, 3030.
- Chaudhari, P., and S. Y. Lin, 1994, *Phys. Rev. Lett.* **72**, 1084.
- Chen, C. H., 1992, in *Physical Properties of High Temperature Superconductors III*, edited by D. M. Ginsberg (World Scientific, Singapore), p. 200.
- Chen, L., C. J. Wei, and A. M. S. Tremblay, 1993, *Phys. Rev. B* **47**, 15316.
- Chesca, B., 1999, *Ann. Phys. (Leipzig)* **8**, 511.
- Chiao, M., R. W. Hill, Ch. Lupien, L. Taillefer, P. Lambert, R. Gagnon, and P. Fournier, 2000, *Phys. Rev. B* **62**, 3554.
- Chien, T. R., W. R. Datars, M. D. Lan, J. Z. Liu, and R. N. Shelton, 1994, *Phys. Rev. B* **49**, 1342.
- Chmaissem, O., J. D. Jorgensen, S. Short, A. Knizhnik, Y. Eckstein, and H. Shaked, 1999, *Nature (London)* **397**, 45.
- Chu, C. W., L. Gao, F. Chen, Z. J. Huang, R. L. Meng, and Y. Y. Xue, 1993, *Nature (London)* **365**, 323.
- Clarke, D. G., S. P. Strong, and P. W. Anderson, 1995, *Phys. Rev. Lett.* **74**, 4499.
- Clarke, J., 1966, *Philos. Mag.* **13**, 115.
- Clarke, J., 1989, *Proc. IEEE* **77**, 1208.
- Clem, J. R., 1998, *Supercond. Sci. Technol.* **11**, 909.
- Clem, J. R., and M. W. Coffey, 1990, *Phys. Rev. B* **42**, 6209.
- Coffey, L., and D. Coffey, 1993, *Phys. Rev. B* **48**, 4184.
- Cohen, M. H., L. M. Falicov, and J. C. Phillips, 1962, *Phys. Rev. Lett.* **8**, 316.
- Cooper, J. R., 1996, *Phys. Rev. B* **54**, R3753.
- Cooper, S. L., and K. E. Gray, 1994, in *Physical Properties of High-Temperature Superconductors IV*, edited by D. M. Ginsberg, (World Scientific, Singapore), p. 61.
- Copetti, C. A., F. Rueders, B. Oleze, C. Buchal, and B. Kobius, 1995, *Physica C* **253**, 63.
- Corson, J., J. Orenstein, S. Oh, J. O'Donnell, and J. N. Eckstein, 2000, "Nodal quasiparticle lifetime in BSCCO," e-print, cond-mat/0003243.
- Covington, M., M. Aprili, E. Paraoanu, L. H. Greene, F. Xu, J. Zhu, and C. A. Mirkin, 1997, *Phys. Rev. Lett.* **79**, 277.
- Cyrot, M., 1973, *Rep. Prog. Phys.* **36**, 103.
- Dagotto, E., 1994, *Rev. Mod. Phys.* **6**, 763.
- Dagotto, E., A. Nazarenko, and M. Boninsegni, 1994, *Phys. Rev. Lett.* **73**, 728.
- Dahm, T., and D. J. Scalapino, 1999, "Nonlinear current response of a *d*-wave superfluid," e-print, cond-mat/9908332.
- Danylenko, O. V., O. V. Dolgov, M. L. Kulić, and V. Oudovenko, 1999, *Eur. Phys. J. B* **9**, 201.
- Das Sarma, S., and E. H. Hwang, 1998, *Phys. Rev. Lett.* **80**, 4753.
- de Gennes, P. G., 1989, *Superconductivity of Metals and Alloys* (Addison-Wesley, New York).
- Demler, E., A. J. Berlinsky, C. Kallin, G. B. Arnold, and M. R. Beasley, 1998, *Phys. Rev. Lett.* **80**, 2917.
- den Hertog, B. C., A. J. Berlinsky, and C. Kallin, 1999, *Phys. Rev. B* **59**, R11645.
- Dessau, D. S., Z. X. Shen, D. M. King, D. S. Marshall, L. W. Lombardo, P. H. Dickinson, A. G. Loeser, J. DiCarlo, C. H. Park, A. Kapitulnik, and W. E. Spicer, 1993, *Phys. Rev. Lett.* **71**, 2781.
- Devereaux, T. P., and D. Einzel, 1995, *Phys. Rev. B* **51**, 16336.
- Devereaux, T. P., D. Einzel, B. Stadlober, R. Hackl, D. H. Leach, and J. J. Neumeier, 1994, *Phys. Rev. Lett.* **72**, 396.

- Dimos, D., P. Chaudhari, and J. Mannhart, 1990, *Phys. Rev. B* **41**, 4038.
- Ding, H., M. R. Norman, J. C. Campuzano, M. Randeria, A. F. Bellman, T. Yokoya, T. Takahashi, T. Mochiku, and K. Kadowaki, 1996, *Phys. Rev. B* **54**, R9678.
- Ding, H., M. R. Norman, T. Mochiku, K. Kadowaki, and J. Giapinzakis, 1996, *Nature (London)* **382**, 51.
- DiVincenzo, D., 1995, *Science* **270**, 255.
- Dolan, G. J., F. Holtzberg, C. Feild, and T. R. Dinger, 1989, *Phys. Rev. Lett.* **62**, 2184.
- Drost, R. J., C. J. van der Beek, H. W. Zandbergen, M. Konczykowski, A. A. Menovsky, and P. H. Kes, 1999, *Phys. Rev. B* **59**, 13612.
- Durst, A. C., and P. A. Lee, 1999, *Phys. Rev. B* **62**, 1270.
- Durusoy, H. Z., D. Lew, L. Lombardo, A. Kapitulnik, T. H. Geballe, and M. R. Beasley, 1996, *Physica C* **266**, 253.
- Dynes, R. C., 1994, *Solid State Commun.* **92**, 53.
- Ekert, A., and R. Jozsa, 1996, *Rev. Mod. Phys.* **68**, 733.
- Ekin, J. W., Y. Xu, S. Mao, T. Venkatesan, D. W. Face, M. Eddy, and S. A. Wolfe, 1997, *Phys. Rev. B* **56**, 13746.
- Emery, V. J., S. A. Kivelson, and O. Zachar, 1997, *Phys. Rev. B* **56**, 6120.
- Feder, D. L., A. Beardsall, A. J. Berlinski, and C. Kallin, 1997, *Phys. Rev. B* **56**, R5751.
- Feenstra, B. J., J. Schützmann, D. van der Marel, R. Pérez Pinaya, and M. Decroux, 1997, *Phys. Rev. Lett.* **79**, 4890.
- Fiske, M., 1964, *Rev. Mod. Phys.* **36**, 221.
- Fogelström, M., D. Rainer, and J. A. Sauls, 1997, *Phys. Rev. Lett.* **79**, 281.
- Fogelström, M., and S.-K. Yip, 1998, *Phys. Rev. B* **57**, R14060.
- Franck, J. P., and D. Lawrie, 1994, *Physica C* **235-240**, 1503.
- Franz, M., and Z. Tešanović, 1998, *Phys. Rev. Lett.* **80**, 4763.
- Franz, M., and Z. Tešanović, 2000, *Phys. Rev. Lett.* **84**, 554.
- Friedel, J., 1987, *J. Phys. (Paris)* **48**, 1787.
- Friedel, J., 1989, *J. Phys.: Condens. Matter* **1**, 7757.
- Fulde, P., J. Keller, and G. Zwicknagl, 1988, *Solid State Phys.* **41**, 1.
- Geim, A. K., S. V. Dubonos, J. G. S. Lok, M. Henini, and J. C. Maan, 1998, *Nature (London)* **396**, 144.
- Geshkenbein, V. B., and A. I. Larkin, 1986, *JETP Lett.* **43**, 395.
- Geshkenbein, V. B., A. I. Larkin, and A. Barone, 1987, *Phys. Rev. B* **36**, 235.
- Ghosh, A., and K. Adhikari, 1998a, *J. Phys.: Condens. Matter* **10**, L319.
- Ghosh, A., and K. Adhikari, 1998b, *Physica C* **309**, 251.
- Gim, Y., A. Mathai, R. Black, A. Amar, and F. C. Wellstood, 1997, *IEEE Trans. Appl. Supercond.* **7**, 2331.
- Ginzburg, V. L., and L. G. Landau, 1950, *Zh. Eksp. Teor. Fiz.* **20**, 1064.
- Gofron, K., J. C. Campuzano, A. A. Abrikosov, M. Lindroos, A. Bansil, H. Ding, D. Koelling, and B. Dabrowski, 1994, *Phys. Rev. Lett.* **73**, 3302.
- Gor'kov, L. P., 1959, *Zh. Eksp. Teor. Fiz.* **36**, 1918.
- Gor'kov, L. P., 1987, *Sov. Sci. Rev., Sect. A* **9**, 1.
- Gough, C. E., M. S. Colclough, E. M. Forgan, R. G. Jordan, M. Keene, C. M. Muirhead, A. I. M. Rae, N. Thomas, J. S. Abell, and S. Sutton, 1987, *Nature (London)* **326**, 855.
- Graf, M. J., M. Palumbo, D. Rainer, and J. A. Sauls, 1995, *Phys. Rev. B* **52**, 10588.
- Graf, M. J., D. Rainer, and J. A. Sauls, 1993, *Phys. Rev. B* **47**, 12089.
- Graf, M. J., S.-K. Yip, J. A. Sauls, and D. Rainer, 1996, *Phys. Rev. B* **53**, 15147.
- Gray, K. E., and D. H. Kim, 1993, *Phys. Rev. Lett.* **70**, 1693.
- Gross, R., 1994, in *Interfaces in Superconducting Systems*, edited by S. L. Shinde and D. Rudman (Springer, New York), p. 176.
- Gurevich, A., and E. A. Pashitskii, 1998, *Phys. Rev. B* **57**, 13878.
- Hadjiev, V. G., X. Zhou, T. Strohm, M. Cardona, Q. M. Lin, and C. W. Chu, 1998, *Phys. Rev. B* **58**, 1043.
- Hamann, D. R., and L. F. Mattheiss, 1988, *Phys. Rev. B* **38**, 5138.
- Han, J. H., and D.-H. Lee, 2000, *Phys. Rev. Lett.* **85**, 1100.
- Hardy, W. N., D. A. Bonn, D. C. Morgan, Ruixing Liang, and Kuan Zhang, 1993, *Phys. Rev. Lett.* **70**, 3999.
- Hasegawa, T., and K. Kitazawa, 1991, *Physica C* **185**, 1743.
- Hatsugai, Y., and P. A. Lee, 1993, *Phys. Rev. B* **48**, 4204.
- Heinzel, Ch., Th. Theilig, and P. Ziemann, 1993, *Phys. Rev. B* **48**, 3445.
- Hensen, S., G. Müller, C. T. Rieck, and K. Scharnberg, 1997, *Phys. Rev. B* **56**, 6237.
- Hess, H. F., R. B. Robinson, R. C. Dynes, J. M. Valles, Jr., and J. V. Waczczak, 1989, *Phys. Rev. Lett.* **62**, 214.
- Hewitt, K. C., T. P. Devereaux, X. K. Chen, X.-Z. Wang, J. G. Naeni, A. E. Curzon, J. C. Irwin, A. Martin, C. Kendziora, and M. Onellion, 1997, *Phys. Rev. Lett.* **78**, 4891.
- Hilgenkamp, H., and J. Mannhart, 1997, *Appl. Phys. A: Mater. Sci. Process.* **64**, 553.
- Hilgenkamp, H., and J. Mannhart, 1999, *IEEE Trans. Appl. Supercond.* **9**, 3405.
- Hilgenkamp, H., J. Mannhart, and B. Mayer, 1996, *Phys. Rev. B* **53**, 14586.
- Hinaus, B. M., M. S. Rzchowski, N. Heinig, X. Y. Cai, and D. L. Kaiser, 1996, *Phys. Rev. B* **54**, 6770.
- Hirschfeld, P. J., and N. Goldenfeld, 1993, *Phys. Rev. B* **48**, 4219.
- Hirschfeld, P. J., W. O. Puttিকা, and D. J. Scalapino, 1993, *Phys. Rev. Lett.* **71**, 3705.
- Hirschfeld, P. J., W. O. Puttিকা, and D. J. Scalapino, 1994, *Phys. Rev. B* **50**, 10250.
- Hirschfeld, P. J., S. M. Quinlan, and D. J. Scalapino, 1997, *Phys. Rev. B* **55**, 12742.
- Hoevers, H. F. C., P. J. M. van Bentum, L. E. C. van de Lemput, H. van Kempen, A. J. G. Schellingerhout, and D. van der Marel, 1988, *Physica C* **152**, 105.
- Hosseini, A., R. Harris, Saeid Kamal, P. Dosanjh, J. Preston, Ruixing Liang, W. N. Hardy, and D. A. Bonn, 1999, *Phys. Rev. B* **60**, 1349.
- Hosseini, A., S. Kamal, D. A. Bonn, Ruixing Liang, and W. N. Hardy, 1998, *Phys. Rev. Lett.* **81**, 1298.
- Hu, C.-R., 1994, *Phys. Rev. Lett.* **72**, 1526.
- Hu, C.-R., 1998, *Phys. Rev. B* **57**, 1266.
- Huang, Q., J. F. Zasadzinski, N. Tralshawala, K. E. Gray, D. G. Hinks, J. L. Peng, and R. L. Greene, 1990, *Nature (London)* **347**, 369.
- Hudson, E. W., S. H. Pan, A. K. Gupta, K.-W. Ng, and J. C. Davis, 1999, *Science* **285**, 88.
- Hussey, N. E., J. R. Cooper, R. A. Doyle, C. T. Lin, W. Y. Liang, D. C. Sinclair, G. Balakrishnan, and D. M. Paul, 1996, *Phys. Rev. B* **53**, 6752.
- Husslein, T., I. Morgenstern, D. M. Newns, P. C. Pattnaik, J. M. Singer, and H. G. Matuttis, 1996, *Phys. Rev. B* **54**, 16179.
- Hyun, O. B., J. R. Clem, and D. K. Finnemore, 1989, *Phys. Rev. B* **40**, 175.
- Iguchi, I., and Z. Wen, 1994, *Phys. Rev. B* **49**, 12388.

- Il'ichev, E., V. Zakosarenko, R. P. J. Ijsselsteijn, H. E. Hoenig, H.-G. Meyer, M. V. Fistul, and P. Müller, 1999a, *Phys. Rev. B* **59**, 11502.
- Il'ichev, E., V. Zakosarenko, R. P. J. Ijsselsteijn, V. Schultze, H.-G. Meyer, H. E. Hoenig, H. Hilgenkamp, and J. Manhart, 1998, *Phys. Rev. Lett.* **81**, 894.
- Il'ichev, E., V. Zakosarenko, R. P. J. Ijsselsteijn, V. Schultze, H.-G. Meyer, H. E. Hoenig, and H. Töpfer, 1999b, *IEEE Trans. Appl. Supercond.* **9**, 3994.
- Imada, M., A. Fujimori, and Y. Tokura, 1998, *Rev. Mod. Phys.* **70**, 1039.
- Ioffe, L. B., V. B. Geshkenbein, M. V. Feigel'man, A. L. Fauchère, and G. Blatter, 1999, *Nature (London)* **398**, 679.
- Jannossy, B., R. Hergt, and L. Fruchter, 1990, *Physica C* **170**, 22.
- Jepsen, O., O. K. Andersen, I. Dasgupta, and S. Savrasov, 1998, *J. Phys. Chem. Solids* **59**, 1718.
- Jha, S. S., 1996, *J. Raman Spectrosc.* **27**, 321.
- Jha, S. S., and A. K. Rajagopal, 1997, *Phys. Rev. B* **55**, 15248.
- Jiang, C., and J. P. Carbotte, 1996, *Phys. Rev. B* **53**, 11868.
- Josephson, B. D., 1962, *Phys. Rev. Lett.* **1**, 251.
- Joynt, R., 1990, *Phys. Rev. B* **41**, 4271.
- Kamal, S., Ruixing Liang, A. Hosseini, D. A. Bonn, and W. N. Hardy, 1998, *Phys. Rev. B* **58**, R8933.
- Kamimura, H., S. Matsuno, Y. Suwa, and H. Ushio, 1996, *Phys. Rev. Lett.* **77**, 723.
- Kaminski, A., J. Mesot, H. Fretwell, J. C. Campuzano, M. R. Norman, M. Randeria, H. Ding, T. Sato, T. Takahashi, T. Mochiku, K. Kadowaki, and H. Hoehst, 2000, *Phys. Rev. Lett.* **84**, 1788.
- Karpińska, K., M. Z. Cieplak, S. Guha, A. Malinowski, T. Skośkiewicz, W. Plesiewicz, M. Berkowski, B. Boyce, T. R. Lemberger, and P. Lindenfied, 2000, *Phys. Rev. Lett.* **84**, 155.
- Karräi, K., E. J. Choi, F. Dunmore, S. Liu, H. D. Drew, Qi Li, D. B. Fenner, Y. D. Zhu, and Fu-Chun Zhang, 1992, *Phys. Rev. Lett.* **69**, 152.
- Kashiwaya, S., T. Ito, K. Oka, S. Ueno, H. Takashima, M. Koyanagi, Y. Tanaka, and K. Kajimura, 1998, *Phys. Rev. B* **57**, 8680.
- Kashiwaya, S., Y. Tanaka, M. Koyanagi, H. Takashima, and K. Kajimura, 1995, *Phys. Rev. B* **51**, 1350.
- Katz, A. S., A. G. Sun, R. C. Dynes, and K. Char, 1995, *Appl. Phys. Lett.* **66**, 105.
- Keene, M. N., T. J. Jackson, and C. E. Gough, 1989, *Nature (London)* **340**, 210.
- Keimer, B., W. Y. Shih, R. W. Erwin, J. W. Lynn, F. Dogan, and I. A. Aksay, 1994, *Phys. Rev. Lett.* **73**, 3459.
- Kendziora, C., R. J. Kelley, and M. Onellion, 1996, *Phys. Rev. Lett.* **77**, 727.
- Ketchen, M. B., W. J. Gallagher, A. W. Kleinsasser, S. Murphy, and J. R. Clem, 1985, in *SQUID'85: Superconducting Quantum Interference Devices and their Applications*, edited by H. D. Hahlbohm and H. Lübbig (Walter de Gruyter, Berlin), p. 865.
- Ketchen, M. B., D. Pearson, A. W. Kleinsasser, C. K. Hu, M. Smyth, J. Logan, K. Stawiasz, E. Baran, M. Jaso, T. Ross, M. Manny, S. Basavaiah, S. Brodsky, S. B. Kaplan, W. J. Gallagher, and M. Bhushan, 1991, *Appl. Phys. Lett.* **59**, 2609.
- Khomskii, D., 1994, *J. Low Temp. Phys.* **95**, 205.
- Kim, J. H., and Z. Tešanović, 1993, *Phys. Rev. Lett.* **71**, 4218.
- King, D. M., Z.-X. Shen, D. S. Dessau, B. O. Wells, W. E. Spicer, A. J. Arko, D. S. Marshall, J. DiCarlo, A. G. Loeser, C. H. Park, E. R. Ratner, J. L. Peng, Z. Y. Li, and R. L. Greene, 1993, *Phys. Rev. Lett.* **70**, 3159.
- Kirtley, J. R., P. Chaudhari, M. B. Ketchen, N. Khare, S. Y. Lin, and T. Shaw, 1995, *Phys. Rev. B* **51**, R12057.
- Kirtley, J. R., M. B. Ketchen, K. G. Stawiasz, J. Z. Sun, W. J. Gallagher, S. H. Blanton, and S. J. Wind, 1995, *Appl. Phys. Lett.* **66**, 1138.
- Kirtley, J. R., K. A. Moler, and D. J. Scalapino, 1997, *Phys. Rev. B* **56**, 886.
- Kirtley, J. R., K. A. Moler, G. Villard, and A. Maignan, 1998, *Phys. Rev. Lett.* **81**, 2140.
- Kirtley, J. R., A. C. Mota, M. Sigrist, and T. M. Rice, 1998, *J. Phys.: Condens. Matter* **10**, L97.
- Kirtley, J. R., C. C. Tsuei, and K. A. Moler, 1999b, *Science* **285**, 1373.
- Kirtley, J. R., C. C. Tsuei, K. A. Moler, V. G. Kogan, J. R. Clem, and A. J. Turberfield, 1999a, *Appl. Phys. Lett.* **74**, 4011.
- Kirtley, J. R., C. C. Tsuei, H. Raffy, Z. Z. Li, A. Gupta, J. Z. Sun, and S. Megert, 1996, *Europhys. Lett.* **36**, 707.
- Kirtley, J. R., C. C. Tsuei, M. Rupp, J. Z. Sun, L. S. Yu-Jahnes, A. Gupta, M. B. Ketchen, K. A. Moler, and M. Bhushan, 1996, *Phys. Rev. Lett.* **76**, 1336.
- Kirtley, J. R., C. C. Tsuei, J. Z. Sun, C. C. Chi, Lock-See Yu-Jahnes, A. Gupta, M. Rupp, and M. B. Ketchen, 1995, *Nature (London)* **373**, 225.
- Kitano, H., T. Hanaguri, and A. Maeda, 1998, *Phys. Rev. B* **57**, 10946.
- Kleiner, R., and P. Müller, 1994, *Phys. Rev. B* **49**, 1327.
- Kleiner, R., A. S. Katz, A. G. Sun, R. Summer, D. A. Gajewski, S. H. Han, S. I. Woods, E. Dnatsker, B. Chen, K. Char, M. B. Maple, R. C. Dynes, and John Clarke, 1996, *Phys. Rev. Lett.* **76**, 2161.
- Klemm, R. A., 1994, *Phys. Rev. Lett.* **73**, 1871.
- Klemm, R. A., G. Arnold, C. T. Rieck, and K. Scharnberg, 1998, *Phys. Rev. B* **58**, 14203.
- Klemm, R. A., and S. H. Liu, 1995, *Phys. Rev. Lett.* **74**, 2343.
- Klemm, R. A., C. T. Rieck, and K. Scharnberg, 1998, *Phys. Rev. B* **58**, 1051.
- Knauf, N., J. Fischer, P. Schmidt, B. Roden, R. Borowski, B. Buechner, H. Micklitz, A. Freimuth, D. Khomskii, and V. Kateev, 1998, *Physica C* **299**, 125.
- Koelle, D., R. Kleiner, F. Ludwig, E. Dantsker, and John Clarke, 1999, *Rev. Mod. Phys.* **71**, 631.
- Kogan, V. G., M. Bullock, B. Harmon, P. Miranović, Lj. Dobrosaljević-Grujić, P. L. Gammel, and D. J. Bishop, 1997, *Phys. Rev. B* **55**, R8693.
- Kogan, V. G., A. Yu. Siminov, and M. Ledvij, 1993, *Phys. Rev. B* **48**, 392.
- Kokales, J. D., P. Fournier, L. V. Mercaldo, V. V. Talanov, R. L. Greene, and S. M. Anlage, 2000, "Microwave electrodynamics and pairing symmetry of electron-doped cuprate superconductors," e-print, cond-mat/0002300.
- Koltenbah, B. E. C., and R. Joynt, 1997, *Rep. Prog. Phys.* **60**, 23.
- Koren, G., E. Polturak, N. Levy, G. Deutscher, and N. D. Zakharov, 1998, *Appl. Phys. Lett.* **73**, 3763.
- Koshelev, A. E., and A. I. Larkin, 1995, *Phys. Rev. B* **52**, 13599.
- Kostić, P., B. Veal, A. P. Paulikas, U. Welp, V. R. Todt, C. Gu, U. Geiser, J. M. Williams, K. D. Carlson, and R. A. Klemm, 1996, *Phys. Rev. B* **53**, 791.
- Kotliar, G., 1988, *Phys. Rev. B* **37**, 3664.

- Kouznetsov, K. A., A. G. Sun, B. Chen, A. S. Katz, S. R. Bahcall, J. Clarke, R. C. Dynes, D. A. Gajewski, S. H. Han, M. B. Maple, J. Giapintzakis, J.-T. Kim, and D. M. Ginsberg, 1997, *Phys. Rev. Lett.* **79**, 3050.
- Krakauer, H., and W. E. Pickett, 1988, *Phys. Rev. Lett.* **60**, 1665.
- Krakauer, H., W. E. Pickett, and R. E. Cohen, 1988, *J. Supercond.* **1**, 111.
- Krishana, K., N. P. Ong, Q. Li, G. D. Gu, and N. Koshizuka, 1997, *Science* **277**, 83.
- Krishana, K., N. P. Ong, Q. Li, G. D. Gu, and N. Koshizuka, 1998, *J. Phys. Chem. Solids* **59**, 2088.
- Kruchinin, S. P., and S. K. Patapis, 1997, *Physica C* **282-287**, 1397.
- Krupke, R., and G. Deutscher, 1999, *Phys. Rev. Lett.* **83**, 4634.
- Kübert, C., and P. J. Hirschfeld, 1998, *J. Phys. Chem. Solids* **59**, 1835.
- Kuboki, K., and M. Sigrist, 1996, *J. Phys. Soc. Jpn.* **65**, 361.
- Kupriyanov, M. Yu., and K. K. Likharev, 1990, *Sov. Phys. Usp.* **33**, 340.
- Kusmartsev, F. V., 1992, *Phys. Rev. Lett.* **69**, 2268.
- Kwo, J., T. A. Fulton, M. Hong, and P. L. Gammel, 1990, *Appl. Phys. Lett.* **56**, 788.
- Labbe, J., 1989, *Phys. Scr.* **T29**, 82.
- Labbe, J., and J. Bok, 1987, *Europhys. Lett.* **3**, 1225.
- Landau, L. D., 1957, *Sov. Phys. JETP* **3**, 920.
- Landau, L. D., and E. M. Lifshitz, 1979, *Statistical Physics* (Pergamon, New York), Part I.
- Laughlin, R. B., 1994, *Physica C* **234**, 280.
- Laughlin, R. B., 1998, *Phys. Rev. Lett.* **80**, 5188.
- Lee, J. D., K. Kang, and B. I. Min, 1995, *Phys. Rev. B* **51**, 3850.
- Lee, P. A., 1993, *Phys. Rev. Lett.* **71**, 1887.
- Lenck, St., and J. P. Carbotte, 1994, *Phys. Rev. B* **49**, 4176.
- Lesueur, J., M. Aprili, A. Goulon, T. J. Horton, and L. Dumoulin, 1997, *Phys. Rev. B* **55**, R3398.
- Levin, K., Ju. H. Kim, J. P. Lu, and Q. Si, 1991, *Physica C* **175**, 449.
- Levin, K., D. Z. Liu, and J. Maly, 1996, in *Proceedings of the 10th Anniversary High-Temperature Superconductors Workshop on Physics, Materials, and Applications*, edited by B. Batlogg, C. W. Chu, W. K. Chu, D. U. Gubser, and K. A. Müller (World Scientific, Singapore), p. 467.
- Levin, K., and O. T. Valls, 1983, *Phys. Rep.* **98**, 1.
- Li, M.-R., P. J. Hirschfeld, and P. Wölfle, 1998, *Phys. Rev. Lett.* **81**, 5640.
- Li, M.-R., P. J. Hirschfeld, and P. Wölfle, 1999, *Phys. Rev. Lett.* **83**, 888.
- Li, Q., Y. N. Tsay, M. Suenaga, G. D. Gu, and N. Koshizuka, 1997, *Physica C* **282-287**, 1495.
- Li, Q., Y. N. Tsay, M. Suenaga, R. A. Klemm, G. D. Gu, and N. Koshizuka, 1999b, *Phys. Rev. Lett.* **83**, 4160.
- Li, Q., Y. N. Tsay, M. Suenaga, G. Wirth, G. D. Gu, and N. Koshizuka, 1999a, *Appl. Phys. Lett.* **74**, 1323.
- Li, Q. P., B. E. Koltenbah, and R. Joynt, 1993, *Phys. Rev. B* **48**, 437.
- Lichtenstein, A. I., and M. L. Kulić, 1995, *Physica C* **245**, 186.
- Likharev, K. K., 1979, *Rev. Mod. Phys.* **51**, 101.
- Liu, M., D. Y. Xing, and Z. D. Wang, 1997, *Phys. Rev. B* **55**, 3181.
- Liu, S. H., and R. A. Klemm, 1994, *Phys. Rev. Lett.* **73**, 1019.
- Loeser, A. G., Z.-X. Shen, D. S. Dessau, D. S. Marshall, C. H. Park, P. Fournier, and A. Kapitulnik, 1996, *Science* **273**, 325.
- Ma, J., C. Quitmann, R. J. Kelley, H. Berger, G. Margaritondo, and M. Onellion, 1995, *Science* **267**, 862.
- MacFarlane, J. C., R. Driver, R. B. Roberts, 1987, *Appl. Phys. Lett.* **51**, 1038.
- Maggio-Aprile, I., Ch. Renner, A. Erb, E. Walker, and Ø. Fischer, 1995, *Phys. Rev. Lett.* **75**, 2754.
- Magnusson, J., P. Nordblad, and P. Svedlindh, 1997, *Physica C* **282-287**, 2369.
- Maki, K., H. Won, M. Kohmoto, J. Shiraishi, Y. Morita, and G.-f. Wang, 1999, *Physica C* **317-318**, 353.
- Mannhart, J., H. Hilgenkamp, B. Mayer, Ch. Gerber, J. R. Kirtley, K. A. Moler, and M. Sigrist, 1996, *Phys. Rev. Lett.* **77**, 2782.
- Mannhart, J., and P. Martinoli, 1991, *Appl. Phys. Lett.* **58**, 643.
- Mannhart, J., B. Mayer, and H. Hilgenkamp, 1996, *Z. Phys. B: Condens. Matter* **101**, 175.
- Markiewicz, R. S., 1990, *J. Phys.: Condens. Matter* **2**, 665.
- Markiewicz, R. S., 1992, *Physica C* **200**, 65.
- Markiewicz, R. S., 1997, *J. Phys. Chem. Solids* **58**, 1179.
- Martin, A. M., and J. F. Annett, 1998, *Phys. Rev. B* **57**, 8709.
- Mathai, A., Y. Gim, R. C. Black, A. Amar, and F. C. Wellstood, 1995, *Phys. Rev. Lett.* **74**, 4523.
- Matsumoto, M., and H. Shiba, 1995a, *J. Phys. Soc. Jpn.* **64**, 1703.
- Matsumoto, M., and H. Shiba, 1995b, *J. Phys. Soc. Jpn.* **64**, 3384 (Part I); 4867 (Part II).
- Mesot, J., M. R. Norman, H. Ding, M. Randeria, J. C. Campuzano, A. Paramekanti, H. M. Fretwell, A. Kaminski, T. Takeuchi, T. Yokoya, T. Sato, T. Takahashi, T. Mochiku, and K. Kadowaki, 1999, *Phys. Rev. Lett.* **83**, 840.
- Michel, L., 1980, *Rev. Mod. Phys.* **52**, 617.
- Mierzejewski, M., J. Zieliński, and P. Entel, 1998, *Phys. Rev. B* **57**, 590.
- Miller, D. J., T. A. Roberts, J. H. Kana, J. Talvacchio, D. B. Bucholz, and R. P. H. Chang, 1995, *Appl. Phys. Lett.* **66**, 2561.
- Miller, J. H., Jr., Q. Y. Ying, Z. G. Zou, N. Q. Fan, J. H. Xu, M. F. Davis, and J. C. Wolfe, 1995, *Phys. Rev. Lett.* **74**, 2347.
- Millis, A., D. Rainer, and J. A. Sauls, 1988, *Phys. Rev. B* **38**, 4504.
- Millis, A. J., 1994, *Phys. Rev. B* **49**, 15408.
- Millis, A. J., H. Monien, and D. Pines, 1990, *Phys. Rev. B* **42**, 167.
- Miyake, K., S. Schmitt-Rink, and C. M. Varma, 1986, *Phys. Rev. B* **34**, 6554.
- Moockly, B. H., and R. A. Buhrman, 1994, *Appl. Phys. Lett.* **65**, 3126.
- Moockly, B. H., D. K. Lathrop, and R. A. Buhrman, 1993, *Phys. Rev. B* **47**, 400.
- Moler, K. A., D. J. Baar, J. S. Urbach, R. Liang, W. N. Hardy, and A. Kapitulnik, 1994, *Phys. Rev. Lett.* **73**, 2744.
- Moler, K. A., J. R. Kirtley, D. G. Hinks, T. W. Li, and M. Xu, 1998, *Science* **279**, 1193.
- Moler, K. A., J. R. Kirtley, R. Liang, D. A. Bonn, and W. N. Hardy, 1997, *Phys. Rev. B* **55**, 12753.
- Moler, K. A., D. L. Sisson, J. S. Urbach, M. R. Beasley, A. Kapitulnik, D. J. Baar, R. Liang, and W. N. Hardy, 1997, *Phys. Rev. B* **55**, 3954.
- Monthoux, P., 1997, *Phys. Rev. B* **55**, 15261.
- Monthoux, P., A. V. Balatsky, and D. Pines, 1991, *Phys. Rev. Lett.* **67**, 3448.
- Morita, Y., H. Kohmoto, and K. Maki, 1997, *Phys. Rev. Lett.* **78**, 4841.

- Morita, Y., M. Kohmoto, and K. Maki, 1998, *Int. J. Mod. Phys. B* **12**, 989.
- Moriya, T., Y. Takahashi, and K. Ueda, 1990, *J. Phys. Soc. Jpn.* **59**, 2905.
- Moshchalkov, V. V., X. G. Qiu, and V. Bruydoncx, 1997, *Phys. Rev. B* **55**, 11793.
- Mössle, M., and R. Kleiner, 1999, *Phys. Rev. B* **59**, 4486.
- Movshovich, R., M. A. Hubbard, M. B. Salamon, A. V. Balatsky, R. Yoshizaki, J. L. Sarrao, and M. Jaime, 1998, *Phys. Rev. Lett.* **80**, 1968.
- Mros, N., V. M. Krasnov, A. Yurgens, D. Winkler, and T. Claeson, 1998, *Phys. Rev. B* **57**, R8135.
- Müller, K. A., 1995, *Nature (London)* **377**, 133.
- Nagato, Y., and K. Nagai, 1995, *Phys. Rev. B* **51**, 16254.
- Nappi, C., and R. Cristiano, 1997, *Appl. Phys. Lett.* **70**, 1320.
- Nappi, C., R. Cristiano, and M. P. Lisitskii, 1998, *Phys. Rev. B* **58**, 11685.
- Nazarenko, A., and E. Dagotto, 1996, *Phys. Rev. B* **53**, R2987.
- News, D. M., P. C. Pattnaik, and C. C. Tsuei, 1991, *Phys. Rev. B* **43**, 3075.
- News, D. M., C. C. Tsuei, R. P. Huebener, P. J. M. van Bentum, P. C. Pattnaik, and C. C. Chi, 1994, *Phys. Rev. Lett.* **73**, 1695.
- News, D. M., C. C. Tsuei, and P. C. Pattnaik, 1995, *Phys. Rev. B* **52**, 13611.
- News, D. M., C. C. Tsuei, P. C. Pattnaik, and C. L. Kane, 1992, *Comments Condens. Matter Phys.* **15**, 273.
- Nie, Y., and L. Coffey, 1999, *Phys. Rev. B* **59**, 11982.
- Niskanen, K., J. Magnusson, P. Nordblad, P. Svedlindh, A.-S. Ullström, and T. Lundström, 1994, *Physica B* **194-196**, 1549.
- Nunner, T. S., J. Schmalian, and K. H. Benneman, 1999, *Phys. Rev. B* **59**, 8859.
- Obhukov, Yu. V., 1998, *J. Supercond.* **11**, 733.
- O'Donovan, C., and J. P. Carbotte, 1995a, *Physica C* **252**, 87.
- O'Donovan, C., and J. P. Carbotte, 1995b, *Phys. Rev. B* **52**, 16208.
- O'Donovan, C., M. D. Lumsden, B. D. Gaulin, and J. P. Carbotte, 1997, *Phys. Rev. B* **55**, 9088.
- Ogata, M., 1999, *Int. J. Mod. Phys. B* **13**, 3560.
- Ong, N. P., Y. F. Yan, and J. M. Harris, 1995, in *High- $T_c$  Superconductivity and the  $C_{60}$  Family*, edited by S. Feng and H. C. Ren (Gordon and Breach, Newark, NJ), p. 53.
- Ong, N. P., K. Krishana, Y. Zhang, and Z. A. Xu, 1999, "Thermal conductivity as a probe of quasiparticles in the cuprates," e-print, cond-mat/9904160.
- Ong, N. P., O. K. C. Tsui, K. Krishana, J. M. Harris, and J. B. Peterson, 1996, *Chin. J. Phys. (Taipei)* **34**, 432.
- Overhauser, A. W., 1999, *Phys. Rev. Lett.* **83**, 180.
- Owen, C. S., and D. J. Scalapino, 1967, *Phys. Rev.* **164**, 538.
- Ozaki, M., and K. Machida, 1989, *Phys. Rev. B* **39**, 4145.
- Ozaki, M., K. Machida, and T. Ohmi, 1985, *Prog. Theor. Phys.* **74**, 221.
- Ozaki, M., K. Machida, and T. Ohmi, 1986, *Prog. Theor. Phys.* **75**, 442.
- Pals, J. A., W. van Haeringen, and M. H. van Marren, 1977, *Phys. Rev. B* **15**, 2592.
- Pan, S. H., E. W. Hudson, K. M. Lang, H. Eisaki, S. Uchida, and J. C. Davis, 2000, *Nature (London)* **403**, 746.
- Pao, C.-H., and N. E. Bickers, 1994, *Phys. Rev. Lett.* **72**, 1870.
- Pearl, Judea, 1966, *J. Appl. Phys.* **37**, 4139.
- Peng, J. L., E. Maiser, T. Venkatesan, R. L. Greene, and G. Czysek, 1997, *Phys. Rev. B* **55**, R6145.
- Pennington, C. H., and C. P. Slichter, 1990, in *Physical Properties of High-Temperature Superconductors II*, edited by D. M. Ginsberg (World Scientific, Singapore), p. 269.
- Pickett, W. E., 1989, *Rev. Mod. Phys.* **61**, 433.
- Pines, D., 1995, in *High- $T_c$  Superconductivity and the  $C_{60}$  Family*, edited by S. Feng and H. C. Ren (Gordon and Breach, Newark, NJ), p. 1.
- Poole, C. P., H. A. Farach, and R. J. Creswick, 1995, *Superconductivity* (Academic, New York), p. 154.
- Pöst, L., L. E. Wenger, and M. R. Koblischka, 1998, *Phys. Rev. B* **58**, 14191.
- Prester, M., 1998, *Supercond. Sci. Technol.* **11**, 333.
- Prozorov, R., R. W. Giannetta, P. Fournier, and R. L. Greene, 2000, "Evidence for  $d$ -wave pairing in electron-doped superconductors," e-print, cond-mat/0002301.
- Radtke, R. J., V. N. Kostur, and K. Levin, 1996, *Phys. Rev. B* **53**, R522.
- Radtke, R. J., S. Ullah, K. Levin, and M. R. Norman, 1992, *Phys. Rev. B* **46**, 1975.
- Ren, Y., J. H. Xu, and C. S. Ting, 1995, *Phys. Rev. Lett.* **74**, 3680.
- Ren, Z. F., J. H. Wang, and D. J. Miller, 1996, *Appl. Phys. Lett.* **69**, 1798.
- Renner, Ch., B. Revaz, K. Kadowaki, I. Maggio-Aprile, and Ø. Fischer, 1998, *Phys. Rev. Lett.* **80**, 3606.
- Revaz, B., J.-Y. Genoud, A. Junod, K. Neumaier, A. Erb, and E. Walker, 1998, *Phys. Rev. Lett.* **80**, 3364.
- Rice, T. M., and M. Sigrist, 1995, *J. Phys.: Condens. Matter* **7**, L643.
- Rojo, A. G., and K. Levin, 1993, *Phys. Rev. B* **48**, 16861.
- Roth, B. J., N. G. Sepulveda, and J. P. Wikswo, Jr., 1989, *J. Appl. Phys.* **65**, 361.
- Russek, S. E., D. K. Lathrup, B. H. Moeckly, R. A. Buhrman, D. H. Shin, and J. Silcox, 1990, *Appl. Phys. Lett.* **57**, 1155.
- Saint-James, D., G. Sarma, and E. J. Thomas, 1969, *Type-II Superconductivity* (Pergamon, New York).
- Sakai, K., Y. Yokoya, and Y. O. Nakamura, 1997, *Physica C* **279**, 127.
- Sakai, T., D. Poilblanc, and D. J. Scalapino, 1997, *Phys. Rev. B* **55**, 8445.
- Salkola, M. I., A. V. Balatsky, and D. J. Scalapino, 1996, *Phys. Rev. Lett.* **77**, 184.
- Salkola, M. I., and J. R. Schrieffer, 1998, *Phys. Rev. B* **58**, R5952.
- Santi, G., T. Jarlborg, M. Peter, and M. Weger, 1996, *Physica C* **259**, 253.
- Sauls, J. A., 1994, *Adv. Phys.* **43**, 113.
- Scalapino, D. J., 1995, *Phys. Rep.* **250**, 329.
- Scalapino, D. J., E. Loh, Jr., and J. E. Hirsch, 1986, *Phys. Rev. B* **34**, 8190.
- Scalapino, D. J., E. Loh, Jr., and J. E. Hirsch, 1987, *Phys. Rev. B* **35**, 6694.
- Schmalian, J., and W. Hübner, 1996, *Phys. Rev. B* **53**, 11860.
- Schoop, U., S. Kleefisch, S. Meyer, A. Marx, A. Alff, R. Gross, M. Naito, and H. Sato, 1999, *IEEE Trans. Appl. Supercond.* **9**, 3409.
- Schopohl, N., and K. Maki, 1995, *Phys. Rev. B* **52**, 490.
- Schrieffer, J. R., 1994, *Solid State Commun.* **92**, 129.
- Schrieffer, J. R., 1995, *J. Low Temp. Phys.* **99**, 397.
- Schultz, R. R., B. Chesca, B. Goetz, C. W. Schneider, A. Schmehl, H. Bielefeldt, H. Hilgenkamp, J. Mannhart, and C. C. Tsuei, 2000, *Appl. Phys. Lett.* **76**, 912.

- Schüttler, H.-B., and M. R. Norman, 1996, Phys. Rev. B **54**, 13295.
- Senthil, T., M. P. A. Fisher, L. Balents, and C. Nayak, 1998, Phys. Rev. Lett. **81**, 4704.
- Setty, A. K., 1998, Phys. Rev. B **58**, 952.
- Shaked, H., P. M. Keane, J. C. Rodriguez, F. F. Owen, R. L. Hitterman, and J. D. Jorgensen, 1994, *Crystal Structure of the High- $T_c$  Superconducting Copper Oxides* (Elsevier Science, Amsterdam).
- Shaw, T. M., S. L. Shinde, D. Dimos, R. F. Cook, P. R. Duncombe, and R. Kroll, 1989, J. Mater. Res. **4**, 248.
- Shen, Z. X., and D. S. Dessau, 1995, Phys. Rep. **253**, 1.
- Shen, Z. X., D. S. Dessau, B. O. Wells, D. M. King, W. E. Spicer, A. J. Arko, D. Marshall, L. W. Lombardo, A. Kapitulnik, P. Diskinson, S. Doniach, J. DiCarlo, A. G. Loeser, and C. H. Park, 1993, Phys. Rev. Lett. **70**, 1553.
- Shen, Z. X., W. E. Spicer, D. M. King, D. S. Dessau, and B. O. Wells, 1995, Science **267**, 343.
- Shen, Z. X., P. J. White, D. L. Feng, C. Kim, G. D. Gu, H. Ikeda, R. Yoshizaki, and N. Koshizuka, 1998, Science **280**, 259.
- Shiraishi, J., M. Kohmoto, and K. Maki, 1999, Phys. Rev. B **59**, 4497.
- Shrivastava, K. N., 1994, Solid State Commun. **90**, 589.
- Sigrist, M., 1998, Prog. Theor. Phys. **99**, 899.
- Sigrist, M., D. Bailey, and R. B. Laughlin, 1995, Phys. Rev. Lett. **74**, 3249.
- Sigrist, M., K. Kuboki, P. A. Lee, A. J. Millis, and T. M. Rice, 1996, Phys. Rev. B **53**, 2835.
- Sigrist, M., and T. M. Rice, 1987, Z. Phys. B: Condens. Matter **68**, 9.
- Sigrist, M., and T. M. Rice, 1992, J. Phys. Soc. Jpn. **61**, 4283.
- Sigrist, M., and T. M. Rice, 1995, Rev. Mod. Phys. **67**, 503.
- Sigrist, M., and T. M. Rice, 1997, Phys. Rev. B **55**, 14647.
- Sigrist, M., and K. Ueda, 1991, Rev. Mod. Phys. **63**, 239.
- Simon, S. H., and P. A. Lee, 1997a, Phys. Rev. Lett. **78**, 1548.
- Simon, S. H., and P. A. Lee, 1997b, Phys. Rev. Lett. **78**, 5029.
- Singh, D. J., 1993a, Physica C **212**, 228.
- Singh, D. J., 1993b, Phys. Rev. B **48**, 3571.
- Singh, D. J., and W. E. Pickett, 1994, Phys. Rev. Lett. **73**, 476.
- Sinha, S., and K.-W. Ng, 1998a, Europhys. Lett. **44**, 648.
- Sinha, S., and K.-W. Ng, 1998b, Phys. Rev. Lett. **80**, 1296.
- Soininen, P. I., C. Kallin, and A. J. Berlinsky, 1994, Physica C **235-240**, 2593.
- Spivak, B. I., and S. Kivelson, 1991, Phys. Rev. B **43**, 3740.
- Stadlober, B., G. Krug, R. Nemetschek, R. Hackl, J. L. Lobb, and J. L. Mackert, 1995, Phys. Rev. Lett. **74**, 4911.
- Strohm, T., and M. Cardona, 1997, Solid State Commun. **104**, 233.
- Sun, A. G., D. A. Gajewski, M. B. Maple, and R. C. Dynes, 1994, Phys. Rev. Lett. **72**, 2267.
- Sun, A. G., S. H. Han, A. S. Katz, D. A. Gajewski, M. B. Maple, and R. C. Dynes, 1995, Phys. Rev. B **52**, R15731.
- Sun, A. G., A. Truscott, A. S. Katz, R. C. Dynes, B. W. Veal, and C. Gu, 1996, Phys. Rev. B **54**, 6734.
- Sun, Y., and K. Maki, 1995, Phys. Rev. B **51**, 6059.
- Svendlinth, P., K. Niskanen, P. Norling, P. Nordblad, L. Lundgren, B. Lönnberg, and T. Lundström, 1989, Physica C **162-164**, 1365.
- Tafari, F., F. M. Granozio, F. Carillo, A. Di Chiara, K. Verbist, and G. van Tendeloo, 1999, Phys. Rev. B **59**, 11523.
- Tafari, F., and J. R. Kirtley, 2000, "Evidence for broken time-reversal symmetry in YBCO thin films," e-print, cond-mat/0003106.
- Taillefer, L., B. Lussier, R. Gagnon, K. Behnia, and H. Aubin, 1997, Phys. Rev. Lett. **79**, 483.
- Tajima, S., J. Schützmann, S. Miyamoto, I. Terasaki, Y. Sato, and R. Hauff, 1997, Phys. Rev. B **55**, 6051.
- Takagi, H., S. Uchida, and Y. Tokura, 1989, Phys. Rev. Lett. **62**, 1197.
- Takagi, H., B. Batlogg, H. L. Kao, J. Kwo, R. J. Cava, J. J. Krajewski, and W. W. Peck, Jr., 1992, Phys. Rev. Lett. **69**, 2975.
- Takigawa, M., P. C. Hammel, R. H. Heffner, and Z. Fisk, 1989, Phys. Rev. B **39**, 7371.
- Tanaka, Y., 1994, Phys. Rev. Lett. **72**, 3871.
- Tanaka, Y., and S. Kashiwaya, 1995, Phys. Rev. Lett. **74**, 3451.
- Terentiev, A., D. B. Watkins, L. E. de Long, D. J. Morgan, and J. B. Ketterson, 1999, Phys. Rev. B **60**, R761.
- Terzioglu, E., and M. R. Beasley, 1998, IEEE Trans. Appl. Supercond. **8**, 48.
- Thomsen, C., 1991, in *Light Scattering in Solids VI*, edited by M. Cardona and G. Güntherodt (Springer, Berlin), p. 285.
- Thomsen, C., and M. Cardona, 1989, in *Physical Properties of High-Temperature Superconductors I*, edited by D. M. Ginsberg (World Scientific, Singapore), p. 410.
- Thompson, D. J., M. S. M. Minhaj, L. E. Wenger, and J. T. Chen, 1995, Phys. Rev. Lett. **75**, 529.
- Timusk, T., and B. Statt, 1999, Rep. Prog. Phys. **62**, 61.
- Tinkham, M., 1964, *Group Theory and Quantum Mechanics* (McGraw-Hill, New York).
- Tinkham, M., 1996, *Introduction to Superconductivity*, 2nd ed. (McGraw-Hill, New York).
- Tokura, Y., H. Takagi, and S. Uchida, 1989, Nature (London) **337**, 345.
- Tomita, N., Y. Takahashi, M. Mori, and Y. Uchida, 1992, Jpn. J. Appl. Phys., Part 2 **31**, L942.
- Tranquada, J. M., 1997, Physica C **282-287**, 166.
- Tsuei, C. C., C. C. Chi, D. M. Newns, P. C. Pattnaik, and M. Däumling, 1992, Phys. Rev. Lett. **69**, 2134.
- Tsuei, C. C., A. Gupta, and G. Koren, 1989, Physica C **161**, 415.
- Tsuei, C. C., and J. R. Kirtley, 1997, J. Alloys Compd. **250**, 615.
- Tsuei, C. C., and J. R. Kirtley, 1998, J. Phys. Chem. Solids **59**, 2045.
- Tsuei, C. C., and J. R. Kirtley, 2000, Phys. Rev. Lett. **85**, 182.
- Tsuei, C. C., J. R. Kirtley, C. C. Chi, L. S. Yu-Jahnes, A. Gupta, T. Shaw, J. Z. Sun, and M. B. Ketchen, 1994, Phys. Rev. Lett. **73**, 593.
- Tsuei, C. C., J. R. Kirtley, Z. F. Ren, J. H. Wang, H. Raffy, and Z. Z. Li, 1997, Nature (London) **387**, 481.
- Tsuei, C. C., J. R. Kirtley, M. Rupp, J. Z. Sun, A. Gupta, and M. B. Ketchen, 1996, Science **272**, 329.
- Tsuei, C. C., J. R. Kirtley, M. Rupp, J. Z. Sun, L. S. Yu-Jahnes, C. C. Chi, A. Gupta, and M. B. Ketchen, 1995, J. Phys. Chem. Solids **56**, 1787.
- Tsuei, C. C., D. M. Newns, C. C. Chi, and P. C. Pattnaik, 1990, Phys. Rev. Lett. **65**, 2724.
- Tsuei, C. C., D. M. Newns, J. R. Kirtley, and P. C. Pattnaik, 1995, in *High- $T_c$  Superconductivity and the  $C_{60}$  Family*, edited by S. Feng and H. C. Ren (Gordon and Breach, Newark, NJ), p. 293.
- Tsvetkov, A. A., D. van der Marel, K. A. Moler, J. R. Kirtley, J. L. de Boer, A. Meetsma, Z. F. Ren, N. Kolesnikov, D.

- Dulic, A. Damascelli, G. Grüninger, J. Schützmann, J. W. van der Eb, H. S. Somal, and J. H. Wang, 1998, *Nature (London)* **395**, 360.
- Uchida, S., K. Tamasaku, K. Takenaka, and H. Takagi, 1994, *J. Low Temp. Phys.* **95**, 109.
- Ueda, K., and T. M. Rice, 1985, *Phys. Rev. B* **31**, 7114.
- Ummarino, G. A., and R. S. Gonnelli, 1997, *Phys. Rev. B* **56**, R14279.
- Valla, T., A. V. Fedorov, P. D. Johnson, B. O. Wells, S. L. Hubert, Q. Li, G. D. Gu, and N. Koshizuka, 1999, *Science* **285**, 2110.
- Van Harlingen, D. J., 1995, *Rev. Mod. Phys.* **67**, 515.
- Van Harlingen, D. J., 1999, *Physica C* **317-318**, 410.
- Varelogiannis, G., 1998a, *Phys. Rev. B* **57**, 13743.
- Varelogiannis, G., 1998b, *Solid State Commun.* **107**, 427.
- Varma, C. M., P. B. Littlewood, S. Schmitt-Rink, E. Abrahams, and A. E. Ruckenstein, 1989, *Phys. Rev. Lett.* **63**, 1996.
- Vernik, I. V., S. Keil, N. Thyssen, T. Doderer, A. V. Ustinov, H. Kohlstedt, and R. P. Huebener, 1997, *J. Appl. Phys.* **81**, 1335.
- Vishveshwara, S., and M. P. A. Fisher, 2000, "Quasiparticle localization transition in dirty superconductors," e-print, cond-mat/0003018.
- Volovik, G. E., 1993, *JETP Lett.* **58**, 469.
- Volovik, G. E., 1997, *JETP Lett.* **65**, 491.
- Volovik, G. E., and L. P. Gor'kov, 1985, *Sov. Phys. JETP* **61**, 843.
- Volovik, G. E., and V. P. Mineev, 1976, *JETP Lett.* **24**, 605.
- Walker, M. B., 1996, *Phys. Rev. B* **53**, 5835.
- Walker, M. B., and J. Luettmmer-Strathmann, 1996a, *Phys. Rev. B* **54**, 588.
- Walker, M. B., and J. Luettmmer-Strathmann, 1996b, *J. Low Temp. Phys.* **105**, 483.
- Walstedt, R. E., and W. W. Warren, Jr., 1990, *Science* **248**, 1082.
- Wang, C. A., Z. F. Ren, J. H. Wang, D. K. Petrov, M. J. Naughton, W. Y. Yu, and A. Petrou, 1996, *Physica C* **262**, 98.
- Wang, J.-L., X. Y. Cai, R. J. Kelley, M. D. Vaudin, S. E. Babcock, and D. C. Larbalestier, 1994, *Physica C* **230**, 189.
- Wang, Y., and A. H. MacDonald, 1995, *Phys. Rev. B* **52**, R3876.
- Weger, M., M. Peter, and L. P. Pitaevskii, 1996, *Z. Phys. B: Condens. Matter* **101**, 573.
- Wei, J. Y. T., C. C. Tsuei, P. J. M. van Bentum, Q. Xiong, C. W. Chu, and M. K. Wu, 1998, *Phys. Rev. B* **57**, 3650.
- Wei, J. Y. T., N. C. Yeh, D. F. Garrigus, and M. Strasik, 1998, *Phys. Rev. Lett.* **81**, 2542.
- Wenger, F., and M. Käll, 1997, *Phys. Rev. B* **55**, 97.
- Wenger, F., and S. Östlund, 1993, *Phys. Rev. B* **47**, 5977.
- Wheatley, J., and T. Xiang, 1993, *Solid State Commun.* **88**, 593.
- White, R. M., and T. H. Geballe, 1979, *Long-range Order in Solids* (Academic, New York).
- Wollman, D. A., D. J. Van Harlingen, J. Giapintzakis, and D. M. Ginsberg, 1995, *Phys. Rev. Lett.* **74**, 797.
- Wollman, D. A., D. J. Van Harlingen, W. C. Lee, D. M. Ginsberg, and A. J. Leggett, 1993, *Phys. Rev. Lett.* **71**, 2134.
- Wollman, D. A., D. J. Van Harlingen, and A. J. Leggett, 1994, *Phys. Rev. Lett.* **73**, 1872.
- Woods, S. I., A. S. Katz, T. L. Kirk, M. C. de Andrade, M. B. Maple, and R. C. Dynes, 1999, *IEEE Trans. Appl. Supercond.* **9**, 3917.
- Wright, D. A., J. P. Emerson, B. F. Woodfield, J. E. Gordon, R. A. Fisher, and N. E. Phillips, 1999, *Phys. Rev. Lett.* **82**, 1550.
- Wu, D. H., J. Mao, S. N. Mao, J. L. Peng, X. X. Xi, T. Venkatesan, R. L. Greene, and S. M. Anlage, 1993, *Phys. Rev. Lett.* **70**, 85.
- Wu, M. K., J. R. Ashburn, C. J. Torng, P. H. Hor, R. L. Meng, L. Gao, Z. J. Huang, Y. Q. Wang, and C. W. Chu, 1987, *Phys. Rev. Lett.* **58**, 908.
- Wysokinski, K. I., 1997, *Physica C* **282-287**, 1701.
- Xu, J. H., J. H. Miller, Jr., and C. S. Ting, 1995, *Phys. Rev. B* **51**, 11958.
- Xu, J. H., Y. Ren, and C. S. Ting, 1996, *Phys. Rev. B* **53**, R2991.
- Xu, J. H., S. K. Yip, and J. A. Sauls, 1995, *Phys. Rev. B* **51**, 16233.
- Yang, C. N., 1962, *Rev. Mod. Phys.* **34**, 694.
- Yang, J., and C.-R. Hu, 1994, *Phys. Rev. B* **50**, 16766.
- Yazdani, A., C. M. Howald, C. P. Lutz, A. Kapitulnik, and D. M. Eigler, 1999, *Phys. Rev. Lett.* **83**, 176.
- Yip, S.-K., 1995, *Phys. Rev. B* **52**, 3087.
- Yip, S.-K., O. F. De Alcantara Bonfim, and P. Kumar, 1990, *Phys. Rev. B* **41**, 11214.
- Yip, S.-K., and A. Garg, 1993, *Phys. Rev. B* **48**, 3304.
- Yip, S.-K., and J. A. Sauls, 1992, *Phys. Rev. Lett.* **69**, 2264.
- Yurgens, A., D. Winkler, T. Claeson, G. Yang, I. F. G. Parker, and C. E. Gough, 1999, *Phys. Rev. B* **59**, 7196.
- Yurgens, A., D. Winkler, N. V. Zavaritsky, and T. Claeson, 1997, *Phys. Rev. Lett.* **79**, 5122.
- Zapotocky, M., D. L. Maslov, and P. M. Goldbart, 1997, *Phys. Rev. B* **55**, 6599.
- Zeyher, R., and M. L. Kulić, 1996, *Phys. Rev. B* **53**, 2850.
- Zhang, S. C., 1997, *Science* **275**, 1089.
- Zhu, J.-X., W. Kim, and C. S. Ting, 1998, *Phys. Rev. B* **57**, 13410.
- Zhu, J.-X., and C. S. Ting, 1998a, *Phys. Rev. B* **57**, 3038.
- Zhu, Y., Q. Li, Y. N. Tsay, M. Suenaga, G. D. Gu, and N. Koshizuka, 1998, *Phys. Rev. B* **57**, 8601.